Master's thesis

NTNU
Norwegian University of Science and Technology
Faculty of Natural Sciences
Department of Chemistry

Tonje Gottenberg Skaalvik

Per- and polyfluoroalkyl substances in shorebirds of Australia

Master's thesis in Environmental Toxicology and Chemistry
Supervisor: Alexandros Asimakopoulos
May 2020

NTNU
Kunnskap for en bedre verden

Tonje Gottenberg Skaalvik

Per- and polyfluoroalkyl substances in shorebirds of Australia

Master's thesis in Environmental Toxicology and Chemistry
Supervisor: Alexandros Asimakopoulos
May 2020

Norwegian University of Science and Technology
Faculty of Natural Sciences
Department of Chemistry

NTNU
Kunnskap for en bedre verden

Abstract

Australian coasts and wetlands are important habitats for wildlife, including avian migrants that accumulate energy for their next trans-equatorial flight by foraging in marine sediments at their Australian non-breeding sites. Shorebirds are prone to exposure of environmental contaminants as marine areas are often sinks for pollution. Exposure of shorebirds to environmental contaminants, such as per- and polyfluoroalkyl substances (PFASs), has not been extensively studied in Australia. This study investigates the exposure of three migratory shorebird species to PFASs at their Australian non-breeding grounds. This is done by determining the concentrations of 15 selected PFASs in red blood cells (rbc) of curlew sandpipers (*Calidris ferruginea*), red-necked stints (*Calidris ruficollis*) and ruddy turnstones (*Arenaria interpres*) sampled between 2013 and 2019 at different Australian shorelines. Differences in PFAS occurrence between species and sites were explored through comparison of concentration levels, detection rates and principal component analysis.

Selected PFASs were perfluoroalkyl sulfonates (PFSAs; C_4, C_6, C_8), perfluoroalkyl carboxylic acids (PFCAs; C_5-C_{14}) and perfluoroalkyl sulfonamides (PFOSA, EtPFOSA). Extraction and clean up was done applying Hybrid-SPE which allowed for rapid sample preparation of a large number of samples. Liquid chromatography tandem mass spectrometry (LC-MS/MS) was used for separation and detection. The method was successfully evaluated through a number of quality control parameters including precision, recoveries and matrix effects. Detection of PFASs in the majority (78%) of the investigated rbc samples (n=110) demonstrated the presence of these contaminants also in the rbc. This is the first study reporting PFASs in rbc as previous studies have only investigated these contaminants in plasma, serum and whole blood.

Occurrence profiles coincided with most previous avian studies, with PFOS being the most detected and dominant PFAS, followed by long-chained PFCAs. Major differences were observed in PFAS occurrence between species, which were mainly attributed to the degree of human influence on the respective sample sites. PFAS rbc concentrations in ruddy turnstones sampled on shorelines of King Island ($\sim$1500 people) were significantly lower than the concentrations found in curlew sandpipers and red-necked stints sampled in marine areas near the city of Melbourne ($\sim$5 million people). Curlew sandpipers and red-necked stints inhabiting areas of a biological wastewater treatment facility, the Western Treatment Plant,

had concerningly high concentrations. The concentrations were in the upper scale of what has previously been reported in avian studies, and similar to concentrations associated with sub-lethal effects such as immunotoxicity.

This thesis provides information regarding the exposure of these shorebirds to environmental pollutants. Such information has previously been scarce. The studied shorebirds are experiencing population declines, and further biomonitoring and ecotoxicological studies with regards to PFASs as well as other contaminants of concern should be carried out to understand the role of pollution in these declines.

Sammendrag

Australske kystområder og våtmarker innehar viktige habitater for dyreliv. I disse områdene forbereder trekkfugler seg på sin kommende reise til hekkeområder i nord, ved å søke etter mat for å samle opp energi. Kystfugler er spesielt utsatt for miljøgifter da slike stoffer ofte opphopes i kystområder. Forekomsten av miljøgifter, eksempelvis per- og polyfluorerte alkylstoffer (PFASer), i australske kystfugler er ikke blitt grundig undersøkt fra før. I dette studiet undersøkes tre forskjellige trekkfuglers eksponering for PFASer i Australia. Dette gjøres ved å bestemme konsentrasjonen av 15 utvalgte PFASer i prøver av røde blodceller (rbc) fra tundrasnipe (*Calidris ferruginea*), rødstrupesnipe (*Calidris ruficollis*) og steinvender (*Arenaria interpres*), som ble tatt i tidsrommet 2013-2019 på forskjellige steder i Australia. Forskjeller i forekomst av PFASer mellom arter og steder ble undersøkt ved sammenligning av konsentrasjoner, deteksjonsfrekvenser og ved bruk av prinsipal komponent analyse.

De utvalgte PFASene var pefluoroalkyl sulfonater (PFSAer; C_4, C_6, C_8), perfluoroalkyl karboksylsyrer (PFCAer; C_5-C_{14}) og perfluoroalkyl sulfonamider (PFOSA, EtPFOSA). Den analytiske metoden besto av Hybrid-SPE for ekstraksjon og væskekromatografi-tandem massespektrometri (LC-MS/MS) for separasjon og deteksjon. Metoden ble evaluert med hensyn på en rekke parametere for kvalitetskontroll, deriblant presisjon, ekstraksjonseffektivitet og matrikseffekter. PFASer ble detektert i de fleste (78%) rbc-prøvene, som viser at disse stoffene også finnes i røde blodceller. Dette er første gang PFASer rapporteres i rbc da tidligere undersøkelser av PFASer er gjort i plasma, serum eller fullblod.

Forekomsten av ulike PFASer samsvarer med de fleste andre studier av fugler ved at PFOS var det mest detekterte stoffet etterfulgt av lange kjeder av PFCAer. Det ble observert store forskjeller i forekomst av PFASer i ulike arter. Disse forskjellene kunne i hovedsak tillegges graden av menneskelig tilstedeværelse på de ulike stedene fuglene oppholdt seg på. PFAS konsentrasjonene i rbc-prøver fra steinvendere som opphold seg på King Island (innbyggertall$\sim$1500) var vesentlig lavere i forhold til konsentrasjonene i tundrasniper og rødstrupesniper som befant seg i kystområder nær Melbourne (innbyggertall$\sim$5 millioner). Tundrasniper og rødstrupesniper som befant seg i området av et biologisk renseanlegg (Western Treatment Plant) hadde høye og bekymringsverdige konsentrasjoner. Disse konsentrasjonene var i øvre sjiktet av hva som tidligere er blitt rapportert i fugler og var i samme størrelsesorden som konsentrasjoner tilknyttet negative helseeffekter

som immuntoksisitet.

Denne avhandlingen gir informasjon vedrørende kystfuglenes eksponering til miljøgifter; informasjon som tidligere ikke har vært kjent. Populasjonsnedgang er observert i de aktuelle fuglene og det er behov for flere slike undersøkelser og økotoksikologiske studier av PFASer og andre miljøgifter for å forstå i hvilken grad forurensning innvirker på populasjonsnedgangen.

Acknowledgement

This thesis concludes my master's degree in Environmental and Analytical Chemistry at NTNU. I wish to express my gratitude towards all the dedicated people making this thesis possible.

First and foremost, I would like to thank my supervisor, Alexandros Asimakopoulos, for your guidance throughout this project. Thank you for sharing all your knowledge as well as your positive energy. Your great availability and mentoring are highly appreciated. This project would also not have been possible without my co-supervisor, Veerle Jaspers. Your insight into this project as well as your motivating words and feedback have been of great value. I wish to thank both my supervisors for introducing me to this exciting project.

I would also like to acknowledge the following people. A very special thank you is given to Kristine Vike (NTNU, IKJ) for the help with LC-MS/MS analysis. Thank you also for always being available to share your knowledge. Thank you, Vishwesh Venkatraman (NTNU, IKJ) for the assistance with principal component analysis and correlations. Syverin Lierhagen (NTNU, IKJ), thank you for your conversations and the help with sample preparation. I am sure the upcoming ICP-MS results will be very interesting. Thank you, Grethe Stavik Eggen (NTNU, IBI), for your practical assistance at numerous occasions during sample handling. I would also like to thank Marcel Klaassen (Deakin University) and Tobias Alexander Ross (Deakin University) for your collaboration and insight into this project. I am grateful for having gotten to take part in it. A huge thank you to Tor Strømsem Haugland and Sigrid Bergseng Lakså for your support and assistance in the finalizing of this thesis.

I also wish to acknowledge the ENVITOX program at NTNU for the opportunity to study this most interesting field. Thank you to my fellow students in the environmental chemistry lab, most notably Hanne and Ragnhild, for the teamwork, discussions and fun. Thank you also to my fellow ENVITOX students, with extra special thanks to Alisa, Hanne and Stine.

Thank you to my family and friends for your loving support and genuine interest in my thesis. Lastly, but far from least, thank you Tor for your immense support throughout this project.

Contents

List of Figures

List of Tables

1. Introduction

1.1. Introduction

Per- and polyfluoroalkyl substances (PFASs) have been in production since the 1950s and have since been used in a variety of industrial and consumer applications utilizing their unique physiochemical properties [1, 2]. The chemical structure of PFASs causes high chemical and thermal stability, low surface tension and dielectric constant, as well as combined hydrophobicity and lipophobicity [2]. This makes PFASs useful in applications such as lubricants, surfactants, impregnating agents, electronics, printing inks, ski gliding wax, textiles, food packaging, pesticides and non-stick cookware [2–5]. Emerging concern of PFASs arose in the early 2000s after the reveal of their global distribution, persistence in the environment, presence in human blood and wildlife, and potential adverse effects [4, 6–9].

Concerns were particularly raised towards perfluorooctane sulfonate (PFOS) and perfluorooctanoic acid (PFOA) which remain the most studied PFASs to this day [7]. This led to volunteered phaseouts of these chemicals by major manufacturers in the beginning of the 21st century. Following this, PFOS was added to the Stockholm Convention on Persistent Organic Pollutants Annex B (restricted production and use) in 2009 [10]. More recently, perfluorohexane sulfonate (PFHxS) has been proposed for listing (2017), and PFOA has been officially included in Annex A of the Stockholm Convention (2019) [11, 12]. Long-chained perfluoroalkyl carboxylic acids (C_{10}-C_{14}), and the short-chained perfluorobutane sulfonate (PFBS) have been included in the Candidate List of Substances of Very High Concern for Authorization under the European Chemicals Agency [13–16]. Despite regulations, PFASs continue to be detected in the global environment, with the highest concentrations found in industrialized and urbanized areas [2]. Particularly, the accumulated concentrations of PFASs in wildlife are concerning.

This study will delve into the PFAS concentration levels in migratory shorebirds at their non-breeding sites. Each year, millions of these birds embark on a thousand of kilometers long journey between their non-breeding grounds in the southern hemisphere and their breeding grounds in northern areas. On their travels, these long-distance migrants stop along the way to rest and refuel. Migratory birds are consequently dependent on multiple habitats, and thus, highly susceptible to local and global change [17]. Australian migratory shorebirds travel from Aus-

tralian coasts and wetlands, through the East Asian-Australasian flyway (EAAF), to their breeding sites in Siberia and Alaska [18]. Major population declines have been observed in the birds of the EAAF [17]. The birds of the EAAF are subjected to habitat destruction from industrial and residential development, pollution from agricultural, industrial and residential run-off, and climate change [19]. While habitat loss and climate change have been identified as major drivers of the population declines [17], the exposure to environmental pollution is less studied. The exposure to environmental contaminants can cause avian mortality directly, but more commonly lead to sub-lethal effects such as decreased reproductive success, impaired immune function, and altered body condition [20]. Studying the exposure of these birds to environmental pollutants may provide powerful insight for their conservation.

Curlew sandpiper (*Calidris ferruginea*), red-necked stint (*Calidris ruficollis*) and ruddy turnstone (*Arenaria interpres*) are migratory shorebirds residing in Australia during the summer months (November-February), before departing to their arctic breeding grounds through the EAAF in autumn (March/April). Their non-breeding grounds in Australia are of importance as this is where the birds recover from migration and accumulate energy for their next flight. Exposure to contaminants here may impact their health and subsequently their migration performance.

The aim of this study was to determine the concentrations of 15 selected PFASs in 110 red blood cell samples of these shorebirds sampled in Australia. This was done using the sample preparation technique Hybrid-SPE [21], which specifically aims for the rapid removal of interfering matrix components from biological matrices. Ultra performance liquid chromatography tandem mass spectrometry (UPLC-MS/MS) was applied for separation and detection. The analyzed sample collection consisted of samples obtained between 2013-2019 from multiple habitats with different degree of human influence, from a biological wastewater treatment facility to the more remote King Island. As PFASs tend to be present in higher concentrations near populated areas, this study also explores spatial trends and species differences.

2. Theoretical background

2.1. Per- and polyfluoroalkyl substances

Per- and polyfluoroalkyl substances (PFASs) are a group of chemicals receiving increased attention the past decades due to their global distribution [6], persistence in the environment [4, 7], ability to bioconcentrate and bioaccumulate [3, 22] and the findings of PFASs in wildlife [6, 9] and human blood [8]. Although simple organic compounds containing fluoride atoms may occur naturally, perfluorinated alkyl chains do not, meaning that all findings of such compounds in the environment are of anthropogenic origin [2, 4].

This chemical group has high structural diversity and the total range of different per- and polyfluoroalkyl substances is broad. In the Swedish Chemical Agency's (KEMI) survey on PFASs in 2015, it was estimated that around 3000 different chemicals on the global market belong to this group [23]. In this study, 15 PFASs, including the ones most commonly monitored, are analyzed. Selected PFASs are presented in Table 2.1.

2.1.1. Classification, terminology and properties

Concerning the various names used for PFASs, a detailed overview of proposed terminology and classification was provided by Buck et al. [24]. Per- and polyfluoroalkyl substances are aliphatic substances containing a perfluorinated moiety, C_nF_{2n+1}, in which all hydrogen atoms bound to carbon are replaced by fluorine atoms. In a *perfluoroalkyl* substance, all carbon atoms of the hydrocarbon analogue are perfluorinated. In a *polyfluoroalkyl* substance, at least one carbon is perfluorinated, but not all [24]. With this regard, all PFASs in this study are perfluorinated with the exception of *N*-Ethyl perfluorooctane sulfonamid (EtPFOSA), which is a polyfluoroalkyl substance.

The persistence of PFASs in the environment, as well as the cause of its wide use in multiple industrial applications, stems from the strong carbon-fluoride bond [5]. This strong bond makes the perfluoroalkyl chain rigid with high chemical and thermal stability [2, 4]. While a hydrocarbon chain is hydrophobic, the perfluoroalkyl chain is both hydrophobic and lipophobic [2]. The presence of a hydrophilic group, such as an acid, at the end of the perfluorinated carbon chain, gives perfluoroalkyl

Table 2.1.: Names, common abbreviations, chemical structure and classification of target analytes.

Chemical	Abbreviation	Structure
Perfluoroalkyl sulfonic acids		
Perfluorobutane sulfonate	PFBS	$CF_3(CF_2)_3SO_3^-$
Perfluorohexane sulfonate	PFHxS	$CF_3(CF_2)_5SO_3^-$
Perfluorooctane sulfonate	PFOS	$CF_3(CF_2)_7SO_3^-$
Perfluoroalkyl carboxylic acids		
Perfluoropentanoic acid	PFPA	$CF_3(CF_2)_3COOH$
Perfluorohexanoic acid	PFHxA	$CF_3(CF_2)_4COOH$
Perfluoroheptanoic acid	PFHpA	$CF_3(CF_2)_5COOH$
Perfluorooctanoic acid	PFOA	$CF_3(CF_2)_6COOH$
Perfluorononanoic acid	PFNA	$CF_3(CF_2)_7COOH$
Perfluorodecanoic acid	PFDA	$CF_3(CF_2)_8COOH$
Perfluoroundecanoic acid	PFUnDA	$CF_3(CF_2)_9COOH$
Perfluorododecanoic acid	PFDoDA	$CF_3(CF_2)_{10}COOH$
Perfluorotridecanoic acid	PFTrDA	$CF_3(CF_2)_{11}COOH$
Perfluorotetradecanoic acid	PFTeDA	$CF_3(CF_2)_{12}COOH$
Perfluoroalkyl sulfonamides		
Perfluorooctane sulfonamide	PFOSA	$CF_3(CF_2)_7SO_2-NH_2$
N-Ethyl perfluorooctane sulfonamide	EtPFOSA	$CF_3(CF_2)_7SO_2-NHCH_2CH_3$
Non-fluorinated		
Decane 1-sulfonate	DecaS	$CF_3(CF_2)_9SO_3^-$

acids (PFAAs) surfactant properties. Krafft et al. reviews the physiochemical aspects of these compounds in great detail [2].

In literature, the term PFAAs refers to the group of perfluoroalkyl carboxylic, sulfonic, sulfinic, phosphonic and phosphinic acids [24]. Perfluoroalkyl carboxylic acids (PFCAs) and perfluoroalkyl sulfonic acids/sulfonates (PFSAs) are more commonly studied and have both been found in wildlife and humans [4, 8, 9]. The term PFAAs will mainly refer to these two groups. PFCAs and PFSAs may exist either in the form of the neutral carboxylic/sulfonic acids or as the corresponding anionic carboxylate/sulfonate salt, depending on the pH and the pKa of the acid. The chemical structures of a PFSA, PFOS, and a PFCA, PFOA, are shown in Figure 2.1. In this thesis, the use of acronyms for PFAAs will refer to both the acid and the dissociated form, unless otherwise stated. It should, however, be noted that the charge of a substance affects its fate in the environment as well as

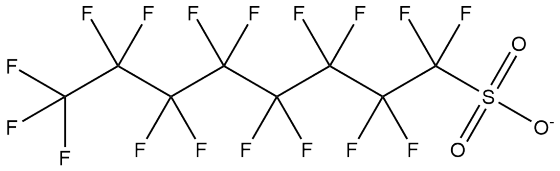

PFOS

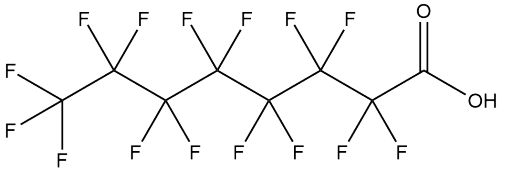

PFOA

Figure 2.1.: Chemical structure of perfluorooctane sulfonate (PFOS) and perfluorooctanoic acid (PFOA).

within organisms [24, 25].

PFASs may be classified in a variety of ways. There are non-polymers such as perfluorooctane sulfonate, PFOS, and polymers such as polytetrafluoroethylene, PTFE. Classification based on production pathway may be done since between the two major manufacturing pathways of PFASs, electrochemical fluorination and telomerization, only the former produces a mixture of linear and branched isomers, while the latter does not [3, 4, 24]. A distinction is often made between "long-chained" and "short-chained" PFASs. Long chained PFCAs and PFSAs are defined as having more than seven and six carbon atoms, respectively [24]. Regulatory approaches have aimed to reduce the emission of long-chained PFASs due to their generally higher persistence and ability to bioaccumulate [2, 7, 26, 27]. Shorter chained PFASs have shorter half-lives in organisms [26] and bioaccumulate less, and may therefore be alternatives to PFOS [7, 28]. Nevertheless, the short-chained homologues are still as persistent in the environment as longer chains.

Classification of PFASs is also done on the basis of persistence. Some PFASs may degrade to more persistent PFAAs. These chemicals are mainly referred to as *precursors* and include fluorotelomer alcohols (FTOH) and perfluoroalkane sulfonamido substances such as perfluoroalkane sulfonamidoethanols (FASEs), sulfonamides (FASAs) and *N*-alkyl perfluoroalkane sulfonamides (e.g. EtFASAs) among others [7, 24]. These compounds are often used as raw materials in the manufacturing of other products [24], but may also be used for specific applications on their own. For instance, *N*-ethyl perfluorooctane sulfonamid (EtPFOSA) is used in the insecticide Sulfluramid [29]. Of the selected PFASs in this study, PFOSA and EtPFOSA are classified as precursors.

2.1.2. Environmental fate

Emission of persistent PFASs may come from direct production, use and disposal, or from the emission of precursors that degrade to PFCAs and PFSAs [3]. For example, EtPFOSA and PFOSA are degradation products and can be further degraded to PFOS [3, 24]. PFCAs and PFSAs may also be found as impurities left from manufacture of other products. For example, perfluorooctanoic acid (PFOA) and perfluorononanoic acid (PFNA) are used as processing aids of polytetrafluoreten (PTFE) and polyvinylidene fluoride (PVDF), and may be found in trace levels in products of these polymers [2, 3, 22].

The highest levels of PFASs are found in industrialized and urbanized areas [30], where PFASs are found in wastewater, landfills, air, coastal environments and biota [22, 31, 32]. Although these areas most often have the highest levels, PFASs have also been found in snow, seawater, sediment, and wildlife in remote locations such as the Arctic [6, 9, 33–35]. The mechanisms of transport from the source to remote locations are not fully understood, though it is thought to be mainly by the long range transport of semi-volatile and volatile precursors followed by degradation to PFAAs [3, 33, 35, 36]. Two major transport routes of PFASs are via the ocean or through the air [7]. On a general basis it is assumed that PFAAs mainly distribute via water, while precursors such as fluorotelomers and perfluoroalkane sulfonamido substances are transported mainly in air [7, 30, 33, 36]. Routes of exposure can be ingestion of contaminated water and soil/sediment and diet. The latter is a major exposure route to wildlife and PFASs have been found in multiple tissues and blood of animals across food webs [6, 22, 37–42].

2.1.3. Adverse effects

While most of the legacy organochloride pollutants are lipophilic and accumulate in fat, PFASs tend to be protein associated and distribute to protein rich compartments [2, 22, 43, 44]. PFASs have been found in the liver, blood, kidney, muscle and eggs of invertebrates, fish, birds and mammals. Long-chained PFCAs and PFSAs are found to bioconcentrate and bioaccumulate in organisms [6, 27, 33]. Studies have also found that some PFASs, such as PFOS, can biomagnify in some food webs, meaning that higher concentrations are found in organisms feeding on higher trophic levels [45]. In their review on biological monitoring of PFASs, Houde et al., summarize that PFOS, perfluorohexanoic acid (PFHxA) and long-chained PFCAs having eight to twelve carbon atoms are able to bioaccumulate and biomagnify [22].

Studies on the toxicity of PFASs in laboratory animals and humans have found evidence of hepatotoxicity, immunotoxicity and developmental toxicity as well as endocrine disruption by altering thyroid hormone levels [43, 46–48]. Interactions

of individual PFASs on organisms varies. For example; the potential to bioconcentrate in fish as well as alter thyroid hormone levels in humans have been found to be dependent on the length of the perfluoroalkyl chain [27, 43]. Inter-species differences are also notable among different PFASs. Bioaccumulation is specie dependent as elimination and uptake may vary between species [30]. The half-life of PFASs in blood is also varying with different species [49, 50]. For example; half-life in blood was found to be 20.7 days in quails (*Coturnix coturnix*) and 13.6 days in mallards (*Anas platyrhynchos*) [51].

Newsted et al. derived avian toxicity reference values (TRV) and predicted no effect concentrations (PNEC) of PFOS based on top predators. Endpoints were mortality, growth, feed consumption, histopathology, egg production, fertility, hatchability, survival and growth of offspring. TRV and PNEC for serum was estimated to $1700\,\mathrm{ng\,mL^{-1}}$ and $1000\,\mathrm{ng\,mL^{-1}}$ respectively. Immunotoxicity was investigated by Peden-Adams et al., who performed *in ovo* injection of PFOS in white leghorn (*Gallus gallus*) chickens. The lowest serum concentration associated with immunological and neurological effects were $154\,\mathrm{ng\,g^{-1}}$ [52]. This is lower than the TRV and also within the concentration range found in some wild birds [52]. Sub-lethal effects should therefor always be considered. Among other sub-lethal mechanism is increased oxidative damage by production of reactive oxygen species and/or downregulation of antioxidant defense [53]. Costantini et al. [53] found a higher protein oxidative damage in black-legged kittiwakes (*Rissa tridactyla*) with higher concentrations of long-chained PFCAs. The authors do however also point out the many discrepancies in literature on oxidative stress biomarkers and PFAS exposure, and that further studies are needed to comprehend this relationship.

2.1.4. Previous studies on birds

PFSAs and PFCAs are the most monitored PFASs, with PFOS being the most studied single PFAS, both with regards to biomonitoring as well as toxicological studies. There are many studies on PFASs in invertebrates, fish and mammals [6, 34, 37–39, 54, 55]. In this chapter, only studies on birds are presented as contamination profiles in birds have been found to differ from those found in mammals [55].

An overview of previous findings of the most detected PFASs in a variety of biological matrices in birds is given in Table 2.2. Among these studies, PFOS is often the dominating PFAS. In addition, long-chained compounds are more detected than shorter homologues. Perfluoroalkyl substances are mostly reported in liver followed by plasma and blood. PFASs have been detected in low levels in birds living in remote locations such as islands of the North Pacific Ocean, Southern Ocean, Northern Norway, Svalbard, Atlantic Ocean and the Mediterranean [41, 56–60]. The highest levels are found in birds collected near industrialized areas or areas

with dense human population [60, 61]. In addition to exposure through anthropogenic sources, diet and trophic position have been found to be important factors affecting PFASs accumulation [58, 60]. Some studies have found blood PFAS levels to be higher than those of legacy contaminants such as polychlorinated biphenyls (PCBs) and organochlorine insecticides [58]. Physiology may also affect levels of PFAS in birds, thus resulting in differences in males and females. Although differences in males and females are not always found, higher relative concentrations of PFOS in males have been reported in northern cardinals (*Cardinalis cardinalis*) at Hawaii [62], lesser black-backed gulls (*Larus fuscus*) in Northern Norway [58] and great skuas (*Stercorarius skua*) from the North Atlantic [63]. Studies on PFASs in eggs have also suggested maternal transfer of these pollutants in some studies [4].

With regards to the toxic reference values for avian predators [51], PFOS levels above these values have been found in liver samples of barn owls (*Tyto alba*) in Belgium [61] and collared scops owl (*Otus lettia*), black-tailed gull (*Larus crassirostris*), brown hawk-owl (*Ninox scutulata*) and northern goshawk (*Accipiter gentilis*) from Korea [64]. Elliot et al. [65] found plasma levels exceeding the TRV in several bald eagles (*Haliaeetus leucocephalus*) sampled in areas with strong human influence. Plasma/serum levels of birds sampled in areas with less human influence such as, white-tailed eagle (*Haliaeetus albicilla*) and northern goshawks nestlings in Northern Norway and Calonectris shearwater of the Mediterranean have been found to be below the toxic reference value [41, 42]. Birds with PFOS concentrations below the TRV can still be subjected to sub-lethal effects such as immunotoxicity [62].

PFBS and short-chained PFCAs have been included in multiple studies, but have mostly not been detected in avian samples and are therefore not included in Table 2.2. In the studies presented in Table 2.2, PFPA is previously not detected in blood or plasma, but is detected in small concentrations of livers of some species in Korean areas [64] and in peregrine falcon (*Falco peregrinus*) eggs in Sweden [66]. PFHxA has been reported in low concentrations in plasma of european shag (*Phalacrocorax aristotelis*) [67], bald eagles [65] and gentoo penguins (*Pygoscelis papua*) [57] and in livers of black guillemot (*Cepphus grylle*) and glaucous gull (*Larus hyperboreus*) [68] as well as some species in Korea [64]. Low plasma concentrations are also reported in a few studies analyzing PFHpA in avian plasma [63, 65, 69]. PFASs of other chemical groups such as PFOSA and EtPFOSA are less studied than PFAAs. PFOSA is included in multiple studies but reported only in some, such as in plasma of lesser black-backed gulls [58], tree swallow (*Tachycineta bicolor*) [70], european shag [67], white-tailed eagle [71] and great skua [63], and livers of common cormorant (*Phalacrocorax carbo*) [40, 72], and tree swallow [70]. There is minimal data on EtPFOSA in birds.

Table 2.2.: Previous findings of some perfluoroalkyl substances in birds in a variety of matrices. Concentrations are given as median or (range) if not stated otherwise.

Species	Matrix	Unit	PFHxS	PFOS	PFOA	PFNA	PFDA	PFUnDA	PFDoDA	PFTrDA	PFTeDA	Location, year	Study
Northern goshawk (n=10)	Plasma	ng/mL	0.65	9.55	0.97	1.4	0.62	1.8	0.74	1	0.04	Norway, 2014	Gómez-Ramírez et al. 2017 [42]
White-tailed eagle (n=14)	Plasma	ng/mL	0.57	32.33	1.07	4.05	1.76	4.01	0.6	1.19	nd	Norway, 2014	Gómez-Ramírez et al. 2017 [42]
Cory's shearwater (n=12)	Blood	ng/mL	nd	5.8[a]	nd	nd	nd	1.2[a]	0.3[a]	nd	nd	Gran Canaria, 2014	Escoruela et al. 2018 [41]
Scopoli's shearwater (n=37)	Blood	ng/mL	nd	(11.8 - 41.9)[b]	nd	nd	nd	(3.5 - 7.3)[b]	(1.1 - 2.6)[b]	(0.2 - 1.2)[b]	nd	Medierranian, 2014	Escoruela et al. 2018 [41]
Kittiwakes (n=44)	Plasma	ng/mL	nd	(8.92 - 10.85)[b]	nd	(1.08-1.21)[b]	(1.63-2.2)[b]	(9.39-12.11)[b]	(1.99-2.54)[b]	(9.68-11.62)[b]	nd	Svalbard, 2014	Blévin et al. 2017 [59]
Lesser black-backed gulls (n=80)	Blood	ng/mL	0.71	33.97	nd	nd	nd	4.39	1.04	1.69	-	Norway, 2005	Bustnes et al. 2008 [58]
Carrion crow (n=5)	Blood	ng/mL	<1	56[a]	-	-	-	-	-	-	-	Japan, 2000	Taniyasu et al. 2003 [73]
Mallard (n=1)	Blood	ng/mL	9	130[a]	-	-	-	-	-	-	-	Japan, 2000	Taniyasu et al. 2003 [73]
Pintail duck (n=2)	Blood	ng/mL	13[a]	126[a]	-	-	-	-	-	-	-	Japan, 2000	Taniyasu et al. 2003 [73]
Northern cardinal (n=40)	Serum	ng/mL	nd	8.4	0.57	0.79	1.3	-[d]	1	0.84	0.92	Atlanta US, 2010	Russell et al. 2019 [62]
Northern cardinal (n=17)	Serum	ng/mL	nd	1	0.83	0.69	0.34	-[d]	0.02	nd	nd	Hawaii US, 2012-13	Russell et al. 2019 [62]
Snow petrel (n=7)	Plasma	ng/g	nd	(0.16-0.84)	-[d]	nd	(nd-0.13)	(nd-0.70)	(nd-0.45)	nd	nd	Antarctica, 2013	Munoz et al. 2017 [69]
King penguin (n=7)	Plasma	ng/g	nd	(nd-0.19)	-[d]	nd	nd	(0.08-0.17)	(nd-0.07)	(nd-0.06)	nd	Subantarctic, 2013	Munoz et al. 2017 [69]

a arithmetic mean; b range of means; c range of medians; d not reported; e geometric mean; f pooled individuals

Species	Matrix	Unit	PFHxS	PFOS	PFOA	PFNA	PFDA	PFUnDA	PFDoDA	PFTrDA	PFTeDA	Location, year	Study
South polar skua (n=7)	Plasma	ng/g	(nd-0.017)	(1.3-9.8)	-[d]	(nd-0.37)	(nd-0.71)	(0.84-4.0)	(0.19-1.0)	(0.45-1.9)	(nd-0.25)	Antarctica, 2013	Munoz et al. 2017 [69]
Tree swallow (n=20)	Plasma	ng/mL	206[e]	856[e]	13.1[e]	4.34[e]	1.72[e]	2.96[e]	0.67[e]	-	-	Michigan, US, 2014-15	Custer et al. 2019 [70]
Gentoo penguin (n=35)	Plasma	ng/mL	(nd-0.14)	(0.25-0.49)	nd	(nd-0.06)	nd	(0.07-0.18)	nd	(nd-0.17)	-	Southern Ocean, 2009-13	Roscales et al. 2019 [57]
Southern giant petrel (n=27)	Plasma	ng/mL	(nd-0.34)	(2.3-46)	(nd-0.05)	(0.14-2.1)	(0.16-0.69)	(0.5-1.4)	(0.09-0.25)	(0.63-2.1)	-	Southern Ocean, 2009-10	Roscales et al. 2019 [57]
Rockhopper penguin (n=36)	Plasma	ng/mL	(nd-0.91)	(0.36-14)	(nd-0.33)	(nd-0.60)	(nd-0.26)	(nd-0.71)	(nd-0.10)	(nd-0.44)	-	Southern Ocean, 2010-13	Roscales et al. 2019 [57]
Brown skua (n=14)	Plasma	ng/mL	nd	1.9	nd	nd	nd	0.09	nd	0.14	-	Southern Ocean, 2013	Roscales et al. 2019 [57]
Black browned albatross (n=8)	Plasma	ng/mL	nd	0.27	nd	nd	nd	nd	nd	nd	-	Southern Ocean, 2013	Roscales et al. 2019 [57]
Scoty shearwater (n=6)	Plasma	ng/mL	0.06	1.2	nd	nd	nd	0.12	0.07	0.53	-	Southern Ocean, 2013	Roscales et al. 2019 [57]
Great shearwater (n=12)	Plasma	ng/mL	0.52	9.2	0.08	0.76	0.51	4	0.97	4.8	-	Southern Ocean, 2010-13	Roscales et al. 2019 [57]
Bald eagle (n=381)	Plasma	ng/mL	0.81	130	1.7	52	22.5	37.3	8.3	15.2	1.7	Midwestern US, 2006-15	Elliott et al. 2019 [65]
European shag (n=11)	Plasma	ng/g	2.4	27.7	5	nd	4.9	1.23	nd	nd	-	Norway, 2004	Herzke et al. 2009 [67]
Glaucous gull (n=20)	Plasma	ng/mL	1.12[a]	134[a]	(<0.70-0.74)	(<2.33-6.33)	6.56[a]	74.4[a]	7.68[a]	11[a]	0.54[a]	Norwegian arctic, 2004	Verreault et al. 2005 [74]
White-tailed eagle (n= 71)	Plasma	ng/mL	(0.09-1.64)[c]	(5.25-16.55)[c]	(0.12-0.53)[c]	(0.56-3.58)[c]	(0.39-1.44)[c]	(1.15-3.59)[c]	(0.22-0.57)[c]	(0.29-0.94)[c]	nd	Norway, 2015-16	Løseth et al. 2019 [71]
Great skua (n=20)	Plasma	ng/g (ww)	(0.406-0.597)[c]	(23-37)[c]	(0.089 - 0.248)[c]	(0.657-1.06)[c]	(1.4 - 2)[c]	(9.06 -14.4)[c]	(2.74-4)[c]	(8.66 -14.7)[c]	(0.994 - 1.8)[c]	Shetland, 2009	Leat et al. 2013 [63]
European shag (n=11)	Liver	ng/g	1.4	26.9	1.38	nd	7.85	nd	nd	nd	-	Norway, 2004	Herzke et al. 2009 [67]
Great skua (n=20)	Eggs	ng/g (ww)	0.115	23	nd	0.493	1.52	9.97	2.93	7.23	0.55	Sheltand, 2008	Leat et al. 2013 [63]
Black guillemot (n=18)	Liver	ng/g (ww)	0.16	11.2	(nd -17.1)	1.28	nd	-[d]	-[d]	-	-[d]	Barents Sea, 2004	Haukås et al. 2007 [68]
Glaucous gull (n=9)	Liver	ng/g (ww)	0.28	38.4	nd	1.46	(nd - 9.43)	-[d]	-[d]	-	-[d]	Barents Sea, 2004	Haukås et al. 2007 [68]

a arithmetic mean; b range of means; c range of medians; d not reported; e geometric mean; f pooled individuals

Species	Matrix	Unit	PFHxS	PFOS	PFOA	PFNA	PFDA	PFUnDA	PFDoDA	PFTrDA	PFTeDA	Location, year	Study
White-tailed eagle (n=14)	Body feathers	ng/g	0.05	6.18	0.3	0.76	0.43	0.92	0.25	1	0.01	Northern Norway. 2014	Gómez-Ramírez et al. 2017 [42]
Eurasian eagle (n=5)	Liver	ng/g (ww)	1.05	296	0.18	1.22	5.15	9.1	8.41	8.71	5.25	Korea, 2010-11	Barghi et al. 2018 [64]
Common kestrel (n=4)	Liver	ng/g (ww)	0.85	168	0.11	1.15	2.38	7.17	5.16	2.72	2.21	Korea, 2010-11	Barghi et al. 2018 [64]
Collared scops owl (n=6)	Liver	ng/g (ww)	0.33	985	0.06	0.94	2.94	6.36	5.44	3.77	2.37	Korea, 2010-11	Barghi et al. 2018 [64]
Black-tailed gull (n=8)	Liver	ng/g (ww)	0.34	475	0.17	2.13	2.97	8.27	3.15	5.37	1.19	Korea, 2010-11	Barghi et al. 2018 [64]
Brown hawk owl (n=9)	Liver	ng/g (ww)	0.19	446	0.31	0.72	2.21	2.03	1.73	2.28	1.2	Korea, 2010-11	Barghi et al. 2018 [64]
Northern goshawk (n=6)	Liver	ng/g (ww)	1.02	710	0.18	1.68	1.39	3.65	2.35	2.34	2.15	Korea, 2010-11	Barghi et al. 2018 [64]
Cinereous vulture (n=7)	Liver	ng/g (ww)	0.21	75.1	nd	0.32	0.56	0.86	0.59	0.42	0.27	Korea, 2010-11	Barghi et al. 2018 [64]
Common buzzard (n=7)	Liver	ng/g (ww)	0.41	97.3	0.15	0.97	1.59	3.83	2.42	3.12	2.76	Korea, 2010-11	Barghi et al. 2018 [64]
Spit-billed duck (n=6)	Liver	ng/g (ww)	2.67	302	nd	2.28	4.56	3.83	6.54	4.31	3.36	Korea, 2010-11	Barghi et al. 2018 [64]
Oriental turtle dove (n=11)	Liver	ng/g (ww)	0.15	103	0.58	0.44	0.5	nd	nd	nd	nd	Korea, 2010-11	Barghi et al. 2018 [64]
Peregrine falcon (n=41)	Eggs	ng/g (dw)	2.07	290	nd	15.7	12.9	39.1	16.5	7.39	0.86	South Greenland, 1986-2014	Vorkamp et al. 2019 [75]
Little egret (n=20)	Egg yolk	ng/g (ww)	2.3[a]	185.4[a]	1.7[a]	25.4[a]	43.6[a]	95.1[a]	19.5[a]	-	-	Korea, 2006	Yoo et al. 2008 [76]
Little ringed plover (n=17)	Egg yolk	ng/g (ww)	2.3[a]	215.1[a]	8.4[a]	51[a]	52.7[a]	153.9[a]	21.4[a]	-	-	Korea, 2006	Yoo et al. 2008 [76]
Parrot bill (n=7)	Egg yolk	ng/g (ww)	1.3[a]	314.1[a]	0.8[a]	40[a]	114.2[a]	201[a]	25.6[a]	-	-	Korea, 2006	Yoo et al. 2008 [76]
Swallow (n=10)	Liver	ng/g (ww)	17.8[e]	209[e]	(nd-1.52)	(nd-0.80)	nd	(nd-1.4)	nd	-	-	Michigan, US, 2014-15	Custer et al. 2019 [70]
Northern goshawk (n=2)	Liver	ng/g (ww)	nd	22.6[a]	1.41	4.28[a]	1.6[a]	3.79[a]	2.8[a]	-	2.36[a]	Japan, 2007	Guruge et al. 2011 [60]

a arithmetic mean; b range of means; c range of medians; d not reported; e geometric mean; f pooled individuals

Species	Matrix	Unit	PFHxS	PFOS	PFOA	PFNA	PFDA	PFUnDA	PFDoDA	PFTrDA	PFTeDA	Location, year	Study
Rural owl (n=1)	Liver	ng/g (ww)	nd	34.1	1.7	7.9	2.4	12.1	10.2	-	9.27	Japan, 2007	Guruge et al. 2011 [60]
Common kestrel (n=1)	Liver	ng/g (ww)	nd	31.4	1.81	7.53	3.94	9.73	7.13	-	3.65	Japan, 2007	Guruge et al. 2011 [60]
Japanese sparrowhawk (n=1)	Liver	ng/g (ww)	nd	210	1.12	44.4	18.4	40.5	21	-	10.1	Japan. 2007	Guruge et al. 2011 [60]
Mallard (n=1)	Liver	ng/g (ww)	nd	6.6	nd	0.78	0.25	0.44	nd	-	nd	Japan, 2007	Guruge et al. 2011 [60]
Northern Goshawk (n=4)	Liver	ng/g (ww)	nd	20[a]	0.77[a]	8.14[a]	3.25[a]	9.82[a]	8.28[a]	-	9.5[a]	Japan, 2008	Guruge et al. 2011 [60]
Brown hawk owl (n=1)	Liver	ng/g (ww)	nd	19.3	nd	1.89	0.78	2.56	1.95	-	2.13	Japan, 2008	Guruge et al. 2011 [60]
Eurasian sparrowhawk (n=2)	Liver	ng/g (ww)	nd	19.7[a]	2.18[a]	16.4[a]	4.92[a]	17.6[a]	12[a]	-	14.8[a]	Japan, 2008	Guruge et al. 2011 [60]
Great egret (n=1)	Liver	ng/g (ww)	nd	113	0.34	4.89	4.26	17.3	10.3	-	7.71	Japan, 2008	Guruge et al. 2011 [60]
Cattle egret (n=1)	Liver	ng/g (ww)	nd	24	0.54	0.94	1.39	6.59	4.98	-	2.6	Japan, 2008	Guruge et al. 2011 [60]
Barn owl (n=13)	Tail feathers	ng/g (ww)	<1.9	15.8	37.1	nd	nd	nd	nd	-[d]	-[d]	Belgium, 2008-09	Jaspers et al. 2013 [61]
Barn owl (n=15	Muscle	ng/g (ww)	<7.6	135.2	<13.3	nd	nd	nd	nd	-[d]	-[d]	Belgium, 2008-09	Jaspers et al. 2013 [61]
Barn owl (n=13)	Liver	ng/g (ww)	21	304.5	<16.2	nd	nd	nd	nd	-[d]	-[d]	Belgium, 2008-09	Jaspers et al. 2013 [61]
Barn owl (n=5)	Preen oil	ng/g (ww)	32.1	431.2	21.5	nd	nd	nd	nd	-[d]	-[d]	Belgium, 2008-09	Jaspers et al. 2013 [61]
Barn owl (n=7)	Adipose tissue	ng/g (ww)	<0.6	202.7	<2.3	nd	nd	nd	nd	-[d]	-[d]	Belgium, 2008-09	Jaspers et al. 2013 [61]
Cormorant (n=5)	Liver	ng/g (ww)	(<0.06-1.5)	(35-238)	(0.64-7.3)	-	-	-	(8.4-28)	-	-	Japan	Senthilkumar 2007 [72]
Eagle (n=2)	Liver	ng/g (ww)	(0.01-0.40)	(25-61)	(1.1-3.0)	-	-	-	(3.7 - 6.1)	-	-	Japan	Senthilkumar 2007 [72]
Large-bill crow (n=2)	Liver	ng/g (ww)	(<0.06-0.10)	(0.15-13)	(nd-0.60)	-	-	-	(<0.03-0.10)	-	-	Japan	Senthilkumar 2007 [72]
Cormorant (n=9)	Eggs	ng/g (ww)	(1.53-8.85)[b]	(76.8-381)[b]	(0.818-15.1)[b]	(2.64-13.7)[b]	(8.29-17.9)[b]	(6.01-5.97)[b]	(7.39-11.4)[b]	-	-	San Francisco, US, 2012	Sedlak 2017 [77]

a arithmetic mean; b range of means; c range of medians; d not reported; e geometric mean; f pooled individuals

Species	Matrix	Unit	PFHxS	PFOS	PFOA	PFNA	PFDA	PFUnDA	PFDoDA	PFTrDA	PFTeDA	Location, year	Study
Black-legged kittiwake (n=10)	Liver	ng/g (ww)	-	(1.19 - 19.97)	nd	-	-	-	-	-	-	Arctic, 1998	Tomy et al. 2004 [45]
Glaucous gull (n=15)	Liver	ng/g (ww)	-	20.2[a]	0.14[a]	-	-	-	-	-	-	Arctic, 1998	Tomy et al. 2004 [45]
Common loon (n=5)	Liver	ng/g (ww)	-	20[a]	nd	nd	nd	1.3[a]	nd	0.88[a]	nd	Canada, 1992	Martin et al. 2004 [55]
Northern fulmar (n=5)	Liver	ng/g (ww)	-	1.3[a]	nd	nd	nd	nd	nd	nd	nd	Canadian arctic, 1992	Martin et al. 2004 [55]
Peregrine falcon (n=10)	Eggs	ng/g (ww)	0.8[a]	83[a]	nd	1.6[a]	3.1[a]	4.2[a]	3.2[a]	7.3[a]	2.7[a]	Sweden, 2006	Holmström et al. 2010 [66]
Black guillemot (n=5)[f]	Liver	ng/g (ww)	nd	(13-16)[f]	nd	-	-	-	-	-	-	Greenland, 2000-02	Bossi et al. 2005 [78]
Fulmar (n=9)[f]	Liver	ng/g (ww)	nd	(19-24)[f]	nd	-	-	-	-	-	-	Faroe Islands, 1998-99	Bossi et al. 2005 [78]
Bald eagle (n=7)	Liver	ng/g (ww)	nd	(26.5-1740)	nd	-	-	-	-	-	-	Michigan US, 2000	Kannan et al. 2005 [79]
Sea gull (n=22)	Liver	ng/g (ww)	<7.5	(40 - 230)[b]	<19	-	-	-	-	-	-	Japan, 1998	Kannan et al. 2002 [40]
Spot-billed duck (n=1)	Liver	ng/g (ww)	<7.5	160	<19	-	-	-	-	-	-	Japan, 1998	Kannan et al. 2002 [40]
Black-headed gull (n=1)	Liver	ng/g (ww)	<7.5	<19	21	-	-	-	-	-	-	Japan, 1998	Kannan et al. 2002 [40]
Black-eared kite (n=2)	Liver	ng/g (ww)	(<7.5 - 34)	(180 - 459)	(<19-21)	-	-	-	-	-	-	Japan, 1999	Kannan et al. 2002 [40]
Gray heron (n=2)	Liver	ng/g (ww)	<7.5	50	<19	-	-	-	-	-	-	Japan, 1997-98	Kannan et al. 2002 [40]
Common cormorant (n=10)	Liver	ng/g (ww)	<7.5	(385 - 390)[b]	<19	-	-	-	-	-	-	Japan, 1999	Kannan et al. 2002 [40]
Bar-tailed godwit (n=3)	Liver	ng/g (ww)	nd	148[a]	nd	-	-	-	-	-	-	Korea. 1993	Kannan et al. 2002 [40]
Black-headed gull (n=5)	Liver	ng/g (ww)	nd	(292 - 296)[b]	nd	-	-	-	-	-	-	Korea, 1994	Kannan et al. 2002 [40]
Black-tailed gull (n=9)	Liver	ng/g (ww)	nd	(71-112)[b]	nd	-	-	-	-	-	-	Korea, 1993-97	Kannan et al. 2002 [40]
Common gull (n=3)	Liver	ng/g (ww)	nd	(28 - 63)	nd	-	-	-	-	-	-	Korea, 1993-94	Kannan et al. 2002 [40]

a arithmetic mean; b range of means; c range of medians; d not reported; e geometric mean; f pooled individuals

Species	Matrix	Unit	PFHxS	PFOS	PFOA	PFNA	PFDA	PFUnDA	PFDoDA	PFTrDA	PFTeDA	Location, year	Study
Common tern (n=2)	Liver	ng/g (ww)	nd	(<10-11.2)	nd	-	-	-	-	-	-	Korea, 1993	Kannan et al. 2002 [40]
Great knot (n=1)	Liver	ng/g (ww)	nd	13.5	nd	-	-	-	-	-	-	Korea, 1993	Kannan et al. 2002 [40]
Greenshank (n=3)	Liver	ng/g (ww)	nd	(13.8 - 112)	nd	-	-	-	-	-	-	Korea, 1993	Kannan et al. 2002 [40]
Herring gull (n=10)	Liver	ng/g (ww)	nd	49.6[a]	nd	-	-	-	-	-	-	Korea, 1993	Kannan et al. 2002 [40]
Sanderling (n=2)	Liver	ng/g (ww)	nd	(21-112)	nd	-	-	-	-	-	-	Korea, 1994	Kannan et al. 2002 [40]
Little egret (n=4)	Liver	ng/g (ww)	nd	24.8[a]	nd	-	-	-	-	-	-	Korea, 1994	Kannan et al. 2002 [40]
Cormorant (n=12)	Liver	ng/g (ww)	<7	(32 - 150)	(29 - 450)	-	-	-	-	-	-	Medierranian sea, 1997	Kannan et al. 2002 [80]
White-tailed sea eagle (n=44)	Liver	ng/g (ww)	nd	(<3.9 - 127)	nd	-	-	-	-	-	-	Germany, Poland, 1979-99	Kannan et al. 2002 [80]
Common merganser (n=20)	Liver	ng/g (ww)	nd	409	nd	-	-	-	-	-	-	New York, 1994-2000	Sinclair et al. 2006 [81]
Hooded merganser (n=2)	Liver	ng/g (ww)	nd	26	nd	-	-	-	-	-	-	New York, 1994-2000	Sinclair et al. 2006 [81]
Bufflehead (n=3)	Liver	ng/g (ww)	nd	550	nd	-	-	-	-	-	-	New York, 1994-2000	Sinclair et al. 2006 [81]
Mallard (n=31)	Liver	ng/g (ww)	nd	130	nd	-	-	-	-	-	-	New York, 1994-2000	Sinclair et al. 2006 [81]
Surf scoter (n=1)	Liver	ng/g (ww)	nd	28	nd	-	-	-	-	-	-	New York, 1994-2000	Sinclair et al. 2006 [81]
Black duck (n=1)	Liver	ng/g (ww)	nd	204	nd	-	-	-	-	-	-	New York, 1994-2000	Sinclair et al. 2006 [81]
Common goldeneye (n=20)	Liver	ng/g (ww)	nd	176	nd	-	-	-	-	-	-	New York, 1994-2000	Sinclair et al. 2006 [81]
Greater scaup (n=2)	Liver	ng/g (ww)	nd	79	nd	-	-	-	-	-	-	New York, 1994-2000	Sinclair et al. 2006 [81]
Lesser scaup (n=6)	Liver	ng/g (ww)	nd	131	nd	-	-	-	-	-	-	New York, 1994-2000	Sinclair et al. 2006 [81]

a arithmetic mean; b range of means; c range of medians; d not reported; e geometric mean; f pooled individuals

2.1.5. PFAS distribution in blood

Studies indicate that PFASs mainly accumulate in the plasma fraction of blood and not in the cellular fraction [82]. Data on PFASs in red blood cells of wildlife are therefore lacking. PFSAs and PFCAs are often described as "proteinophillic"[83], and are primarily found in the serum fraction of blood, associated with albumin [82, 84]. A plasma/serum to whole-blood ratio (P/WB) of 2 has often been used for PFOS and PFOA when comparing results from these matrices [73, 85].

Since PFASs have surfactant properties, they may distribute to lipid-water interfaces, and onto biological membranes [86]. Kärrmann et al. calculated mean P/WB for PFOS, PFOA, PFHxA and PFNA to 1.2, 1.4, 1.2, and 1.1 respectively, indicating that most of the compound is distributed in plasma, but a partial distribution to cellular fractions can not be ruled out [87]. Interestingly, Kärrmann et al. found that the P/WB of PFOSA was lower (0.2) than PFOS and PFOA, suggesting that the perfluorooctane sulfonamide has a different distribution than the PFAAs in blood [87]. A preference to whole-blood for PFOSA was also reported by Hanssen et al. in their study assessing PFASs in whole-blood and plasma in maternal and umbilical cord blood [88]. A study by Garcia et al. on cellular accumulation and lipid binding of PFASs showed that PFOS will bind to lung epithelial cells and adipocytes, but this binding was decreased in the presence of plasma [86]. In the same study, PFOA cell-accumulation was measurable but low, and the short chained PFBS and PFHxA did not show accumulation. These studies combined illustrate that distribution of PFASs in blood is compound dependent and not fully understood.

2.2. Study populations

There are multiple purposes for monitoring pollutants in birds, including measuring contaminant levels, assessing biological effects, investigating bioaccumulation of environmental contaminants and assessing the hazards to ecosystems as well as the human population [89, 90]. Birds have historically provided early warning signs of pollution [91], such as the well-known revelation of the damaging effects of the household pesticide dichlorodiphenyl-trichloroethane (DDT) on birds of prey, which lead to observed population declines worldwide during the 1960-70s [89, 92]. Migratory birds of the East Asian-Australasian Flyway are currently experiencing major population declines as they are subjected to multiple threats such as habitat disturbance, pollution of coastal wetlands and climate change [17, 93]. In their trans-equatorial flight, the birds make stops along some of the most polluted marine areas of the world, such as the Yellow Sea. In addition, birds may be exposed to contaminants at their non-breeding sites where they recover from the intense migration and prepare for the next [93, 94]. As the role of pollutant exposure in these birds has not been explored, measuring their contaminant levels may contribute to important insights for their conservation.

In their travels to a variety of environments, migratory birds are exposed to different ecosystems, each with a unique composition of environmental contaminants. Their non-breeding sites are important, as this is where the birds accumulate energy for their next flight. Migrating shorebirds in Australia may increase their body weight by 70-80% before migration [95], by storing mainly fat. Shorebirds are primarily exposed to environmental contaminants through their foraging in marine sediments [91]. If their diet is contaminated, the shorebirds will rapidly be exposed to contaminants before their migration, with potentially adverse effect on their migratory performance. In addition, stored pollutants may be re-released to the blood stream during the high intensity migration as energy reserves are used.

2.2.1. Curlew sandpipiper

The curlew sandpiper (*Calidris ferruginea*) (Figure 2.2a) is a medium to small sized Arctic-breeding shorebird, nesting from June-July on the tundra of Siberia, before migrating southwards to Africa, South Asia and Australia [96, 97]. At their non-breeding grounds in Australia the birds are often found foraging on intertidal mudflats in large mixed flocks together with red-necked stints [96, 98]. Curlew sandpipers preferably feed on small marine invertebrates on exposed mudflats [97, 99]. Curlew sandpipers are listed as *Vulnerable* in the International Union for Conservation of Nature (IUCN) *Red List of Threatened Species* [100]. The population decline of the curlew sandpiper is estimated to be 80% since the 1980s [93]. The species was listed as *critically endangered* under the Australian government's

Environment Protection and Biodiversity Conservation Act (EPBC) act in 2015 [18].

2.2.2. Red-necked stint

The red-necked stint (*Calidris ruficolis*) (Figure 2.2b) is small sized but one of the most abundant migratory birds in Australia with an estimated population of 270 000 in 2007 [96, 101]. Nesting occurs on the Siberian tundra or in Alaska in May-July, before southwards migration with stop-over sites on muddy shorelines along the Yellow Sea [102]. After arriving in Australia late August through November, they are found foraging on intertidal mudflats, sandy beaches, lagoons and estuaries, often in dense flocks [96, 102]. The red-necked stint is omnivorous with a diet consisting of insects, small vertebrates, gastropods, crustaceans, mollusks, plants and seeds [102]. The population is estimated to have declined 29% in Australia and New-Zealand over three generations, and the species is listed as *Near Threatened* on the IUCN *Red List* [103].

2.2.3. Ruddy turnstone

The ruddy turnstone (*Arenaria interpres*) (Figure 2.2c) got its name from its distinct foraging behavior using its strong bill to turn stones and seaweed, collecting feed such as small crustaceans, insects, mollusks, and sometimes small fish and eggs [97, 104]. In the non-breeding season, these medium sized birds are found in small groups on rocky and sometimes sandy coasts [97, 105]. Breeding occurs in high arctic tundra and non-breeding sites can be found in Europe, South Asia, Australasia and South America [96]. The global population is regarded as decreasing, but the species is assessed *Least Concern* on the IUCN *Red List* [104].

a) **b)** **c)**

Figure 2.2.: **a)** Curlew sandpiper (*Calidris ferruginea*), winter adult by JJ Harrison, licensed under CC BY-SA 3.0 (https://creativecommons.org/licenses/by-sa/3.0). **b)** Red-necked stint (*Calidris ruficollis*) - Marion Bay, by JJ Harrison, licensed under CC BY-SA 3.0. **c)** Ruddy turnstone (*Arenaria interpres*), by Arnstein Rønning.

2.3. Analysis of organic pollutants

Organic pollutants can be present in minuscule concentrations in biological and environmental samples that otherwise contain high levels of a variety of molecules that are not of interest [106]. In order to detect and quantify such target analytes, sufficient methods of separation and detection are required. Liquid chromatography tandem mass spectrometry (LC-MS/MS) is widely used for this purpose, providing high resolution, specificity and sensitivity [107]. A major issue when analyzing trace organics in biological matrices is co-elution of endogenous matrix components, which is described further in Chapter 2.3.4. Matrix effects cause problems in quantification and affect the overall sensitivity, reproducibility and accuracy of analysis [108]. Adequate sample preparation steps are therefore necessary in order to isolate target analytes from the interfering matrix.

2.3.1. Sample preparation

Sample preparation steps are necessary for nearly all organic analysis [109]. The sample preparation process can include extraction, solvent exchange, concentration and clean-up. The purpose of this is to transfer target analytes from the bulk matrix into a known solvent matrix, with minimal co-extraction of interfering compounds [106]. The components of the sample extracts are further separated by chromatography. The ideal sample preparation process isolates target analytes completely from matrix components using minimal steps, avoiding contamination from laboratory personnel and equipment [110, 111]. The major components in biological samples causing matrix effects and reduced instrument performance in LC-MS/MS analysis are proteins and phospholipids. Sample preparation is important to remove these components prior to analysis.

Solid-phase extraction

Solid-phase extraction (SPE) is a sample preparation technique applicable in extraction, clean-up, solvent exchange and pre-concentration procedures [112]. A sample in liquid or dissolved form is applied to a solid phase by passing the liquid through a cartridge pre-packed with a sorbent material [109]. Depending on their relative affinity to the solid phase and solvent, components are either retained or eluted. Isolation of analytes can happen in either of two ways; by retaining impurities while analytes elute, or by adsorption of analytes and elution of impurities [113].

A general procedure for SPE consists of washing and conditioning the cartridge before loading the sample. This solvates the sorbent material and washes out potential impurities left in manufacture [106]. When compounds of interest are

retained, impurities can be washed out with a suitable solvent. Analytes are recovered by passing through a solvent favoring elution of these compounds. Vacuum is often applied to mediate flow through the cartridge [106].

The sorbent material is important since it changes the selectivity and efficiency of the method. The choice of sorbent depends on the physiochemical properties of the analytes, as well as the nature of the sample matrix [114]. Common sorbent materials are silica, carbon, and polymeric based with chemically bonded phases [114]. Silica has conventionally been modified with octyl (C8), octadecyl (C18), phenyl, cyano (CN), amino, cyclohexyl and ion-exchange phases [106, 115]. Interactions between the sorbent and retained molecules may be of hydrophobic, polar or electrostatic kind, depending on the type of sorbent [115]. In mixed mode sorbents, multiple modes of interactions are occurring between the solutes and stationary phase [116]. Mixed mode ion exchange sorbents in particular combines ion exchange and reverse phase interactions and can be used to remove phospholipids from biological matrices [117].

Protein precipitation

Protein precipitation (PPT) is a simple sample preparation step used before the analysis of biological matrices with LC-MS/MS [118]. Contact with the mobile phase in LC-MS/MS may leave proteins to precipitate in the analytical column, thereby reducing performance [119]. Removing proteins with sample preparation is therefore preferable. The procedure involves the addition of a precipitating agent which induces protein aggregation. Precipitates are removed by centrifugation, and the supernatant is used for further analysis. Precipitating agents can be organic solvents (e.g. methanol, acetonitrile), salts, acids and metal ions [119, 120]. Water miscible organic solvents decrease the solubility of proteins by facilitating electrostatic protein interactions leading to protein aggregation [120, 121]. PPT is simple and inexpensive but leads to a high degree of matrix effects compared to SPE [108, 122]. Major matrix components such as phospholipids remain in the sample and interfere with the subsequent LC-MS/MS analysis, causing variability in analyte signal [108, 117, 122]. Because of this, protein precipitation is used in combination with other extraction and clean-up steps.

Hybrid-SPE

Hybrid-SPE combines protein precipitation and solid-phase extraction with the aim of removing interfering matrix components, specifically phospholipids, from biological matrices [123]. Endogenous proteins are removed by the addition of a precipitating agent and phospholipids are subsequently removed using a zirconia-coated silica sorbent following the principles of solid phase extraction [111, 123].

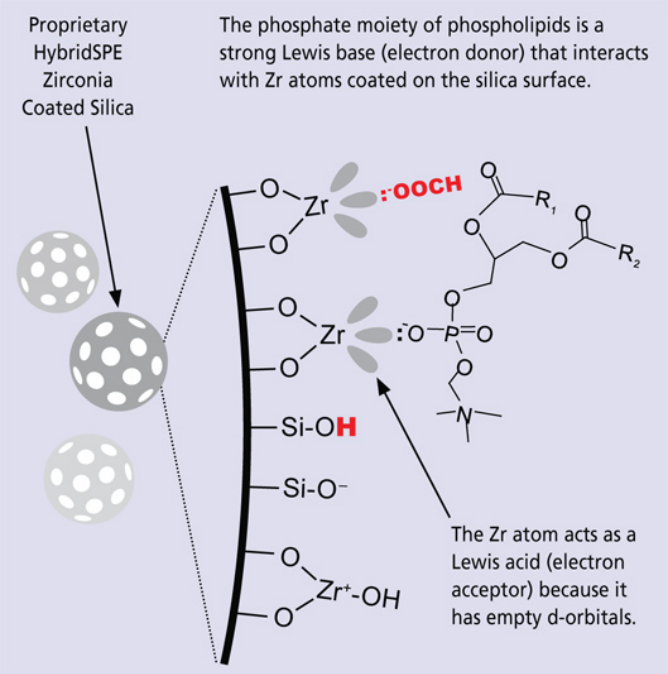

Figure 2.3.: Hybrid-SPE interactions between phospholipids and zirconia. Illustration by Sigma-Aldrich [125].

PPT and SPE can either be performed separately, by the transfer of PPT-supernatant to a Hybrid-SPE cartridge or 96-well plate, or combined by using in-well precipitation 96-well plates [123].

The interaction between zirconia and phospholipids is illustrated in Figure 2.3. Phospholipids are selectively retained on the Hybrid-SPE solid phase. This is because phospholipids contain a phosphate group that binds to zirconia through Lewis acid-base interaction [122]. The solid phase remains non-selective towards a range of other compounds [122]. Hence, interfering compounds are retained, while analytes of interest elute. The eluent can be directly transferred to LC-MS/MS analysis [124]. Interactions between target organic acids and the solid phase is avoided by the addition of formate ions to the sample [123]. Formate ions are weak Lewis bases that occupy the zirconia, thus reducing retention of sample analytes.

Hybrid-SPE is mainly used in pharmaceutical applications [123, 126], but has recently been applied in extraction of environmental pollutants such as bisphenols and PFASs from human plasma [21, 127]. The technique is especially effective in extractions from plasma samples, as plasma/serum contains high levels of phospholipids that will interfere in LC-MS/MS analysis [122]. With Hybrid-SPE, phos-

pholipids can effectively be removed from plasma by means of rapid preparation with little solvent consumption [108, 127].

Ultrasound assisted extraction

Ultrasound assisted extraction (UAE), referred to as ultrasonication, is used to accelerate the mass transfer of analytes from various solid matrices to solvents [128]. When ultrasound propagates through a sample of solids in a liquid solution, small vacuum bubbles (cavities) are formed by the expansion and compression of the liquid. The rupture of cavities releases mechanical energy in the form of high energy shock waves, which propagate through the media and disrupts tissues and thus enhancing the mass transfer of analytes to solution [128–130]. The technique is widely applied in extractions of natural products and can also be applied in environmental analysis in extraction of trace organics in sediments, soil and biological matrices [128, 131].

2.3.2. Liquid chromatography

Liquid chromatography is a widely used separation technique applied in analysis of a wide range of non-volatile and thermic labile compounds from low to high molecular weight [132]. The purpose of chromatographic separation is to effectively separate compounds in a mixture in order to identify and quantify analytes of interest [109].

Chromatographic separation is obtained by injecting a sample into a liquid mobile phase (MF) that flows through a column packed with a solid or liquid-coated solid material, the stationary phase (SF) [133]. Compounds distribute differently between the two phases depending on their physiochemical properties. Separation occurs when the time spent to migrate through the system to the detector (retention time) differs. Interactions with the stationary phase lead to retardation, resulting in longer retention times, while compounds having greater affinity to the mobile phase have shorter retention times [109].

The chromatographic efficiency can be measured by the resolution, meaning the degree of separation between analyte peaks [109]. With ultra performance liquid chromatography (UPLC) a very high resolution, sensitivity and accuracy is obtained by utilizing very small particles ($<2\,\mu m$) in the packing material [109].

2.3.3. Liquid chromatography mass spectrometry

Liquid chromatography mass spectrometry (LC/MS) combines the separation of compounds based on their physiochemical properties in LC with separation according to mass in MS. This allows for a precise quantification and identification of

compounds that otherwise co-elute in the chromatographic method [134]. Liquid chromatography tandem mass spectrometry (LC-MS/MS), using an atmospheric pressure ionization source, such as electrospray ionization (ESI), has become the method of choice when analyzing bio-molecules, pharmaceuticals and environmental contaminants like PFASs in complex matrices [31, 107].

Mass spectrometry

A mass spectrometer separates molecules and atoms according to their mass-to-charge ratio, m/z. Sample components can only be separated by mass in ion form as the mass analyzer operates by controlling the velocity and direction of ions by the application of an electric field and magnetic force [135]. The three major components of a mass spectrometer are the ion source, which ensures the ionization of sample components into gas phase ions, the mass analyzer, which separates ions based on their m/z, and the detector, which measures and amplifies the ion-current that reaches it [133, 135]. The ion source also works as the LC/MS interface, producing ions from non-volatile and thermally labile compounds as well as removing the mobile phase [109, 136, 137].

Electrospray ionization

Electrospray ionization (ESI) is commonly the ion source of choice when coupling UPLC and HPLC to MS, allowing high sensitivity and analysis of a wide range of compounds [138]. ESI is a soft ionization technique producing little to no fragmentation of the molecular ion [133]. It is therefore applicable when analyzing proteins, identifying and elucidating structures of compounds in complex mixtures and more [135].

The ESI process involves passing the LC eluent through a metal capillary tube with an applied electric field at atmospheric pressure [136, 138]. By imposing a potential difference of 3-6 kV between the capillary tip and a counter electrode, an accumulation of charge in the liquid occurs, creating highly charged Taylor cone-shaped droplets emerging from the tip of the capillary [133, 138]. Droplets decrease rapidly in size by evaporation of the solvent while ions are retained [137]. Thus, the mobile phase used in the chromatographic separation must be volatile. The evaporation process is aided by an inert drying gas, usually nitrogen [133].

Reducing the droplet size further increases repulsive forces between charges at the droplet surface, eventually leading to electrohydrodynamic disintegration of the droplets to even smaller sizes [137, 139]. The formation of gas-phase ions from droplets are not fully understood, but can be explained either by the size reduction reaching a point in which the surface charge is high enough for ion evaporation from the droplets (ion-evaporation model), or by repeating the electrohydrodynamic

disintegration and evaporation until only a single analyte ion is left (charge-residual model) [134].

Electrochemical processes also play a role in ion production. ESI is operated in either positive or negative mode depending on the charge of the analyte. Cations are analyzed in positive mode and anions are analyzed in negative mode [135]. When anions are analyzed, negative ions will migrate towards the counter electrode and a positive charge is supplied in the capillary by the reduction of the solvent or sample. Additional ions are produced by reduction in negative mode and by oxidation in positive mode [138].

Many parameters affect the electrospray ionization process, including the nature of the analyte, electrolytes and presence of other analytes [138]. ESI is particularly sensitive to analyte signal suppression caused by co-eluting analytes competing for charge [133].

Mass analyzers

The purpose of a mass analyzer is to separate the gas-phase ions based on their m/z before reaching the detector [133]. A range of mass analyzers exist, differing in the way electric and magnetic fields are used to obtain ion separation [138].

The quadrupole mass analyzer (Q) consists of four parallel rods arranged symmetrically, with each pair of opposite rods being connected. A combination of direct-current (dc) and a radio frequency (RF) potential is applied to the rods, with the two pairs having the same magnitude but opposite sign of potential [133]. The path of ions traveling through the quadruple is influenced by a dc/RF oscillating field. For a given combination of dc and RF potential and frequencies, only ions within a particular m/z-range will have a stable path through the quadrupole. Ions outside of this m/z-range will have unstable paths and collide with the rods before ever reaching a detector. Thus, controlling the dc/RF field makes it possible to select ions of a certain mass-to-charge range to be detected. [133, 135, 136]. By changing the dc and RF potential, but keeping their ratio constant, a mass spectrum can be obtained [135]. The quadrupole can operate in a scanning mode by successively transmitting ions of different masses along a time scale, or in selected-ion monitoring (SIM), in which only ions of a few selected ions are transmitted and recorded repeatedly [135, 138].

Tandem mass spectrometry

Tandem mass spectrometry (MS/MS) is performed by combining two mass analyzers allowing multiple stages of scanning and mass selection [133]. By combining two mass analyzers with a collision cell, high sensitivity is reached [133, 136].

The triple quadrupole (QqQ) is widely used in analysis of molecules present in

low concentration in complex mixtures [133]. Three quadrupoles are coupled in in space. The first and third quadrupoles (Q1,Q3) operates as mass analyzers as described above. The middle quadrupole (q2) operates as a reaction chamber, commonly referred to as a collision cell, in which all ions can pass through but are subjected to activation in the form of reaction or fragmentation [135, 136]. A two-step mass filtering is obtained by selecting a precursor ion in the first mass analyzer, which undergoes fragmentation in the collision cell (q2), before the product ion(s) are analyzed in the second mass analyzer (Q3) [133].

As the two mass analyzers can operate either in scanning mode or selected-ion monitoring, there are four common scan modes used. In a *product ion* scan only selected precursor ions are transmitted from Q1 to the collision cell. Fragmentation information of the precursor ion is obtained by scanning all product ions in Q3 [136]. A *precursor ion* scan is used to detect all ions that fragment to a selected common product ion [138]. This is done by selecting ions of a certain m/z in Q3, while scanning all ions through Q1 [135]. The *neutral loss* scan mode is also used to detect molecules with a common fragmentation product. Both mass analyzers operate in scan mode, but with a constant offset of mass between the two [138]. Ions are only detected if they lose a common neutral product [136].

The most specific scan mode is *selected-reaction monitoring* (SRM), which is most commonly used in LC-MS/MS techniques where trace compounds are analyzed in complex matrices [133, 136]. When the fragmentation pattern of the analyte is known, Q1 and Q3 are both set to select a specific precursor and product ion pair, further referred to as a transition [136]. In this way, only ions of a specific m/z producing a characteristic fragment are detected, thus obtaining high selectivity [138]. The term *multiple-reaction monitoring* (MRM) is used when the SRM monitors multiple fragmentation reactions [135].

2.3.4. Matrix effects

Although LC-MS/MS is a highly suitable method for analyzing complex matrices, one should pay attention to matrix effects as the electrospray ionization technique is susceptible to such effects impacting accuracy, precision and reproducibility of analysis [108]. Matrix effects result in the same amount of analyte having different signal responses when analyzed in the sample matrix and in pure solution [117]. This leaves uncertainties in quantification, if the sample analyte signal is compared to those in a calibration mixture of a different matrix. In addition to this, matrix effects can cause shifts in retention times, elevated baselines, and impaired sensitivity [108].

Compounds that co-elute with analytes will also be present during the ionization process in the LC-MS interface. Suppression or enhancement of the analyte signal occurs by matrix components influencing the ionization of analytes, thus altering

the amount of charged analyte reaching the mass analyzer [140]. A mechanism to explain this phenomenon is through competition between co-eluting compounds and analyte with regards to ionization, droplet formation or the formation of gas-phase ions in the ESI-source [117, 141, 142].

Matrix effects can be caused by endogenous sample matrix components, mobile phase additives, buffers, salts and other compounds originating from sample work up and analysis [142, 143]. The degree of matrix effect is both analyte and sample matrix specific. Different analytes present in the sample are not equally affected by the matrix, and the same analyte may have varying matrix effects in similar sample matrices, such as in different blood samples [109, 117]. Phospholipids (PLs) are a major group of endogenous compounds causing matrix effects in bioanalysis [108]. Phospholipids are cell membrane constituents found in high levels in blood, plasma and other biological samples [144]. PLs cause matrix effects not only by signal disturbance, but can also adhere strongly to the chromatography columns, thus reducing column life-time as well as eluting in subsequent analysis [117]. This may further cause elevated baselines [108].

Eliminating and assessing matrix effects

Efforts should be made to both avoid the presence of interfering compounds as well as assessing to what degree matrix effects occur. As described in section 2.3.1, elimination of such compounds can be done with an adequate sample preparation technique. Sample dilution can also reduce matrix effects but may be troublesome in trace analysis [107].

Matrix effects can be assessed qualitatively by identifying chromatographic regions where co-eluting compounds affects analyte signal. This can be done using the post-column infusion method, where clean matrix extracts are analyzed with a constant analyte flow delivered between the column and detector [140]. Co-elution of strongly interfering compounds can thus be avoided by manipulating chromatographic conditions to facilitate better separation [117]. A quantitative measure of matrix effects can be obtained by comparing the response of a known amount of analyte spiked into the sample matrix to the response of the same analyte amount in pure solution [117, 140]. Calculations of matrix effects are further described in section 2.3.5. A widely used method for compensating matrix effects is the use of internal standards, which is further described in Chapter 2.3.5.

2.3.5. Quantification and quality control

The use of LC-MS/MS makes certain analyte confirmation possible by combining retention characteristics, mass and fragmentation patterns [139]. In this chapter, a series of parameters used to achieve confident identification and quantification are introduced in addition to quality control parameters. Sample preparation is often the major source of variability in measurements which makes quality assurance and quality control during this stage important [145].

Retention time and relative retention time

Chromatographic retention time (RT) of a compound is the time spent migrating through the column and is measured from injection to detection. Peak identification of analytes can be done comparing analyte retention times in samples to those of external standards analyzed with the same conditions [134]. In order to increase intralaboratory reproducibility, relative retention times (RRT) are used. The relative retention time is the analyte retention time, $\mathrm{RT_A}$, relative to the internal standard retention time, $\mathrm{RT_{IS}}$, [146, 147],

$$\mathrm{RRT} = \frac{\mathrm{RT_A}}{\mathrm{RT_{IS}}} \tag{2.1}$$

While retention times (RT) are dependent on chromatographic conditions like flow rates, relative retention times are not, thus providing a more reliable peak identification [146, 148]. Peak identification solely based on retention characteristics requires complete separation of the analyte as any co-eluting unknown compound could result in incorrect determination. Combining relative retention times with selected-reaction monitoring data from the MS detector allows for strong peak confirmation.

Ion ratio

Using selected reaction monitoring or multiple reaction monitoring, the most abundant ion of the transition is called a *quantifier ion* and is used in quantification. The other product ion is referred to as a *qualifier* or *confirmative ion* as it is used as an additional confirmation of analyte identity [149]. The ion ratio (IR%) can be used as a confirmation parameter for analytes and is expressed as

$$\mathrm{IR\%} = \left(\frac{A_{\mathrm{qualifier}}}{A_{\mathrm{quantifier}}}\right) \cdot 100\% \tag{2.2}$$

where, the peak areas A of ions are compared [150].

Relative response

Variations in instrument response and sample preparation efficiency can lead to analyte signal variations between different samples. A way of compensating for this is by using internal standards to express the relative response of the analyte [150]. The internal standard and target analyte are ideally subjected to equal variations. A relative response ratio (RR) is used, and expresses the relative signal response of the analyte and internal standard,

$$\mathrm{RR} = \frac{A_{\mathrm{A}}}{A_{\mathrm{IS}}}. \tag{2.3}$$

The relative response is further used in quantification of target analytes using the internal standard method described below.

Quantification

Analytes are generally quantified using a relationship between the detector signal and concentration of the analyte [151]. The *internal standard method* is one way of accomplishing this, while simultaneously compensating for analytical errors such as sample loss during extraction and matrix effects [133]. A known amount of internal standard (IS) is added to all samples as well as calibration mixtures of target analytes. The added amount is ideally in the same concentration range as target analytes in the sample [135]. A calibration curve is constructed for each target analyte expressing the ratio of peak areas for analytes and internal standards as a function of analyte concentration [109, 151]. In environmental LC-ESI/MS analysis with complex matrices and signal disturbance, matrix matched calibration with internal standards can be used to compensate for matrix effects [152].

A chemical must satisfy certain requirements in order to be used as an internal standard. Most importantly is that the internal standard is not naturally present in the sample, as the detector signal needs to originate solely from the added amount. In addition, the IS should behave similarly to the target analyte in a chromatographic system and in extraction, experiencing a similar degree of matrix effects and sample loss [133, 134]. Thus, the internal standard and target analyte should have similar physiochemical properties. In order to satisfy both requirements simultaneously, homologues, analogues, isomers and stable isotope labeled compounds are used [151]. When applying mass spectrometry, stable isotope analogues of the target analytes are the most ideal internal standards since they are structurally equivalent, but still differentiable by mass [135].

Accuracy of quantification is affected by the similarity between the internal standard and target analytes. When analyzing several compounds of interest in a mixture, multiple internal standards may be necessary as matrix effects and sample loss differ depending on the analyte [133, 140].

Limit of detection and quantification

The limit of detection (LOD) is the lowest amount of detectable analyte, meaning that the signal is confidently differentiated from noise. Noise is the change in detector response caused by drift, chemicals, electrical components and other variations in the system in absence of analyte [134]. Signals above the LOD are not necessarily quantifiable and a limit of quantification (LOQ) is used as the lowest concentration that can be quantified with high levels of accuracy and precision [135, 153]. Detection limits are usually determined using a signal-to-noise ratio, S/N, which is the analyte signal intensity relative to the noise level. In analysis of multiple analytes, the limit of detection and quantification are to be determined for each analyte individually. In this study LOD was determined as the concentration of analyte yielding S/N = 3. The limit of quantification was further determined as

$$\mathrm{LOQ} = 3 \cdot \mathrm{LOD} \tag{2.4}$$

which corresponds to a signal-to-noise ratio of nine.

Precision and accuracy

Assessing precision and accuracy of measurements is important when validating a method. The accuracy expresses the closeness between measurements and the true value and can be assessed when this is known. Precision is the closeness of repeated measurements and is assessed through analysis of replicates [145, 154, 155]. The precision is usually expressed through standard deviation (STD) or relative standard deviation (RSD%) [109, 154]. Standard deviation relates to the spread of measurements relative to the mean, $\bar{x}$, and is calculated as

$$\mathrm{STD} = \sqrt{\sum_i \frac{(x_i - \bar{x})^2}{n-1}} \tag{2.5}$$

where x_i is individual measurements x_1, x_2, ..., x_n, with n being the number of samples. (n-1) is the degree of freedom. The mean is calculated as the sum of all measurements divided by n.

The relative standard deviations (RSD%) expresses the percent of the STD relative to the mean,

$$\mathrm{RSD\%} = \left(\frac{\mathrm{STD}}{\bar{x}}\right) \cdot 100\% \tag{2.6}$$

The RSD% is usually the preferred measure of precision as it provides a clearer picture of the data variation, especially when comparing results [145, 156]

Repeatability and reproducibility are common ways of considering precision. The repeatability of a method expresses the variability of measurements made under the same conditions, meaning that results are obtained at a particular time, in the same laboratory, by the same operator using the same equipment [154]. The reproducibility expresses variability in measurements made under changing conditions and can express the interlaboratory precision [109].

Matrix effects

A quantitative measure of matrix effects can be assessed by the post-extraction addition method, where the response of analyte in a post-extraction spiked sample is compared to the response of analyte in a standard solvent [157]. A matrix factor (MF) can be calculated by the following equation;

$$\mathrm{MF} = \frac{\mathrm{A_{post-ext.spiked}} - \mathrm{A_{sample/blank}}}{\mathrm{A_{solvent}}}, \tag{2.7}$$

where $\mathrm{A_{post-ext.spiked}}$ is the peak area of analyte in a post-extraction spiked sample, further referred to as a matrix match sample. $\mathrm{A_{solvent}}$ is the peak area of the spiked amount in a standard solvent. The area of analyte in method blanks or naturally present in the sample, $\mathrm{A_{sample/blank}}$ is subtracted to ensure comparison based on equal amounts of analyte. A matrix factor normalized to internal standard lowers the variability in MF and can be obtained by substituting peak areas with analyte/internal standard peak ratio [158].

The matrix effect percentage (ME%) for each analyte can be expressed as

$$\mathrm{ME\%} = (\mathrm{MF} - 1) \cdot 100\%, \tag{2.8}$$

where MF is the matrix factor described in equation 2.7. Analytes with a high, negative ME% are subjected to a large degree of ion suppression, while positive ME%s indicate signal enhancement.

Recovery

When analytes in complex matrices are analyzed, the amount detected is usually lower than the original sample amount. This is due to sample loss, mainly during sample preparation and work-up [153]. Recovery calculations are used as a measure of sample preparation efficiency with regards to analyte recovery. By spiking the sample matrix with known amounts of analyte before and after the extraction procedure it is possible to obtain a measure of absolute and relative recoveries.

The absolute recovery (AR) of an analyte is calculated as

$$\mathrm{AR\%} = \left(\frac{\mathrm{A_{Ssp}} - \mathrm{A_{Sb/rb}}}{\mathrm{A_{Smm}} - \mathrm{A_{Sb/rb}}} \right) \cdot 100\% \tag{2.9}$$

where A_{Ssp} and A_{Smm} are the peak areas of analyte in samples spiked before and after extraction, respectively [159]. Peak area of analyte present naturally in the sample (A_{Sb}) or in blanks (A_{rb}) are subtracted to ensure a true comparison between only spiked amounts.

Relative recovery (RR) expresses the analyte recovery relative to a surrogate internal standard;

$$RR\,\% = \left(\frac{\frac{A_{Ssp} - A_{Sb}}{A_{ISsp}}}{\frac{A_{Smm} - A_{Sb}}{A_{ISmm}}} \right) \cdot 100\% \tag{2.10}$$

where A_{ISsp} and A_{ISmm} are the internal standard peak areas of a pre-extraction spiked sample and matrix match sample, respectively. Higher recovery values are obtained using RR [159, 160].

In literature, recoveries are at times calculated by comparing the pre-extraction spiked sample with analyte in a standard solution [157, 160]. These calculations measure the overall efficiency, but are not measures of the true recovery of extraction as they include matrix effects, which influences the peak area ratio [157]. Although the recovery and matrix effects are connected, they will be assessed separately using equations 2.7 - 2.10.

2.4. Statistics

A brief introduction to statistics applied in this thesis is described below.

2.4.1. Statistical tests

Observed differences in results obtained with different circumstances, i.e. mean toxicant concentrations in two populations, are either caused by the populations being different, or by random variations in the data. Significance tests are used to determine if differences in two results can be accounted for by random variation [145]. The choice of the statistical test depends on the distribution of data. Parametric tests assume a normal distribution, while non-parametric tests do not. To confirm normal distribution of data, a Shapiro-Wilk test can be applied. If data are confirmed normal, a Student's t-test is applied when comparing two groups, while one-way ANOVA can be used when comparing multiple groups. The non-parametric alternatives to these are the Mann-Whitney U-test and the Kruskal-Wallis test, respectively. Pairwise comparisons to identify where significance lies in a Kruskal-Wallis test can be done with a Dunn's post hoc test with Bonferroni correction [161].

2.4.2. Principal component analysis

When a data set consists of many variables it can be challenging to observe patterns and relationships. Principal component analysis, PCA, is a widely used multivariate mathematical technique to reduce the dimensions of data, while retaining trends [162, 163]. In PCA, the original variables, of which some are correlated, are transformed into non-correlating principal components (PCs), in which most of the data variation is retained. The principal components are linear combinations of the original variables [162]. The associated coefficients of original variables can be referred to as loadings. The first principal component (PC1 or Dim1) is the PC accounting for most data variation, and the second principal component (PC2 or Dim2) accounts for the second most variation [145].

In a PCA-biplot, data points (i.e. individual blood samples) are plotted in the dimensions of PC1 and PC2, together with loading plots of the original variables. The plot is interpreted by observing positions of data points and loadings. Clustering of points is indicative of similarities in some way. The position of loadings reflects the variable's influence on each PC. Using PCA, one can obtain further understanding of relationships and key variables in data [162]. Applying PCA on biological data can reveal differences between species, age-groups, sexes, locations etc. [145].

3. Methods and materials

3.1. Study population and sample collection

3.1.1. Sampling

Red blood cell (rbc) samples of curlew sandpipers (*Calidris ferruginea*), red-necked stints (*Calidris ruficollis*) and ruddy turnstones (*Arenaria interpres*) from 2013-2019 from different locations in Australia were obtained through collaborators at Deakin University (Victoria, Australia). Sampling occurred some time after migration return as well as later in the season. Blood was sampled from branchial or leg veins by using microvette capillaries. Blood samples were split into plasma and red blood cells (rbc). Red blood cells were freeze-stored at -20°C. From a larger collection of samples, 110 rbc samples were selected for this study. Information (sample ID, banding number, age, sample collection date and location) about each selected sample is presented in Table A.1.

The selection of samples was based on the available sample volumes as well as the collaborators' prioritization for analysis. In addition, samples were selected from a reduced number of locations to gain a sufficient number of samples per site.

3.1.2. Sampling sites

The sample sites are presented on the map in Figure 3.1. The number of samples from each year at different sample sites is given in Table 3.1- 3.2. Curlew sandpipers and red-necked stints were sampled at the Western Treatment Plant (WTP and WTP270S) on the coast of Port Phillip Bay and at Yallock Creek in Western Port Bay. The Western Treatment Plant is a biological wastewater treatment plant (WWTP) as well as an internationally recognized bird habitat [164]. Tens of thousands of birds are found at the site and over 200 species, including Australia residents and East Asia migrants, are recorded [165]. The two collection sites at this habitat, WTP and WTP 270S, were combined to represent the Western Treatment Plant location. Yallock Creek is located in Western Port Bay, which is a semi-enclosed bay in Victoria, also of great importance for aquatic birds [166]. The highest abundance of birds in Western Port Bay is found near Yallock Creek [166].

Ruddy turnstones were mainly sampled on the west coast of King Island; an island located in the Bass Strait between Australia and Tasmania. King Island is regarded as a relatively remote island with a human population of around 1500 [167]. Of the sample sites on King Island, Denby Bay is the most remote. Burges Bay is in vicinity of the largest township on the island. Central and North Manuka are 6-7 km away from the small regional airport on the island. A few ruddy turnstones were also sampled in rural areas of the mainland of South-Australia; Blackfellows Cave (2015) and Nene Valley (2016).

Location	**Year**	**Curlew sandpiper**	**Red-necked stint**
WTP	2013	4	4
	2014	4	4
	2016	-	4
	2017	-	3
	2018	4	-
Yallock Creek	2017	-	2
	2018	5	-
	2019	6	2

Table 3.1.: Number of samples per year at sampling sites of curlew sandpipers and red-necked stints.

	Ruddy turnstone					
Location	2014	2015	2016	2017	2018	2019
North Manuka	5	4	-	-	4	3
Central Manuka	4	4	5	4	3	4
Burges Bay	4	-	4	5	4	-
Denby Bay	-	4	-	-	-	-
Blackfellows Cave	-	5	-	-	-	-
Nene Valley	-	-	2	-	-	-

Table 3.2.: Number of samples each year at sampling sites of ruddy turnstones.

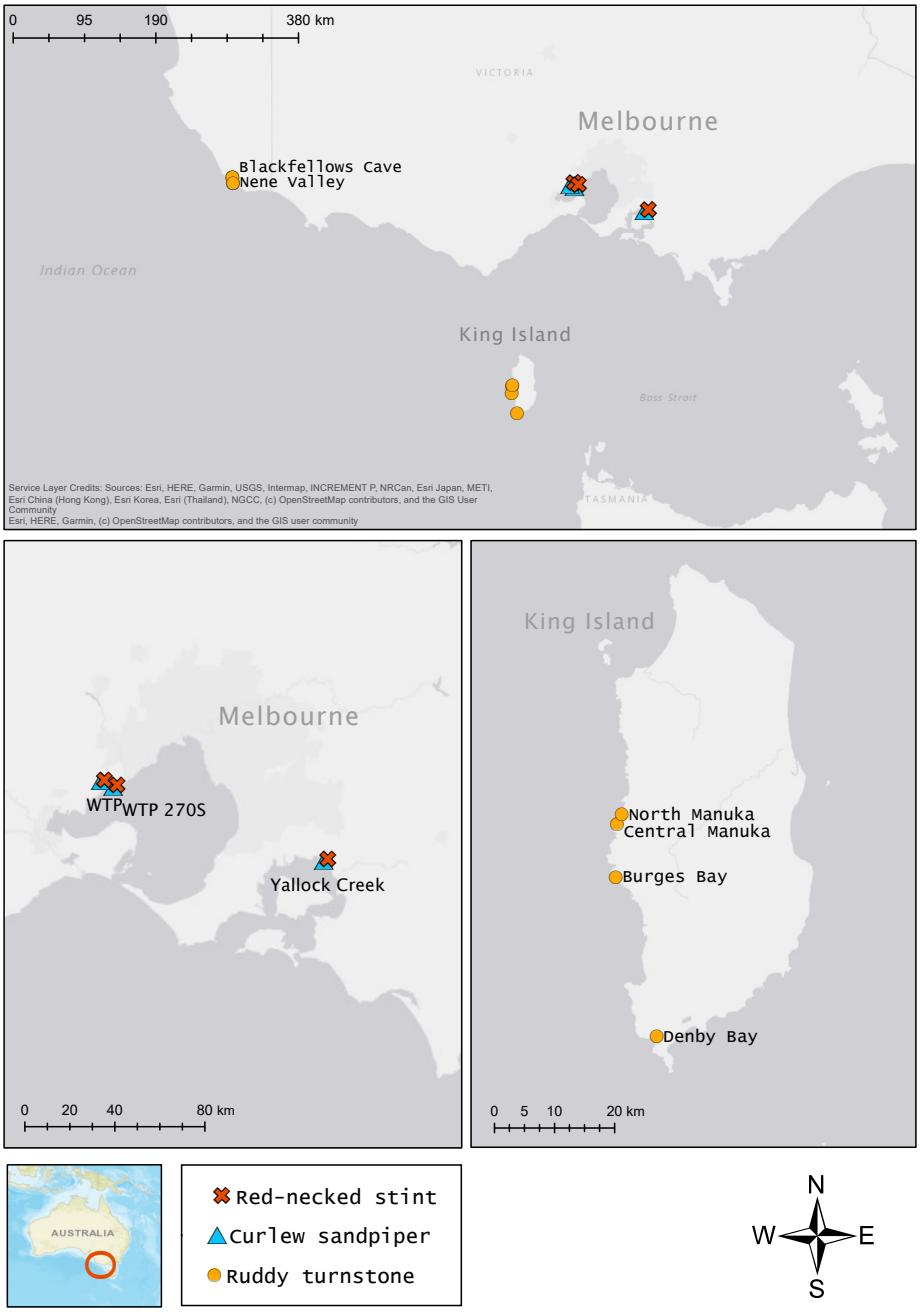

Figure 3.1.: Study sites of curlew sandpipers (*Calidris ferruginea*), red-necked stints (*Calidris ruficollis*) and ruddy turnstones (*Arenaria interpres*) in Australia and at King Island. Created with ArcMap 10.7 Sources: Esri, HERE, Garmin, USGS, Intermap, INCREMENT P. NRCan, Esri Japan, METI, Esri China (Honk Kong), Esri Korea, Esri (Thailand), NGCC, (c) OpenStreetMap contributors, and the GIS User Community.

3.1.3. Sample handling prior to extraction

Individual rbc samples (n=110) were prepared for analysis of both PFASs and elements. In order to perform organic and element analysis, each sample was split in two. Samples were weighed by transferring 20-70 mg to a 15 mL Eppendorf tube using an Eppendorf pipette tip (100 µL). Due to challenges in transferring samples with very low volumes, some samples (n=59) were treated with ethanol prior to transfer. 30 µL ethanol (100% pure) was added to the sample vial to assist the transfer into Eppendorf tubes (15mL) as described above. These samples were left to evaporate overnight. Sample weights and treatment method of each sample is presented in Table A.1. Due to the special circumstances during the spring of 2020, the element analysis could not be presented in this thesis. The sample preparation for element analysis is described in Appendix G.

3.2. Chemicals and materials

Analytical standards of one non-fluorinated compound and 15 perfluorinated alkyl substances were obtained from Sigma-Aldrich (Steinheim, Germany) and Chrion AS (Trondheim, Norway). Target analyte standards included: sodium 1-decane sulfonate (DecaS), perfluoropentanoic acid (PFPA), perfluorohexanoic acid (PFHxA), perfluoroheptanoic acid (PFHpA), perfluorooctanoic acid (PFOA), perfluorononanoic acid (PFNA), perfluorodecanoic acid (PFDA), perfluoroundecanoic acid (PFUnDA), perfluorododecanoic acid (PFDoDA), perfluorotridecanoic acid (PFTrDA), perfluorotetradecanoic acid (PFTeDA), perfluorobutane sulfonate tetrabutylammonium salt (PFBS), perfluorohexane sulfonate potassium salt (PFHxS), perfluorooctane sulfonate tetrabutylammonium salt (PFOS), perfluorooctane sulfonamide (PFOSA) and *N*-Ethyl perfluorooctane sulfonamide (EtPFOSA). Specific information regarding purity and supplier for each standard is presented in Table B.1. Standard concentrations of target analytes were 100 µg mL^{-1} in methanol. See Table B.2 for exact concentrations. ^{13}C-labeled internal standards of perfluorooctanoic acid (^{13}C-PFOA, 50 µg mL^{-1} in methanol) and perfluorooctane sulfonate sodium salt (^{13}C-PFOS, 50 µg mL^{-1} in methanol) were obtained from Cambrigde Isotope Laboratories Inc. (Tewksbury, MA, USA).

Methanol (MeOH, analytical grade) used in extraction and standard solutions was purchased from VWR Chemicals (Rue Carnot, Fontenay-sous-Bois, France). Ammonium formate (anhydrous, reagent grade 97%) was purchased from Sigma-Aldrich (Steinheim, Germany). Solutions of 0.001% and 1% ammonium formate (w/v) in methanol were prepared by dissolving 11.2 mg and 10.0 g ammonium formate, respectively, in 1000 mL MeOH.

Hybrid-SPE®-Phospholipid cartridges (Supelco, Bed wt. 30mg, 1 mL) and dis-

posable liners (PFTE) were purchased from Sigma-Aldrich (Steinheim, Germany). A 12-port disposible liner Visiprep SPE vacuum manifold was obtained from Supelco (PA, U.S.). Eppendorf pipettes and tips were obtained from VWR.

3.2.1. Standard solutions

Sample spikes and matrix match samples were spiked with a 1000 ng mL^{-1} target analyte mixture (TA). This mixture was prepared by mixing 10 µL of each target analyte solution 100 µg mL^{-1} (DecaS, PFBS, PFHxA, PFOS, PFPA, PFHxA, PFHpA, PFOA, PFNA, PFDA, PFUnDA, PFDoDA, PFTrDA, PFTeDA, PFOSA, EtPFOSA), and diluting to 1000 µL in MeOH. This 1000 ng mL^{-1} TA mixture was also used for preparing calibration standards (Section 3.2.2).

^{13}C-labeled standards of PFOA and PFOS were used as internal standards. All samples were spiked with a 1000 ng mL^{-1} mixture of the two internal standards. The internal standard mixture (IS) was prepared by mixing and diluting 20 µL 50 µg mL^{-1} perfluorooctanoic acid and perfluorooctane sulfonate sodium salt to 1000 µL MeOH. All standard solutions were stored in glass vials at -18°C.

3.2.2. Calibration curve

Standard calibration solutions of target analytes with concentrations 0.01, 0.02, 0.05, 0.1, 0.2, 0.5, 1, 2, 5, 10, 20 and 50 ng mL^{-1} in MeOH were prepared. Calibration solutions were prepared using the 1000 ng mL^{-1} TA mixture, and from solutions 100 ng mL^{-1}, 10 ng mL^{-1} and 1 ng mL^{-1} prepared by dilution of the former. All calibration solutions were spiked with 33 µL of the 1000 ng mL^{-1} IS-mixture to contain 33 ng mL^{-1} isotope labeled internal standards. Calibration curve solutions had total volumes of 1000 µL. Calibration curves of all target analytes based on absolute and relative response are presented in Figures C.1-C.6.

3.3. Sample preparation

Hybrid-SPE was the extraction method of choice due to its rapid methodology and known effectiveness in removing matrix interferences from biological matrices. Extraction of PFASs from serum using Hybrid-SPE was described by Honda et al. [21]. For method development and validation, method testing of the Honda et al. method was done on bovine serum. The method was further adjusted and scaled down for the extraction of smaller volumes of avian red blood cells. Bovine blood was used as a matrix standard for method development and validation of the adjusted method.

3.3.1. Method testing on bovine serum

Method for extracting PFASs from serum described by Honda et al. [21] was tested to investigate method recoveries and matrix effects. Quality control parameters were assessed for three fortification levels (10, 20, 50 ng mL^{-1}) of pre- and post-spiked bovine serum samples. Three sample-spikes (pre-extraction spiked) and two matrix match (post-extraction spiked) samples were prepared for each spike-concentration in addition to a total of three sample blanks of bovine serum and three method blanks.

Freeze-stored (-18°C) homogenized bovine serum was thawed to room temperature before extraction. 250 µL serum was spiked with 10 µL internal standard mixture (1000 ng mL^{-1}) in a 15 mL polypropylene (PP) tube using Eppendorf pipettes. Sample spikes were spiked with 10, 20 or 50 µL TA mixture (1000 ng mL^{-1}) to obtain final spike-concentrations of 10, 20 and 50 ng mL^{-1}, respectively. Protein precipitation was done by adding 750 µL precipitating agent (MeOH containing 0.001% ammonium formate (w/v)) to the sample. Samples were vortex mixed (30 seconds) and centrifuged (4000g, 5 minutes) at room temperature.

Hybrid-SPE cartridges were washed with 1 mL MeOH containing 0.001% ammonium formate for conditioning and to remove potential impurities. Sample supernatants were loaded and passed directly through the Hybrid-SPE cartridges. Eluents were collected in 1 mL amber vials. Vacuum was applied during the rinsing and eluting and the vacuum manifold was lined with PTFE liners.

Matrix match samples were prepared using the above protocol, spiking with internal standards and target analytes only after extraction. Method blanks were made by following the extraction protocol of sample blanks, replacing 250 µL serum with MeOH.

3.3.2. Extraction of PFASs from red blood cells

Red blood cell samples were pre-weighed in 15 mL PP-tubes as described in Section 3.1.3. Samples were spiked with 10 µL 1000 ng mL^{-1} ^{13}C-isotope labeled IS-mixture before addition of 300 µL MeOH containing 1% ammonium formate (w/v). To ensure interaction between internal standard and the sample matrix, the internal standard was applied directly onto the samples that had adhered to the PP-tube wall. To obtain contact between the sample matrix and methanol solution, the solvent was used to wet the tube walls by rotation of the tube, before vortex mixing (30 seconds) and centrifuging (5 min, 4000g) to guide the sample matrix to the bottom the PP-tube. Samples were ultrasonicated for 30 minutes before centrifuging again (4000g, 5 minutes) to allow sedimentation.

Hybrid-SPE was performed using Hybrid-SPE (30 mg, 1 mL) cartridges. Disposable PFTE liners were used in the SPE-vacuum manifold. Cartridges were con-

ditioned and rinsed with 1 mL MeOH containing 1% ammonium formate (w/v) to remove impurities. The sample supernatant was loaded onto the cartridge and directly passed through under vacuum. Extracts were collected in 1 mL amber vials for LC-MS/MS analysis. Due to small extraction volumes, glass inserts (150 µL) were used.

3.4. Analysis

The analytical method was extrapolated from Silock et al. [168] and Arvaniti et al. [147]. Chromatographic separation of 16 target analytes was carried out with Waters Acquity UPLC Thermo system equipped with Waters Acquity Column Manager, Waters Acquity Sample Manager and Waters Acquity UPLC class Binary Solvent Manager. A Kinetex C18 column (30 x 2.1 mm, 1.3 µm, 100 Å Phenomex) for separation was serially connected to a Phenomex C18 guard column.

The mobile phase was a mixture of MilliQ-water with 2 mM ammonium acetate (A) and MeOH (B). The gradient elution program using mobile phase A and B is presented in Table 3.3. Injection volume was 4 µL and the flow rate was 0.4 µL min^{-1}. Column oven temperature was set to 30°C.

Table 3.3.: Gradient elution analysis using Kinetex C18 column (30 x 2.1 mm). (A) Water phase: Milli-Q water with 2 mM ammonium acetate. (B) Organic phase: methanol. Constant flow rate of 0.4 µL min^{-1}

Time [min]	**A [%]**	**B [%]**
0	90	10
0.2	90	10
3.0	0	100
3.5	0	100
3.6	90	10
4.0	90	10

Waters Xevo TQ-s, triple quadrupole mass analyzer with ZSpray ESI in negative ionization mode was used for detection. The electrospray ionization (ESI) voltage was 1.8 kV. Desolvation gas and cone gas flow rates were 900 L h^{-1} and 150 L h^{-1}. Collision gas flow rate was 0.15 mL min^{-1}. Source temperature was 150°C and desolvation temperature was 450°C. Specific MS/MS parameters are shown in Table B.3 and B.4. Parent → parent transitions were used for PFSAs due to the reported sensitivity [147].

3.5. Quality assurance and control

Due to small volumes of avian red blood cells, quality control samples could not be obtained from this matrix and bovine blood was instead used as a matrix standard. Spiked samples and matrix match samples were prepared from 50 mg bovine blood following the extraction protocol used when extracting PFASs from red blood cells (Chapter 3.3.2). Samples were pre- and post-extraction spiked with 10 and 20 µL target analyte mixture (1000 ng mL^{-1}) to investigate extraction recovery and matrix effects at fortification concentrations 33 and 66 ng g^{-1}. Pre-spiked samples were made in replicates of four and post-extraction spiked samples were in duplicates for each fortification level.

A critical quality assurance step when analyzing PFASs is avoiding contamination during sample treatment. In addition to making efforts to avoid contamination, blank samples were prepared to monitor it. To avoid contamination from sample equipment, samples were stored and contained in vials and tubes of polypropylene, which has been described as a suitable material when analyzing PFASs [169]. Due to the absence of alternative materials of disposable manifold liners, polytetrafluoroethylene (PFTE) liners were used to line the SPE- vacuum manifold. Any potential contamination originating from the sample preparation was monitored by multiple method blanks. Method blanks were prepared following the same extraction protocol as rbc samples, with no sample matrix added. Potential contamination in samples handled with the ethanol pre-treatment (Chapter 3.1.3) was assessed by analyzing blank samples of ethanol (30 µL) treated with the same extraction protocol as samples. Potential contamination from the ethanol evaporation step was assessed by preparing a fume hood blank, which consisted of ethanol (30 µL) in a PP-tube left to evaporate with samples, and treated using the same protocol as rbc samples.

Solvent blanks (MeOH) were regularly analyzed in-between samples in LC-MS/MS to monitor potential cross contamination and carry-over in the instrument. To monitor potential signal drifting, the calibration standard solution of 0.5 ng mL^{-1} was regularly analyzed in the LC-MS/MS sequence.

3.6. Data analysis and statistical treatment

MassLynx and TargetLynx v4.1 (Waters) were used to acquire LC-MS/MS data. Data was processed in Microsoft Excel (2016) and statistics was done in IBM SPSS Statistics 26 and R (principal component analysis). Data was checked for normality using the Shapiro-Wilk Test and showed non-normal distributions ($p<0.05$). Non-parametric tests were therefore used (Mann-Whitney U test and Kruskal-Wallis test). p-values below 0.05 were determined significant. Quantification was based on

the internal standard method with matrix-matched calibration standards that were pre-extraction spiked (33 ng mL^{-1} and 66 ng mL^{-1})[170]. Signals were adjusted for blank sample response. Concentrations were reported as ng g^{-1}. Data analysis did not include data<LOD.

4. Results and discussion

4.1. Method performance and quality control

The analytical method was validated with regards to a number of quality control parameters, including analyte recoveries, matrix effects, ion ratios, relative retention times, linearity of standard calibration curves and contamination. Ion ratios and relative retention times (RRTs) of analytes in calibration standards and matrix standards are presented in Table B.4. The ion with lower signal was chosen as the quantifying ion if the most intense peak had substantially more noise, as was the case for PFBS, PFOS and PFHpA. Otherwise, the most intense peak was chosen as the quantitative ion. All ion ratios showed sufficient precision with coefficient of variance (RSD%) <10%, with the exception of PFHxS and PFHxA with RSD% of 12% and 13%. Target analytes were quantified using relative response to associated internal standards based on calibration in matrix standards (bovine blood). Analytes were corrected with the ^{13}C-labeled internal standard closest in retention time, as this reflects similar chemical properties. To ensure certainty of peak identification, peaks with RRT outside of the range of standards were omitted. Chromatograms of MRM transitions for target analytes and internal standards in a pre-extraction spiked matrix sample is presented in Figures D.2-D.7.

Standard calibration solutions in methanol, fortified with target analytes at 0.01, 0.02, 0.05, 0.1, 0.2, 0.5, 1, 2, 5, 10, 20 and 50 $\mathrm{ng\,mL^{-1}}$ and internal standards at 33 $\mathrm{ng\,mL^{-1}}$, were used to plot calibration curves based on absolute and relative response. Calibration curves are presented in Figures C.1-C.6. The coefficient of determination (R^2) was assessed and showed linearity with R^2>0.985 in all calibration curves.

To assess the common problem of background contamination of PFASs in trace analysis [44], contamination was monitored through a number of blank samples described in Chapter 3.5. Out of the 16 target analytes, most compounds were not detected in any of the method blanks prepared with samples. PFOS and PFHxA were found in low but detectable levels in method blanks, indicating cross contamination or impurities from equipment. Honda et al. also reported background contamination of PFHxA from Hybrid-SPE cartridges [21]. Cartridges were pre-washed to avoid such contamination, but PFHxA was still found in low levels in some method blanks, indicating that the washing step was not completely

effective with regards to this chemical. To assess if the ethanol treatment step described in Chapter 3.1.3 affected the results, two treatment groups were compared with a non-parametric test. A Mann-Whitney U-test of the most abundant PFAS (PFOS) showed no statistical difference (p=0.79) between samples treated with ethanol (n=59) and samples that were not treated with ethanol (n=51). Three analytes (PFNA, PFUnDA, PFTrDA) were detected in a fume hood blank prepared in the evaporation step. All sample analyte signals were corrected with associated blanks.

Detection limits of target PFASs and the non-fluorinated decane-1-sulfonate (DecaS) are presented in Table 4.1. The limit of detection (LOD) was estimated based on a signal-to-noise ratio of three in standard calibration solutions (0.01-50 $\mathrm{ng\,mL^{-1}}$). If signals were not visible throughout the calibration curve, the LOD was estimated to the lowest calibration solution in which an identifiable peak was visible. Limit of quantification (LOQ) was estimated using LOD and Equation 2.4. The LODs of target analytes ranged from 0.0006 to 0.2 $\mathrm{ng\,mL^{-1}}$, thus most analytes were detected with high sensitivity.

Table 4.1.: Limit of detection (LOD) and limit of quantification (LOQ) of target analytes.

	LOD [$\mathrm{ng\,mL^{-1}}$]	**LOQ** [$\mathrm{ng\,mL^{-1}}$]
PFBS	0.003	0.009
PFHxS	0.10	0.3
PFOS	0.0018	0.005
PFPA	0.2	0.6
PFHxA	0.10	0.3
PFHpA	0.10	0.3
PFOA	0.09	0.27
PFNA	0.05	0.15
PFDA	0.03	0.09
PFUnDA	0.02	0.06
PFDoDA	0.03	0.09
PFTrDA	0.02	0.06
PFTeDA	0.02	0.06
PFOSA	0.003	0.009
EtPFOSA	0.0006	0.0018
DecaS	0.2	0.6

4.1.1. Precision and accuracy

Method precision was evaluated from RSD% values of pre-extraction spiked bovine blood replicates (n=4) at two fortification levels (33 and 66 ng mL^{-1}). These samples were analyzed in the same LC-MS/MS sequence as avian rbc samples. Results are presented in Table 4.2 for both absolute and relative values. Most target analytes showed acceptable precision (RSD%<16%) at both fortification concentrations. The most noteworthy exception was PFHxS, which showed higher RSD% (27-29%) compared to other analytes at the 33 ng mL^{-1} spike-concentration. The reason for this increased variation was not identified. The precision was, however, increased for samples spiked with the highest concentration for this compound.

Internal standards could to some degree compensate for variations by experiencing the same fluctuations as target analytes. The precision of relative signals showed lower RSD% on a general basis, but other than that, no trends in increased repeatability of relative values were observed.

Signal variations could stem from variability in matrix effects, recovery loss and other conditions during sample preparation. As the spiked samples were sub-samples from the same batch of bovine blood, variations in the amount of endogenous matrix components, causing signal disturbance and analyte loss, were assumed to be minimal, thus increasing precision. However, variations in interacting sample components could be induced through variable efficiency of protein precipitation, ultrasonication as well as retardation of matrix components in Hybrid-SPE.

The trueness of the method was not evaluated due to lack of certified reference materials. Accuracy was evaluated by back-calculating the spiked samples used in quantification. All target analytes remained within ±15% of target values.

4.1.2. Recoveries

Recoveries of target analytes were calculated using Equations 2.9-2.10 and evaluated in two extraction protocols applying Hybrid-SPE on biological matrices. Recoveries of analytes following the extraction protocol for smaller volume blood/rbc samples (Chapter 3.3.2) were determined using bovine blood as a matrix standard. This was the protocol used for all avian rbc samples in this study. Recoveries were compared with those following the extraction protocol of bovine serum (Chapter 3.3.1), which was tested for the purpose of method evaluation. Absolute and relative recoveries in both protocols are presented in Table 4.3.

Table 4.2.: Precision of target analytes in replicates (n=4) of pre-extraction spiked samples with concentrations 33 ng mL^{-1} (SP_{33}) and 66 ng mL^{-1} (SP_{66}). Mean, STD and RSD% of analyte signal (area) and signal relative to internal standard are reported.

		Absolute values			**Relative values**		
		Mean	**STD**	**RSD %**	**Mean**	**STD**	**RSD %**
DecaS	SP_{33}	11736	891	8	2.2	0.10	5
	SP_{66}	23411	2399	10	4.7	0.19	4
PFBS	SP_{33}	5716	912	16	1.0	0.11	10
	SP_{66}	11264	253	2	2.3	0.3	13
PFHxS	SP_{33}	2464	712	29	0.5	0.12	27
	SP_{66}	4101	467	11	0.8	0.08	10
PFOS	SP_{33}	17499	1233	7	0.7	0.05	8
	SP_{66}	35361	2236	6	1.5	0.05	3
PFPA	SP_{33}	17000	1479	9	3.1	0.15	5
	SP_{66}	34132	4276	13	6.8	0.5	7
PFHxA	SP_{33}	22483	1307	6	4.2	0.4	8
	SP_{66}	45529	5232	11	9.1	0.5	5
PFHpA	SP_{33}	3836	673	18	0.7	0.08	11
	SP_{66}	7621	934	12	1.5	0.15	10
PFOA	SP_{33}	44218	4003	9	8.2	0.5	6
	SP_{66}	91395	11688	13	18.2	1.3	7
PFNA	SP_{33}	81426	6547	8	3.1	0.3	10
	SP_{66}	160840	22296	14	6.6	0.5	7
PFDA	SP_{33}	98984	12102	12	3.8	0.4	9
	SP_{66}	204081	20175	10	8.4	0.4	4
PFUnDA	SP_{33}	128971	10556	8	4.9	0.6	12
	SP_{66}	252339	25545	10	10.4	0.6	5
PFDoDA	SP_{33}	128178	13413	10	4.9	0.5	9
	SP_{66}	251804	22800	9	10.4	0.5	5
PFTrDA	SP_{33}	140823	13387	10	5.4	0.5	9
	SP_{66}	280014	30132	11	11.5	0.8	7
PFTeDA	SP_{33}	107719	8520	8	4.1	0.5	13
	SP_{66}	212800	34234	16	8.7	0.9	10
PFOSA	SP_{33}	71870	8132	11	2.7	0.13	5
	SP_{66}	136563	6212	5	5.6	0.4	7
EtPFOSA	SP_{33}	42855	5419	13	1.6	0.08	5
	SP_{66}	81451	2268	3	3.4	0.2	6

Table 4.3.: Average absolute (AR%) and relative recoveries (RR%) of target analytes in two Hybrid-SPE protocols for biological matrices. Recoveries in the extraction protocol for smaller volume avian red blood cells are given for two fortification levels (33 and 66 ng mL^{-1}). Recoveries in the serum protocol are given as an average of three fortification levels (10, 20 and 50 ng mL^{-1}).

	Rbc protocol*				**Serum protocol****	
	33 ng mL^{-1}		66 ng mL^{-1}			
	AR%	**RR%**	**AR%**	**RR%**	**AR%**	**RR%**
DecaS	18 (8)	92 (5)	17 (12)	82 (4)	66 (18)	133 (30)
PFBS	16 (16)	82 (11)	16 (11)	80 (13)	57 (9)	111 (9)
PFHxS	17 (29)	86 (27)	17 (11)	83 (22)	57 (9)	111 (9)
PFOS	18 (7)	100 (8)	19 (6)	105 (3)	56 (9)	108 (10)
PFPA	19 (9)	97 (5)	20 (13)	98 (7)	57 (9)	113 (12)
PFHxA	19 (6)	96 (8)	19 (12)	95 (5)	56 (13)	110 (9)
PFHpA	21 (18)	105 (11)	22 (12)	111 (10)	59 (11)	117 (9)
PFOA	21 (9)	109 (6)	23 (13)	113 (7)	60 (9)	119 (11)
PFNA	22 (8)	121 (10)	25 (14)	136 (7)	59 (12)	115 (13)
PFDA	19 (12)	104 (9)	22 (10)	118 (4)	59 (12)	114 (13)
PFUnDA	19 (8)	104 (12)	20 (10)	112 (4)	58 (9)	112 (12)
PFDoDA	20 (11)	108 (9)	22 (9)	119 (5)	57 (10)	110 (9)
PFTrDA	20 (10)	109 (9)	21 (11)	113 (7)	55 (14)	106 (15)
PFTeDA	18 (8)	98 (13)	19 (16)	106 (10)	57 (18)	110 (14)
PFOSA	18 (11)	98 (5)	18 (5)	98 (7)	55 (9)	107 (11)
EtPFOSA	17 (13)	92 (5)	16 (3)	86 (6)	52 (9)	101 (11)

* Recoveries in bovine blood extracts
** Recoveries in bovine serum extracts.

Target analytes demonstrated somewhat low absolute recoveries (16-25%) when extracted with the protocol for rbc samples. This indicates a considerable amount of sample loss during the sample preparation stage. Although absolute recoveries were on the lower end, target analytes demonstrated relative recoveries in the range 80-136%, illustrating the compensating effects of internal standards on sample loss. Analyte recoveries using the serum extraction protocol were considerably higher compared to those of the rbc protocol. Recoveries were acceptable with absolute recoveries in the range 52-66%, and relative recoveries in the range 101-133%, which were similar to relative recoveries reported by Honda et al. [21] using the same method. Analyte recoveries were corrected with either ^{13}C-labeled PFOS or PFOA. The structural similarity of analyte and internal standard varied between the 16 target analytes, which can cause dissimilar behavior in the extraction process.

The high relative recoveries demonstrate that although the internal standard has a different structure than the target analyte, it is reasonably similar in terms of physiochemical properties and thus sufficient in compensating analyte loss.

When transferring analytes from complex matrices, like biological tissues and blood, to simple solvents, some degree of analytes loss is to be expected [153]. Although calculations of absolute recoveries include matrix effects in the determination step [160], matrix components may still affect the absolute recoveries through interactions with analytes during sample preparation. During the protein precipitation step, which was performed in both protocols, proteins aggregate, and bound analytes are released to the solvent. However, analytes binding strongly to proteins may co-precipitate instead of dissociating [130]. As PFASs tend to associate to proteins, incomplete removal of matrix proteins before they are filtrated in Hybrid-SPE is a potential source of sample loss. Interestingly, the analyte with the best recovery in the serum extraction was the non-fluorinated DecaS, which is not regarded as "proteinophilic". Another potential source of sample loss during Hybrid-SPE is co-retardation of analytes with phospholipids on the stationary phase [171]. The presence of formate ions interacting with the stationary phase usually prevents this. However, when extracting target analytes from serum, a solution of 0.001% ammonium formate in methanol (w/v) was used instead of the recommended 1% solution. Experiments in the same lab, using the same Hybrid-SPE equipment to extract the same target analytes from harbor porpoise (*Phocoena phocoena*) livers showed that the use of the 0.001% formate concentration had no effect on recovery [172].

The causes of the relatively low absolute recoveries in the rbc protocol were not confidently identified. This extraction method differed from the serum protocol by using lower volumes and applying an additional extraction step (ultrasonication). In general, multiple stages of sample preparation increases the opportunities of sample loss. The ultrasonication step is expected to release various cellular components that can interact with analytes. Another likely reason for the sample loss is of more practical origin. Unlike serum samples, the bovine blood was considerably more difficult to work with. Although most of the matrix was in contact with the precipitating agent at all times, blood was consistently observed sticking to the PP-tube walls above the liquid. To facilitate extraction from this blood, the tubes were vortexed mixed and manually rotated to re-gain contact with the solvent (See Chapter 3.3.2). However, the contact time between the solvent and this part of the sample was considerably lower than that of the rest of the sample. Although the amounts lost to the sample walls were small, the relative amount may have been considerable due to the low total sample volume of this extraction protocol. Nevertheless, the acceptable relative recoveries illustrate the importance of internal standards to compensate for such loss.

Low absolute recoveries are not necessarily detrimental to analysis if the recoveries show consistency [130]. Absolute recoveries in the rbc protocol showed consistency across the two fortification levels. In addition, recovery test showed acceptable precision for most analytes (RSD%<15%), with the exception of PFHxS, which had RSD%=29% at the lowest fortification level. However, this chemical was barely detected in the avian blood cells, thus, the variable recoveries of this compound did not greatly impact the study. Although precision and consistency of absolute recoveries were acceptable, a high degree of sample loss is undesirable in trace analysis when analytes are present in concentrations already close to detection limits. Further work should aim to increase the extraction efficiency.

4.1.3. Matrix effects

Matrix effects (ME%) of 15 perfluoroalkyl substances and one non-fluorinated surfactant in bovine blood and serum extracts analyzed with UPLC-MS/MS are presented in Figure 4.1. Calculated matrix factors (MF) are presented in Table B.5. Matrix effects of all target analytes showed subjection to signal enhancement (ME%>0) relative to standard solvent when extracted from blood, indicating that matrix components facilitated the ionization rather than impeding it [173]. In serum extracts, the non-fluorinated surfactant DecaS showed signal suppression, while signal enhancement remained for all PFASs with the exception of PFPA, for which ion suppression was observed in the higher concentrations of serum extracts. Efforts were made to reduce the known contribution of endogenous phospholipids to matrix effects by applying Hybrid-SPE. However, considerable amounts of matrix effects were still observed, especially in blood extracts.

Although ion suppression is generally the most common matrix effect in LC-MS/MS using electrospray ionization [133], previous studies have also reported signal enhancements of PFASs. Positive matrix effects of similar magnitude were previously reported for PFASs extracted from wastewater and sludge [147]. Honda et al. [21] also reported signal enhancement as well as suppression of PFASs depending on the choice of precipitating agent in Hybrid-SPE. For the majority of PFASs, a trend of decreasing matrix effects with increased analyte concentration could be observed in both matrices (Figure 4.1). Increasing analyte concentration alters the ratio of analytes to co-eluting matrix components, thus increasing the number of analyte molecules competing for droplet formation and/or formation of gas phase ions in the electrospray ionization (ESI) source (Chapter 2.3.3 and 2.3.4). This also implies decreasing the relative number of matrix components to facilitate ion enhancement.

Matrix effects are both compound and matrix specific, something that becomes evident when comparing ME% between blood and serum extracts. Matrix effects were compared for similar fortification levels; 33 and 66 $\mathrm{ng\,g^{-1}}$ blood and 50 $\mathrm{ng\,g^{-1}}$

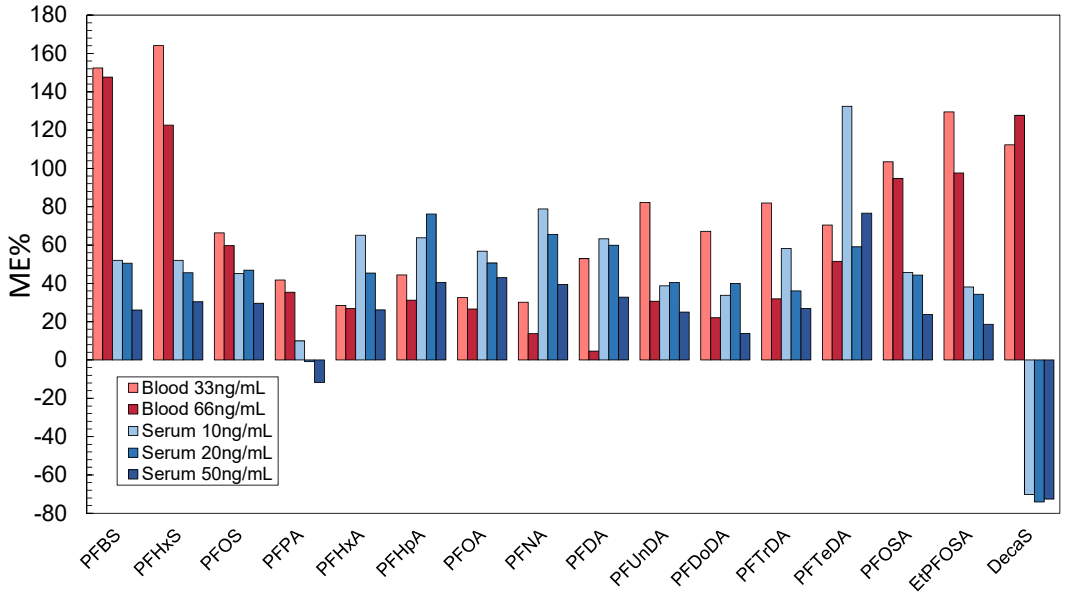

Figure 4.1.: Matrix effects (ME%) of 15 PFASs and DecaS in bovine blood and serum extracts at different fortification levels.

serum. Compounds of similar chemical nature showed similar trends between matrices, as seen in Figure 4.1. ME% in blood extracts were considerably higher than in serum extracts for the sulfonate and sulfonamide based PFASs, PFSAs, PFOSA and EtPFOSA. This was not the case for PFCAs, where the ME% were similar between matrices, or even higher in serum extracts. For the alkyl sulfonate DecaS, a shift to ion suppression was observed in serum extracts, illustrating the effect of the matrices' nature on the matrix effects. Matrix components that co-elute with analytes and cause alterations of the ESI-process can be both of endogenous origin, such as proteins and phospholipids, and exogenous origin, which are compounds introduced through sample preparation and analysis [174]. When comparing the ME% in blood and serum, a note should be made, that in addition to the matrices naturally containing different profiles of endogenous compounds, the extracts were obtained using extraction protocols that differed in salt content, preparatory steps, scale and ratio between sample and solvent volume. Differences in sample to MeOH ratios have been shown to affect the purity of extracts through different degrees of protein breakthrough in Hybrid-SPE [159].

As matrix effects appeared to increase with lower fortification levels, the matrix effects of analytes detected in trace amounts in avian blood cells could be substantially bigger. In order to compensate for matrix effects and sample loss, quantification was based on the internal standard method with matrix-matched

calibration from pre-extraction spiked samples. Internal standards with structural similarity to target analytes compensate for matrix effects as well as loss of absolute recovery by interacting similarly with matrix components and other variability in LC-MS/MS analysis. The use of ^{13}C-labeled analogues ensures nearly identical physiochemical properties, thus a better ability to compensate. In this study, two ^{13}C-labeled internal standards were used between 16 target analytes. Although analytes were corrected with the internal standards closest in retention time, relative retention times deviating from 1 (Table B.4) imply that the chemical properties of analytes and respective internal standards were not equal. In addition, the differences in RT also implied that not all target analytes were ionized together with their respective internal standard. When analytes and the internal standard enter the ESI-source at different times, their co-eluting components differ, thus they experience different matrix effects [175]. Compensation of matrix effects is therefore expected to be more accurate for PFOA and PFOS as these are structural analogues of the internal standards that were used.

4.2. Occurrence of PFASs in avian red blood cells

All 15 target PFASs were detected in avian red blood cell samples, with detection rates ranging from 1-51%, differing between species and sites. PFASs were detected in 78% of the analyzed rbc samples, indicating that although most PFASs primarily accumulate in plasma [82], they are also found in detectable levels in the cell fraction of blood. To the best of my knowledge, PFASs are not previously analyzed in the rbc alone.

Overall detection rates and concentrations of target analytes are presented in Table 4.4. Detection rates, median concentrations and range of target analytes in individual species are presented in Table 4.5. Descriptive statistics and results are only presented for concentrations found above the LOD. Detection rates varied greatly between samples collected at different sites, illustrated in Figure 4.2. The most detected PFAS was PFOS, which was found in 51% of rbc samples, and the only chemical with detection rate above 50% when combining all species. The target analytes detected with highest mean concentrations overall were PFOS (75.6 $\mathrm{ng\,g^{-1}}$), PFHxS (20.7 $\mathrm{ng\,g^{-1}}$), PFNA (13.9 $\mathrm{ng\,g^{-1}}$), PFPA (7.90 $\mathrm{ng\,g^{-1}}$) and PFUnDA (7.90 $\mathrm{ng\,g^{-1}}$). However, with the exception of PFOS, these compounds were less frequent with low detection rates (<18%, Table 4.4). PFHxS had the second highest mean concentration, but was detected in one sample only. Since results are only calculated for data above the LOD and left-censored data (concentrations<LOD) were omitted, compounds should have 50% detection rates at *minimum* in order to be representative. Therefore, the discussion and comparison between species and sites will focus on compounds with high detection frequencies.

Table 4.4.: Detection rates (DR), mean, median, minimum and maximum detected concentrations of 15 PFASs and one non-fluorinated compound (DecaS) in avian red blood cells (n=110).

	DR [%]	**Mean** [ng g^{-1}]	**Median** [ng g^{-1}]	**Min** [ng g^{-1}]	**Max** [ng g^{-1}]
PFBS	10	1.08	0.74	0.03	5.39
PFHxS	0.9	20.7	20.7	20.7	20.7
PFOS	51	75.6	10.7	0.04	804
PFPA	7	7.90	7.94	1.17	24.0
PFHxA	6	4.36	2.87	1.70	9.37
PFHpA	2	6.30	6.30	3.43	9.18
PFOA	28	4.71	3.87	0.70	12.8
PFNA	18	13.9	12.3	1.39	39.9
PFDA	22	4.47	1.93	0.39	19.8
PFUnDA	13	7.90	4.97	1.06	20.5
PFDoDA	30	2.08	1.29	0.17	15.9
PFTrDA	37	2.19	1.57	0.10	8.78
PFTeDA	24	5.05	3.89	0.90	20.4
PFOSA	16	4.85	1.84	0.12	41.3
EtPFOSA	5	0.28	0.19	0.05	0.65
ΣPFAS	78	62.6	7.89	0.05	837
DecaS	15	16.5	8.74	1.33	65.8

Regarding comparison of results to previous studies in the following chapters, some caution should be taken. Different biological matrices differ not only in matrix effects, which was demonstrated through method evaluation in this study (Figure 4.1), but PFASs distribute differently between biological compartments as well. In addition, observed contaminant levels may differ between species due to differences in body size, habitat use, trophic position and metabolic capacity [176]. Because PFASs are not previously studied in these shorebirds nor analyzed in the same matrix, comparison with previous studies is done semi-quantitatively only. Conversion factors have previously been applied to compare PFAS levels in whole-blood and plasma [73, 85]. However, the distribution of individual PFASs in the different compartments of blood is not fully understood and seems to be compound dependent (Chapter 2.1.5). In addition, the distribution to red blood cells alone is less studied. For these reasons, conversion factors were not applied when comparing the following results to previous studies in blood and plasma.

From a general point of view, if a compound distributes mainly to plasma proteins, levels reported in blood cells could be regarded as the lower estimate of what is expected in the whole-blood of the individual. However, for compounds associ-

Table 4.5.: Detection rates (DR) and concentrations (median and range) in $ng\,g^{-1}$ of PFASs in red blood cells of curlew sandpipers (n=23), red-necked stints (n=19) and ruddy turnstones (n=68). Only concentrations>LOD are presented.

	Curlew sandpiper		**Red-necked stint**		**Ruddy turnstone**	
	DR [%]	Median (range) [$ng\,g^{-1}$]	DR [%]	Median (range) [$ng\,g^{-1}$]	DR [%]	Median (range) [$ng\,g^{-1}$]
PFBS	9	0.53 (0.03-1.04)	11	3.06 (0.74-5.39)	10	0.25 (0.09-1.73)
PFHxS	4	20.7*	0	-	0	-
PFOS	96	24.9 (0.62-804)	68	112 (13.1-396)	31	0.63 (0.04-1.28)
PFPA	0	-	16	8.07 (8.00-24.0)	7	3.03 (1.17-8.98)
PFHxA	13	2.03 (1.71-3.71)	5	7.67*	3	5.53 (1.70-9.37)
PFHpA	4	3.43*	5	9.18*	0	-
PFOA	52	3.90 (0.76-9.70)	58	6.16 (2.37-12.8)	12	2.89 (0.70-8.47)
PFNA	52	14.1 (2.35-39.9)	26	9.15 (1.39-27.6)	4	10.7 (2.57-17.1)
PFDA	48	3.96 (1.01-17.5)	26	6.29 (1.31-19.8)	12	0.92 (0.39-1.68)
PFUnDA	30	4.51 (1.06-19.3)	32	5.12 (1.66-20.5)	1	15.1*
PFDoDA	43	1.52 (0.95-5.52)	42	3.11 (1.38-15.9)	22	0.47 (0.17-1.41)
PFTrDA	57	2.89 (1.29-8.78)	47	2.65 (1.08-5.06)	28	0.54 (0.10-3.66)
PFTeDA	52	4.30 (1.44-10.63)	53	5.00 (1.34-20.4)	6	1.61 (0.90-8.26)
PFOSA	43	2.75 (0.50-41.3)	37	0.77 (0.12-8.65)	0	-
EtPFOSA	4	0.42*	5	0.65*	4	0.08 (0.05-0.19)
ΣPFAS	100	40.2 (6.48-837)	84	117 (0.12-467)	69	7.89 (0.05-27.9)
DecaS	30	19.9 (1.85-65.8)	5	5.27*	12	5.05 (1.33-47.4)

* Detected in one sample

ating less to plasma proteins, which seems to be the case for PFOSA [87, 88], the blood cells may be more representative of the whole-blood. Thus, if distribution varies greatly between PFASs, the profiles observed in blood cells may differ from those in plasma. Further studies on PFAS distribution in blood, including blood cells as a separate fraction, would potentially make for a more solid comparison.

Perfluorooctane sulfonate

In addition to the highest overall mean concentration of $75.6\,ng\,mL^{-1}$, PFOS showed the highest maximum concentration of $804\,ng\,g^{-1}$, which was found in a curlew sandpiper at the Western Treatment Plant (WTP) in 2013. This concentration was notably higher than other concentrations found in this study. The maximum PFOS concentration was in fact double the second highest concentration of PFOS ($396\,ng\,g^{-1}$), found in a red-necked stint at the same location the same year. PFOS was the dominating PFAS, which coincides with previous studies across multiple species and matrices [55, 61, 64, 67, 70, 74, 76]. The concen-

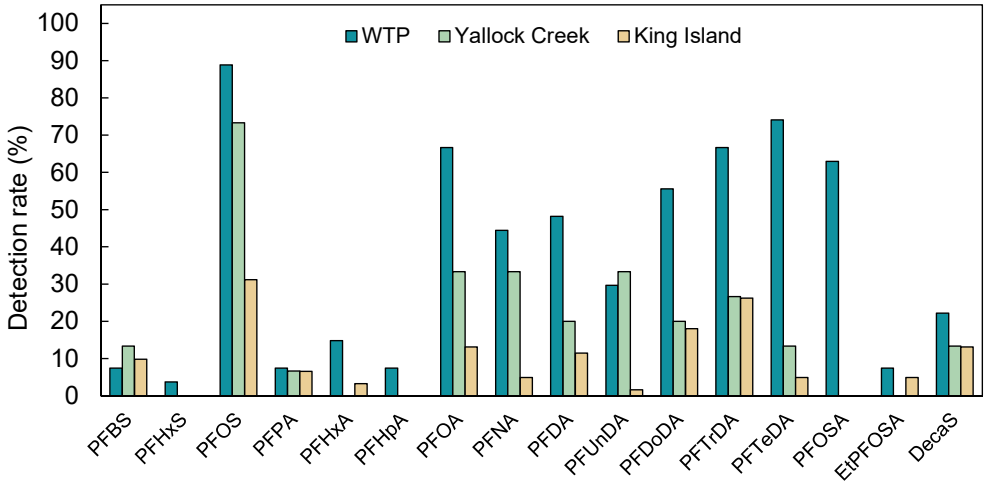

Figure 4.2.: Detection rates (%) of PFASs and one non-fluorinated compound (DecaS) in rbc samples from different sample locations, species combined. WTP and Yallock Creek are sample sites of curlew sandpipers and red-necked stints. Ruddy turnstones were sampled on King Island.

tration ranges varied greatly between ruddy turnstones sampled at King Island (0.04-1.28 ng g^{-1}), and curlew sandpipers (0.62-804 ng g^{-1}) and red-necked stints (13.1-396 ng g^{-1}) that were sampled near the city of Melbourne. Within the latter two species, detection rates and PFOS concentrations also varied between sites. PFOS is further discussed throughout the following chapters.

Short-chained perfluoroalkyl substances

The short-chained PFASs, PFPA, PFHxA, PFHpA, PFBS and PFHxS had very low detection rates across species (<16%). Following regulatory efforts and volunteered phase-outs of PFOS and PFOA, short-chained PFAAs have been proposed as alternatives as they are regarded as less bioaccumulative [177, 178]. Even though short-chained PFAAs are still as persistent and more mobile than their long-chained homologues, the global market for these chemicals has nevertheless been increasing [30, 177]. Findings of PFPA, PFHxA, PFHpA and PFBS in avian samples have previously been scarce and the low detection rates of these compounds concurs with previous studies. The absence of these compounds could be explained by lower exposure to these chemicals and/or by lower bioavailability. In addition, the distribution of these compounds to the cell fraction of blood has not been elucidated.

PFHxS has been reported more frequently in previous avian studies (Table

2.2), but was the least detected compound in rbc of the three studied shorebird species. When detected, previously reported PFHxS concentrations in plasma and blood have most often been low $<2.5\,\mathrm{ng\,mL^{-1}}$, with the exception of tree swallow nestlings from contaminated sites in Michigan USA, which had a geometric mean plasma PFHxS concentration of $206\,\mathrm{ng\,mL^{-1}}$. PFHxS was detected in one out of 110 rbc samples, however with relatively high concentration ($20.7\,\mathrm{ng\,g^{-1}}$). Although the sampled bird frequented the biological wastewater treatment facility, where the contamination levels varied in individuals, the reliability of this PFHxS concentration was regarded as low.

Long-chained perfluoroalkyl carboxylic acids

Along with PFOS, long-chained PFCAs are frequently reported in birds. In this study the long-chained PFCAs were the dominating PFCAs comprising on average 96%, 84% and 85% of ΣPFCA in curlew sandpipers, red-necked stints and ruddy turnstones, respectively. Following PFOS, long-chained PFCAs were the most detected compounds of the analyzed rbc samples. Detection rates of these compounds did, however, vary greatly between species. Detection rates in ruddy turnstones were all-around low (<28%), while detection rates in curlew sandpipers and red-necked stint were higher and varied between sample sites. PFTrDA was among the most detected compounds in all species (curlew sandpiper, 57%; red-necked stint, 47%; ruddy turnstone, 28%) with median concentrations 2.89, 2.65 and $0.54\,\mathrm{ng\,g^{-1}}$ in curlew sandpipers, red-necked stints and ruddy turnstones, respectively. These levels were of similar magnitude to most previous studies.

Most PFCAs were not detected in a representative number of samples, making comparison with previous studies challenging. For instance, PFNA was the long-chained PFCA with highest median concentration in all species (curlew sandpiper, $14.1\,\mathrm{ng\,g^{-1}}$; red-necked stint, $9.15\,\mathrm{ng\,g^{-1}}$; ruddy turnstone, $10.7\,\mathrm{ng\,g^{-1}}$), which were of the same magnitude as some of the highest concentrations reported in avian plasma. However, due to the varying detection rates (curlew sandpiper, 52%; red-necked stint, 26%; ruddy turnstone, 4%), and censored data not being included in some way, this comparison is not representative. PFTeDA was of the most detected compounds in curlew sandpiper (52%) and red-necked stints (53%), but barely present in samples of ruddy turnstones (6%). With the exception of PFUnDA, all long-chained PFCAs had higher detection rates among birds sampled at the WTP site (Figure 4.2). The occurrence of long-chained PFCAs at the WTP is further discussed in Chapter 4.4.2.

N-Ethyl perfluorooctane sulfonamide and perfluorooctane sulfonamide

Two compounds known to be less stable and degradable to persistent PFASs were investigated. EtPFOSA was detected in only a few of the analyzed samples (5%). EtPFOSA is most known for its use in the pesticide Sulfluramid, which has been linked to PFOS and PFOA emissions through degradation [23]. Sulfluramid has been phased out by the EU, the American Environmental Protection Agency and more [23] and has not been registered for use in Australia [179]. The low abundance and occurrence in this study population could therefore be due to the lower emissions of this chemical, in addition to it being susceptible for biotransformation to PFOSA and PFOS [85]. This chemical is not excessively studied in birds and there is minimal data for comparison.

PFOSA was frequently detected (63%) in samples collected at the wastewater treatment facility, but was otherwise not detected in samples from any other sites (Figure 4.2), making the overall detection rate low (16%). At the WTP site, median PFOSA concentrations were 2.75 and 0.77 $\mathrm{ng\,g^{-1}}$ in curlew sandpipers and red-necked stint, respectively, with similar distribution between species. Of the studies presented in Chapter 2.1.4, PFOSA is often not reported in blood and plasma, with some exceptions. The median PFOSA concentration in blood cells of red-necked stint was of the same magnitude as previously reported plasma PFOSA levels in lesser black-backed gulls [58] and european shag in Norway [67]. In curlew sandpipers, the median PFOSA concentration at the WTP was of the same magnitude as reported plasma concentrations in tree swallows sampled in areas with influence from wastewater treatment plants, urban runoff and more [65]. Emissions of PFOS precursors like PFOSA are linked to increased PFOS levels, which is further discussed in Chapter 4.4.2.

Decane-1-sulfonate

DecaS is a non-fluorinated alkyl sulfonate primarily included in this study to investigate method validation parameters against perfluoroalkyl sulfonates. In the absence of the perfluorinated carbon chain, alkyl sulfonates do not have the combined hydrophobic and lipophobic nature that is known for perfluorinated surfactants [2]. The chemical structure of DecaS more resembles lipids and the behavior is expected to deviate from PFASs to some degree. This was also observed by the different matrix effects particularly in bovine serum. The compound also had the highest LOD, and by far the most background noise in the parent $\rightarrow$ parent transition used for PFSAs (Figure D.2).

DecaS was detected in all investigated species with detected concentrations ranging from 1.33 to 65.8 $\mathrm{ng\,g^{-1}}$ (Table 4.4). The overall mean (16.5 $\mathrm{ng\,g^{-1}}$) and median (8.74 $\mathrm{ng\,g^{-1}}$) DecaS concentrations were among the higher concentrations in this

study, although overall detection rate was low (15%). Due to low detection rates, relationships between this compound and PFASs in the avian rbc were not further investigated.

Study groups

Comparing detection rates and results showed a difference in PFAS abundance and frequency among the three species. Median ΣPFAS concentrations were $40.2\,\mathrm{ng\,g^{-1}}$ in curlew sandpipers, $117\,\mathrm{ng\,g^{-1}}$ in red-necked stints and $7.89\,\mathrm{ng\,g^{-1}}$ in ruddy turnstones. Overall occurrences of PFASs in the three species are presented in Figure 4.3. The box plots in Figure 4.3 are color-coordinated according to detection rate within each species, as the observed concentrations are more representative among the chemicals with high detection rate. From Table 4.5 and Figure 4.3 it is evident that abundance and contamination levels of PFASs were lower in ruddy turnstones compared to curlew sandpipers and red-necked stints.

In addition to lower PFAS concentrations overall, no compounds showed detection rates above 31% in the ruddy turnstone population. Detection rates were higher in samples of curlew sandpipers and red-necked stints, with PFOS, PFTeDA, PFOA all detected above 50% in both species. In the curlew sandpiper population, PFNA and PFTrDA also had detection rates above 50%. A Kruskal-Wallis test of species-differences in PFOS and ΣPFAS concentrations confirmed that the distribution was not the same across species ($p<0.0001$). This is possibly explained by the samples site of the three species. Curlew sandpipers and red-necked stints were sampled at locations with more human and industrial influence (Yallock Creek and WTP) compared to ruddy turnstones, which were sampled at the more remote King Island. Finding higher levels of PFASs in areas more influenced by human activity is expected from previous studies on these compounds in wildlife [6, 60, 180]. Due to the difference in sample sites between species, further results and discussion will mainly be based on two study groups; (1) ruddy turnstones sampled on shorelines of King Island and rural areas of South-Australia and (2) curlew sandpipers and red-necked stint sampled at sites near the city of Melbourne.

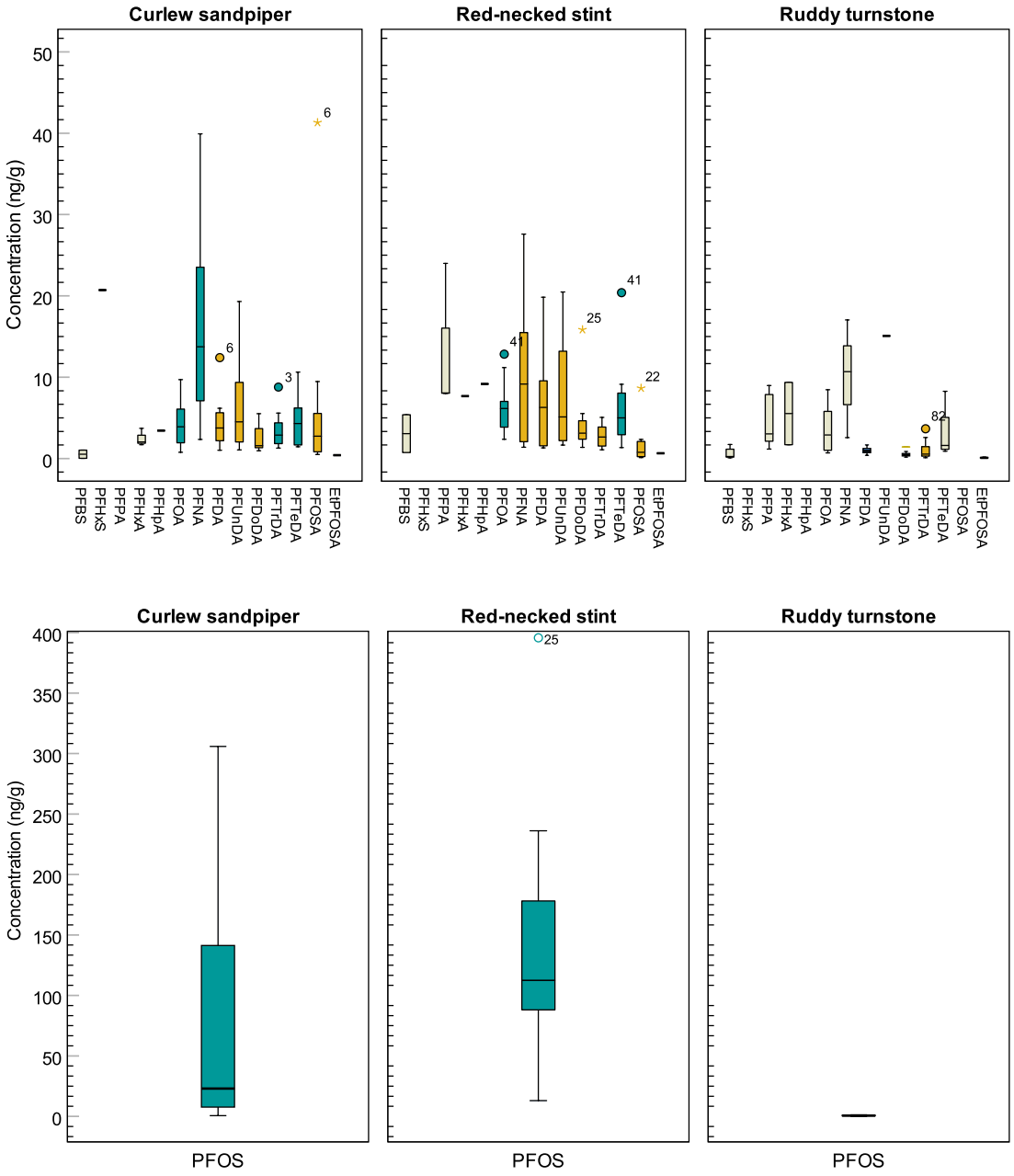

Figure 4.3.: Rbc concentrations of selected PFASs in curlew sandpipers (n=23), red-necked stints (n=19) and ruddy turnstones (n=68) presented as box and whisker plots. Only concentrations above the detection limit (LOD) are presented. Boxes are color-coded after detection rate; Green boxes represent DR>50%, yellow boxes represent 50%>DR>25% and white boxes represent compounds with DR<25% within each species.

4.3. PFASs in ruddy turnstones

Levels of PFASs in red blood cells of ruddy turnstones on King Island (n=61) and in South Australia (n=7) were assessed. PFASs were found in 69% of analyzed samples. 11 PFASs were detected with low detection rates (<31%). The most detected compounds were PFOS (31%), PFTrDA (28%) and PFDoDA (22%). PFBS, PFPA, PFHxA, PFOA, PFNA, PFDA, PFUnDA, PFTeDA and EtPFOSA were detected in few samples (<12%), while PFHxS, PFHpA and PFOSA were not detected in rbc samples of ruddy turnstones. Of the three most detected compounds, medians ranged PFOS ($0.63\,ng\,g^{-1}$), PFTrDA ($0.54\,ng\,g^{-1}$) and PFDoDA ($0.47\,ng\,g^{-1}$). Compared to previous avian studies, these levels are among the lowest reported. PFOS was the dominating contaminant overall, constituting 55% of ΣPFAS on average. This predominance was considerably lower than in the other studied species.

Due to the low detection rates of individual PFASs, temporal and spatial trends were only investigated based on ΣPFAS in the ruddy turnstone population. Figure 4.4 and 4.5 show ΣPFAS rbc concentrations in ruddy turnstones across sample sites and years. Figures 4.4 and 4.5 show that median ΣPFAS did not vary considerably across sample sites or years. A few samples from rural parts of mainland South-Australia (Blackfellows Cave 2015 (n=5) and Nene Valley 2016 (n=2)) were included for comparison. There were no observable differences in ΣPFAS concentrations in ruddy turnstones sampled at King Island and mainland Australia in 2015 and 2016.

Among ruddy turnstone sample sites, Denby Bay was hypothesized to be the cleanest area based on less influence by the human population on the island. North and Central Manuka are in vicinity (6-7km) of the local airport and Burges Bay is closer to the largest township on the island. Interestingly, maximum ΣPFAS concentration ranked North Manuka>Central Manuka>Burges Bay>Denby Bay. These ΣPFAS concentrations were influenced by a few compounds with otherwise low detection rates having considerably high concentrations. Airports have sometimes been linked to emissions of PFASs due to the use of aqueous film-forming foam (AFFF) for fire protection [3, 26]. For example, in Russel et al.'s study on PFASs in northern cardinals of Atlanta and Hawaii, the distance to the nearest international airport affected PFAS serum levels in birds on Hawaii, however, not in birds of Atlanta. The airport near the Manuka sites is a small regional airport, and the use of AFFFs may not be prominent. In addition, local contamination of the below lying sediments of airports may not always spread widely to the surrounding environment and wildlife [33].

Regarding ΣPFAS levels in ruddy turnstones over time, the median ΣPFAS concentrations were consistent across sample years, but an interesting trend of higher maximum concentration in earlier sample years was observed (Figure 4.5).

However, this trend was merely an interesting observation, and the distribution of ΣPFAS across years suggests no significant temporal trends.

The findings of PFASs in blood cells indicate that ruddy turnstones are yearly exposed to these contaminants. As these birds are migrants, contaminant levels can reflect the exposure from other locations than the sample site [91]. Consequently, the observed ΣPFAS concentrations are either a result of low exposure on King Island or traces of accumulation somewhere else. Sampling of ruddy turnstones occurred earlier in the season compared to other species in this study, making it more challenging to assess the origin of exposure. In 2014-2018 birds were sampled early in the season (late November/early December), and in 2019, birds were sampled closer to their next migration departure (March). 2019 median ΣPFAS concentrations were comparable to other sampling years (Figure 4.5), indicating that the levels were somewhat consistent throughout the season. Regardless of the origin of the detected PFASs, assuming similar elimination and uptake between species, the exposure to ruddy turnstones on King Island was lower than of the other studied species. The occurrence of PFASs in avian rbc sampled at King Island and rural areas of South-Australia were comparable to previously reported plasma levels of birds inhabiting smaller islands. Levels were of the same magnitude as reported plasma levels in seabirds of the Southern Ocean [57, 69] and the Atlantic Ocean [41]. The predominance of PFOS also coincides with these studies. The findings of PFASs in birds inhabiting areas with low human density also reflects the wide spread of these contaminants.

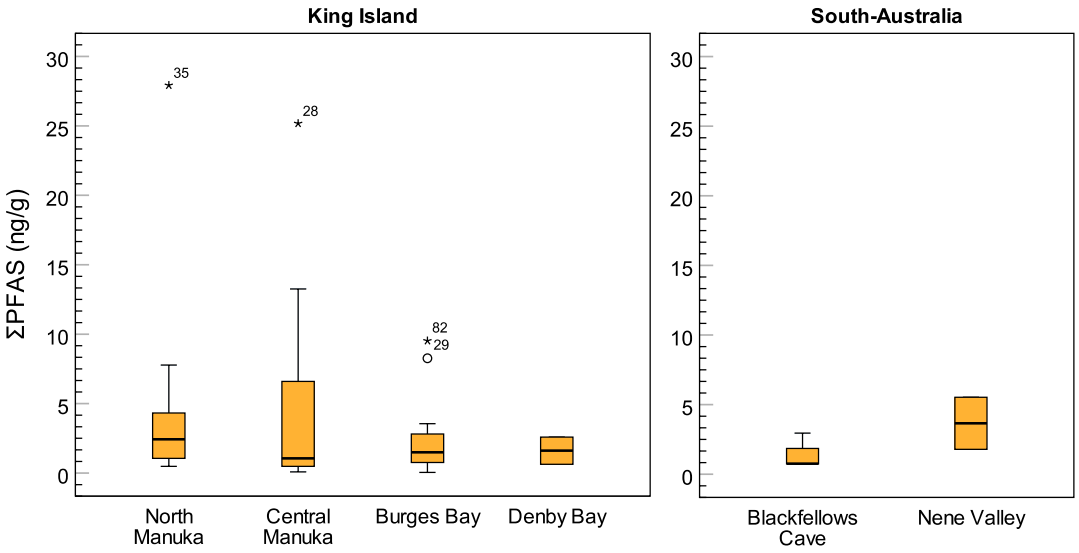

Figure 4.4.: ΣPFAS rbc concentrations in ruddy turnstones sampled on King Island and South-Australia locations. Outliers are labeled (o) and (*) if outside 1.5 and 3 times the interquartile range, respectively

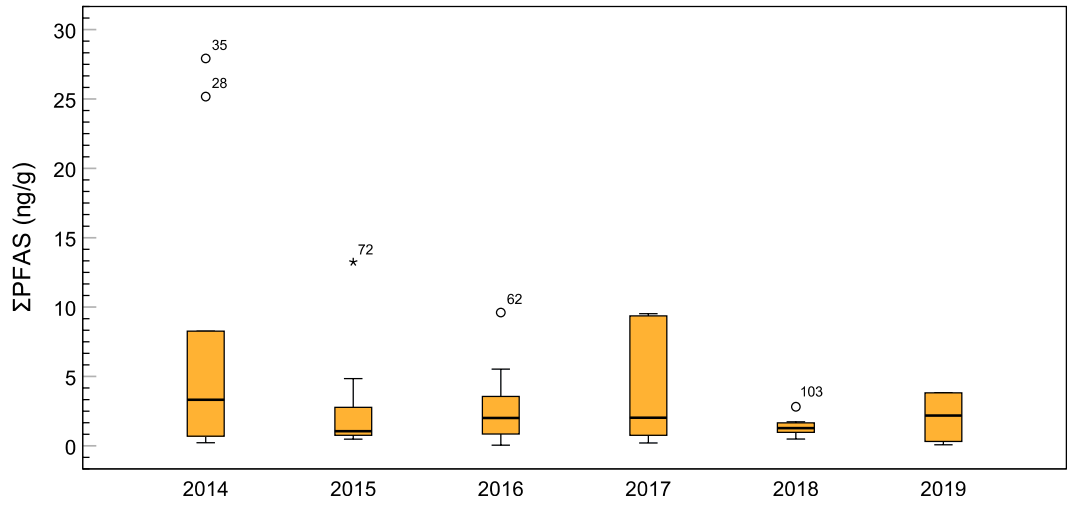

Figure 4.5.: Yearly ΣPFAS rbc concentrations in ruddy turnstones sampled at King Island and South-Australia. Outliers are labeled (o) and (*) if outside 1.5 and 3 times the interquartile range, respectively.

4.4. PFASs in curlew sandpipers and red-necked stints

Occurrence of PFASs was overall higher in the populations of curlew sandpipers and red-necked stints in this study, most likely due to the sites the birds frequented. Birds at the Western Treatment Plant (WTP) were sampled in late December (2013-2018) and birds near Yallock Creek were sampled later in the season (January-April, 2017-2019). Both sites are areas with human and industrial influence. Yallock Creek is however regarded as a site with less human impact.

4.4.1. Yallock Creek

Nine PFASs were detected in rbc samples of curlew sandpipers in Yallock Creek (n=11; 2018, 2019) with median ΣPFAS of 15.1 $\mathrm{ng\,g^{-1}}$. Detected PFASs were PFBS (18%), PFOS (91%), PFOA (45%), PFNA (45%), PFDA (27%), PFUnDA (36%), PFDoDA (18%), PFTrDA (27%) and PFTeDA (18%). PFOS was the most ubiquitous of the selected PFASs analyzed in curlew sandpiper rbc from Yallock Creek, and the only PFAS detected in more than half of the samples. PFOS was the predominating PFAS, constituting 41% of ΣPFAS on average. Detected PFOS concentrations ranged from 0.62 to 26.9 $\mathrm{ng\,g^{-1}}$ and were similar between years, with median PFOS concentration of 7.29 and 8.27 $\mathrm{ng\,g^{-1}}$ in 2018 and 2019, respectively. Detected PFOS rbc concentrations in curlew sandpipers at Yallock Creek were of the same magnitude as previously reported plasma levels in northern goshawk nestlings in Northern Norway [42]. Similar PFOS median concentrations were also reported in serum of northern cardinals in metropolitan areas of Atlanta USA, however, with a much larger range (2.9-180 $\mathrm{ng\,mL^{-1}}$ plasma).

Only a total of four red-necked stint samples from Yallock Creek (2017,2019) were analyzed. Representative PFAS occurrence profiles for red-necked stints could thus not be assessed for this site. Of the analyzed samples of red-necked stints, PFOS and long-chained PFCAs, PFUnDA, PFDoDA and PFTrDA were detected in one bird in 2019. Of the other three samples, PFPA was detected in one bird in 2017, and otherwise none of the target analytes were detected.

ΣPFAS concentrations in curlew sandpipers at the Yallock Creek site were significantly higher ($p<0.0001$) than the concentrations found in ruddy turnstones on King island. Although there are no known identifiable point sources of PFASs in the Yallock Creek area, diffuse inputs of nutrients, pesticides and agricultural runoff are identified in the Western Port Bay area [166]. The bay is semi-enclosed with some oceanic input from the Bass Strait, however, water residence time in Western Port Bay is much longer than what is expected in the Bass Strait exposed King Island. The time for contaminants to accumulate in sediments of Western

Port Bay is therefore expected to be longer. In addition, human influence on the Yallock Creek sample site is expected to be much more significant than the impacts on King Island based on human population density.

4.4.2. The Western Treatment Plant

Median ΣPFAS concentrations in curlew sandpipers (n=12) and red-necked stints (n=15) sampled at the WTP location were 186 and 129 ng g^{-1}, respectively. These levels were considerably higher than what was found at other investigated locations. In addition, detection rates of PFASs in birds of this site were considerably higher (Figure 4.2), with several chemicals frequently detected. This was not unexpected as PFASs tend to be found in higher concentrations in wildlife sampled near identifiable point sources such as wastewater treatment plants and industrial areas. 96% of samples analyzed from the WTP site contained detectable levels of one or more target PFASs, and all target analytes were detected at some point. PFOS was ubiquitous and most abundant, with overall detection rates and median concentrations of 100% and 149 ng g^{-1}, and 80% and 116 ng g^{-1} in curlew sandpipers and red-necked stints, respectively. PFOA, PFTrDA and PFTeDA were the only other chemicals with overall (all years combined) detection rates above 50% in both curlew sandpipers and red-necked stints at the WTP site.

13 PFASs were detected in curlew sandpipers. PFOS, PFTrDA, PFTeDA and PFOSA were detected most frequently with high detection rates overall (>80%). PFOA, PFNA, PFDA and PFDoDA had medium detection rates (58-67%), while PFHxS, PFHxA, PFHpA, PFUnDA and EtPFOSA had low overall detection rates (8-25%). The shortest chained perfluoroalkyl acids, PFBS and PFPA, were not detected in curlew sandpipers at the WTP site.

In red-necked stints, 14 target PFASs were detected, but detection rates were generally lower than those of curlew sandpipers. PFASs were detected in all samples with the exception of one bird sampled in 2016. PFOA was the second most detected chemical after PFOS with overall detection rate of 73%. Similar to curlew sandpipers, the longest chained PFCAs, PFDoDA, PFTrDA and PFTeDA and the PFOS precursor PFOSA, were of the most detected compounds, however, with medium detection rates (47-67%). PFNA, PFDA and PFUnDA were detected in 33% of red-necked stints samples at the WTP. Occurrence of PFBS, PFPA, PFHxA, PFHpA and EtPFOSA was low (7%) and PFHxS was not detected. The lower overall detection rate compared to curlew sandpipers was heavily influenced by little occurrence of PFASs in samples analyzed from 2017 (n=4). In 2017, PFBS, PFOS, PFPA and PFOSA were the only detected chemicals, with each compound detected once.

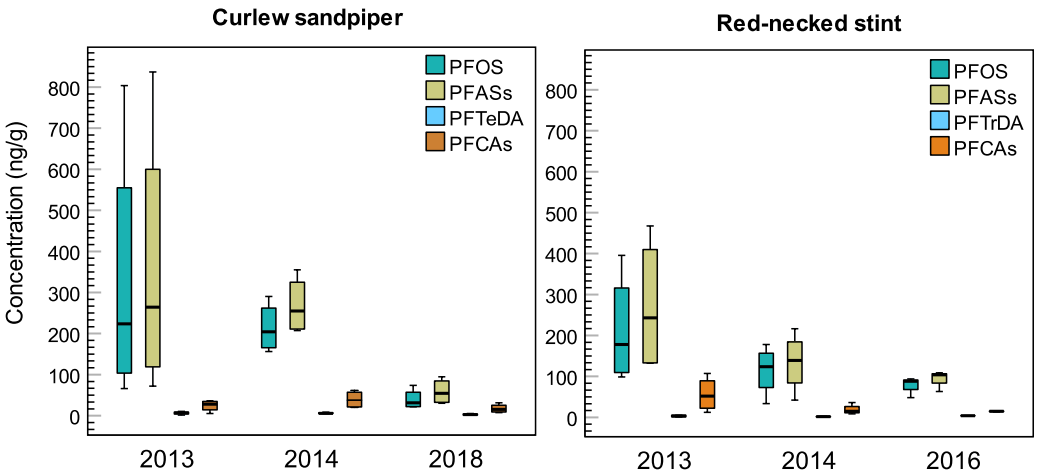

Figure 4.6.: Yearly PFOS, ΣPFAS (PFASs) and ΣPFCA (PFCAs) rbc concentrations in curlew sandpipers (2013, 2014, 2018) and red-necked stints (2013, 2014, 2016) at the Western Treatment Plant. PFOS distribution in curlew sandpipers was significantly different across years (p=0.039).

Yearly PFAS concentrations at the Western Treatment Plant

Figure 4.6 shows concentrations of chemicals with DR>50% every single year (PFOS and PFTeDA), ΣPFAS and ΣPFCA each year in curlew sandpipers and red-necked stints at the Western Treatment Plant. It should be noted that the only overlapping sampling years between these species were 2013-14. 2017 results from red-necked stints were omitted from Figure 4.6 due to insufficient data this year. For the record, the ΣPFAS median concentrations for red-necked stints of 2017 was 241 ng g^{-1}, due to the PFOS detect of 235 ng g^{-1}.

PFOS was the dominant PFAS in WTP samples, constituting on average 75% and 77% of ΣPFAS in curlew sandpipers and red-necked stints, respectively. The combined sum of perfluoroalkyl sulfonates (ΣPFSA) was also predominated by PFOS, which constituted on average 99.5% and 99.8% of ΣPFSA in sandpipers and stints, respectively. PFOS will therefore parallel and represent ΣPFSA in Figure 4.6. ΣPFCA was predominated by long-chained PFCAs, which constituted on average 94% and 90% of ΣPFCA in sandpipers and stints at this site.

From Figure 4.6, a trend of decreasing PFOS and ΣPFAS concentration in later sample years could be observed for both species. Median PFOS concentration de-

creased from 223 and 204 ng g^{-1} in 2013 and 2014, to 31.3 ng g^{-1} in 2018 among curlew sandpipers, and from 178 and 124 ng g^{-1} in 2013 and 2014 to 88.0 ng g^{-1} in 2016 among red-necked stints. Median ΣPFCA did not seem to change considerably with time. Detection rates of most PFCAs were, however, lower in 2016-17 in the red-necked stint population. The observed decreasing trends of PFOS and ΣPFAS, was only significant for PFOS concentrations across years in the curlew sandpiper population (p=0.039). PFOS levels in the earlier sampling years, 2013 and 2014, were not significantly different, which can also be seen in Figure 4.6.

Although PFOS was the dominant PFAS, the distribution of ΣPFAS in curlew sandpipers was not statistically different across years (p=0.058). It should be noted that the number of samples per year-group was low (n=3-4) and making conclusions regarding temporal trends should be done with caution. Although trends of decreasing median PFOS and ΣPFAS concentrations were observed in red-necked stints (Figure 4.6), no trends were significant. The observation is interesting, since some studies have reported a decrease in PFOS in later years after the phase out and regulatory efforts of this chemical [34, 181–183]. This trend has not been consistent globally and others report an increase or no trends at all [63]. Temporal differences do often not emerge when comparing shorter time intervals [57], and trends could possibly be more evident if the missing time intervals between 2014 and 2018 were investigated for curlew sandpipers. In addition, increasing sample size per year would be needed to be able to make definite interpretations and conclusions regarding temporal trends.

Is the Western Treatment Plant a hotspot for PFASs?

The high occurrence of PFASs and high PFOS concentration at the WTP site compared to other study sites was not surprising as PFASs are almost always found in higher concentrations in wildlife inhabiting areas of human influence. Wastewater treatment serves as a link between humans and the environment and is often a source of a variety of contaminants of emerging concern, such as personal care products, pharmaceuticals, surfactants, flame retardants, plasticizers, pesticides and more [184, 185]. PFASs have previously been detected in wastewater worldwide [31, 182]. The Western Treatment Plant treats half of the sewage in Melbourne; a city with a human population of approximately 5 million. A study on perfluoroalkyl sulfonates, perfluoroalkyl carboxylic acids, fluorotelomer sulfonates and chlorinated perfluoroether sulfonic acids (F53-B) in Australian WWTPs showed that PFASs were detected across all matrices in all 19 investigated plants [186]. The Western Treatment Plant was not included in the latter study.

Elevated levels of PFASs in tissues of wildlife inhabiting areas with wastewater effluents have previously been reported [70, 76, 81]. PFOS concentrations in blood cells sampled at WTP are concerning as they were in the same magnitude as some

of the highest previously reported plasma and serum concentrations, such as in tree swallow nestlings in areas with polluted grounds and surface waters [70], pintail ducks (*Anas acuta*) feeding in Tokyo Bay [73] and top-predators such as bald eagle nestlings from areas influenced by WWTPs and industrial discharges [65] and the avian top-predator glaucous gull in the Norwegian Arctic [74]. Comparing the 2013-14 levels of PFOA, PFNA, PFDA, PFDoDA and PFTrDA to previously reported concentration in plasma and blood, the observed concentrations in birds from the WTP were in the upper scale of what has previously been reported. PFTeDA is less frequently detected and/or included in previous studies on plasma and blood. The observed rbc concentrations of PFTeDA was an order of magnitude higher than most previously reported plasma concentrations, and the same magnitude as what is reported in liver samples in birds of Korea [64].

Biological treatment of sewage is performed in multiple large anaerobic and aerobic lagoons at the WTP. PFSAs and PFCAs are, however, regarded as recalcitrant to biodegradation [6, 31]. The biological treatment may therefore not be effective in removing PFAAs released in sewage. In addition, previous studies on wastewater have reported increased concentrations of some PFAAs in wastewater effluents compared to influents, thus indicating the formation of stable PFASs through biotransformation of precursor compounds during treatment [186–188]. The high levels of PFOS and PFCAs may therefore stem from a combination of direct releases and transformation of emitted precursors. Interestingly, the PFOS precursor PFOSA was detected frequently in samples collected at the WTP site, but was completely absent from samples obtained from all other sites (Figure 4.2). This indicates the emission of such precursors at the WTP site. Median PFOSA rbc concentrations in curlew sandpipers ($4.48\,\mathrm{ng\,g^{-1}}$) and red-necked stints ($1.84\,\mathrm{ng\,g^{-1}}$) at the WTP in 2013-14 were of the same magnitude as some of the highest reported plasma PFOSA levels, which were reported in tree swallows collected in areas influenced by numerous human activities, including wastewater treatment [65]. The latter study also reported some of the highest PFOS levels in avian plasma (Table 2.2), which were of the same magnitude as the 2013-14 PFOS levels at the WTP.

ΣPFAS and PFOS concentrations were significantly ($p<0.0001$) higher in curlew sandpiper samples collected at the WTP site compared to Yallock Creek. These results suggest that the WTP could be a hotspot for PFOS exposure. The distribution of ΣPFCA was not significantly different across sample sites. This comparison is, however, not representative as Yallock Creek data was obtained from later sample years only, and a decrease in PFOS and ΣPFAS concentrations at the WTP in 2018 was observed (Figure 4.6). As samples from other locations than the WTP were not obtained from the 2013 and 2014 seasons, it was not possible to assess whether the higher contaminant load these years were site specific to WTP or represented in all curlew sandpipers and red-necked stints at this time. Of curlew

sandpipers, samples were obtained from both the WTP and Yallock Creek in the 2018/19 season, making a representative comparisons of sites possible. This was done comparing samples collected at the WTP late December of 2018 with Yallock Creek samples collected mid-January of 2019.

In the 2018/19 season, median ΣPFAS concentration in curlew sandpiper blood cells was $54.0\,\mathrm{ng\,g^{-1}}$ at the WTP (n=4) site, while $8.84\,\mathrm{ng\,g^{-1}}$ at Yallock Creek (n=5), indicating that the contaminant load in birds sampled near the wastewater treatment plant was higher than in those residing in the Western Port Bay area. This difference was primarily impacted by differences in PFOS concentrations and overall detection rates. Median PFOS concentrations were three times higher at the WTP site ($31.4\,\mathrm{ng\,g^{-1}}$) than in Yallock Creek ($8.27\,\mathrm{ng\,g^{-1}}$) in the 2018/19 season. This site difference is accordant with expectations made from previous studies reporting increased plasma concentrations near point sources [70]. The differences in PFOS and ΣPFAS concentrations between sites in the 2018/19 season were, however, not statistically significant (ΣPFAS, p=0.067; PFOS, p=0.063).

Shorebirds are particularly prone to exposure of contaminants because they feed on marine invertebrates from sediments, which are sinks for environmental pollutants [189]. During migration, these birds feed and rest on shorelines of stop-over sites, and the measured contaminant levels in these migratory birds could potentially stem from exposure during migration and not from the non-breeding grounds in Australia. Determining the origin of the observed contaminant levels is thus not straightforward. In this case, because the birds were sampled weeks after their migration return, and blood concentrations reflect a more short-term dietary exposure [190], it is likely that the elevated blood ΣPFAS concentrations are a result of exposure at the Western Treatment Plant. Nevertheless, since the high PFOS levels in 2013-14 at the WTP site could not be compared with other habitats these years, it remains unclear if the high exposure is attributed to the non-breeding habitat or if levels were generally high in the arriving migrants these years. Further studies should look into PFOS concentrations in curlew sandpipers and red-necked stint at other sample locations than the WTP these years.

4.5. Correlations and species differences

The major trends of the presented results were clearly visualised by principal component analysis (PCA). PCA biplots with loadings of age and absolute concentrations of PFOS, ΣPFAS, ΣPFSA and ΣPFCA and sample scores grouped by species and sample regions are presented in Figure 4.7 and Figure 4.8. A similar biplot grouped by year is presented in Figure F.1. PC1 (Dim1) accounted for 70.5% of the observed variation and was mostly influenced by PFOS, which was strongly correlated with ΣPFAS. PC2 (Dim2) accounted for 20.1% of variation and seemed to be influenced mostly by age. A heat map of correlations was constructed and is presented in Figure F.2. This revealed a slightly positive correlation between ΣPFCA and age. Such correlation was not significant for PFOS and ΣPFAS. Relationships between age and PFASs in birds are not comprehensively studied [59]. A few previous studies report a difference between PFOS liver concentrations in adults and juvenile birds [81], but most studies do not investigate this relationship, or report a lack of it [62, 191]. Many mammalian studies report a negative correlation between age and PFAAs, while some find no differences [191]. The correlation between age and ΣPFCA is interesting and may be a reflection of the bioaccumulative properties of the long-chained homologues, which were the dominating PFCAs [27]. Factors potentially influencing relationships between age and contaminant levels are body-size, diet and tropic position [192]. Other biological factors potentially influencing the PFAS concentrations, such as sex, were not investigated.

The most evident differences between species could be observed in the PCA biplots. As seen from Figure 4.7 and 4.8, the contaminant concentrations were considerably lower in ruddy turnstones sampled at shorelines of King Island compared to curlew sandpipers and red-necked stints sampled near the city of Melbourne (WTP and Western Port (=Yallock Creek)). The clear observable pattern of ruddy turnstone samples to the left in the plot is consistent with the observed low ΣPFAS concentrations with low variability between sample sites in the ruddy turnstone population (Figure 4.4). This clustering was not observed in curlew sandpipers and red-necked stints (Figure 4.7) due to considerably different sample sites and high variability of concentrations at the WTP (Figure 4.8). The median ΣPFAS concentration in ruddy turnstones ($1.58\,\mathrm{ng\,g^{-1}}$) was significantly lower ($p<0.0001$) than median ΣPFAS concentrations in curlew sandpipers ($40.1\,\mathrm{ng\,g^{-1}}$) and red-necked stints ($117\,\mathrm{ng\,g^{-1}}$). This difference could be attributed to the degree of human influence at the site the birds frequented. Sample regions distributed according to expected degree of human influence in the regional grouped biplot (Figure 4.8), with King Island samples appearing furthest to the left in the plot, Yallock Creek to the right, and WTP rightmost, closest to the contaminant variables.

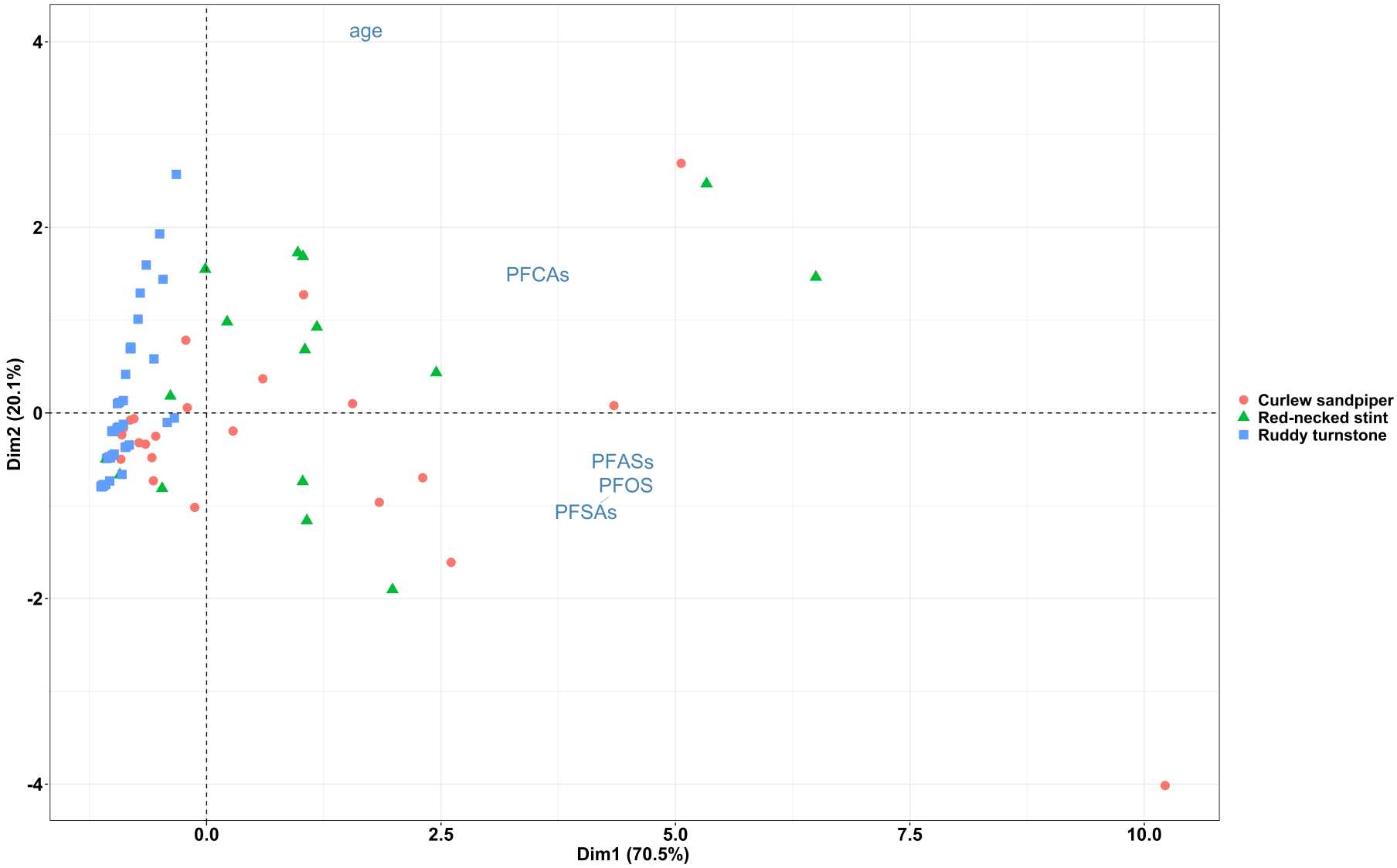

Figure 4.7.: PCA biplot of age and absolute concentrations of PFOS, PFCAs (ΣPFCA), PFSAs (ΣPFSA) and PFASs (ΣPFAS) grouped by species.

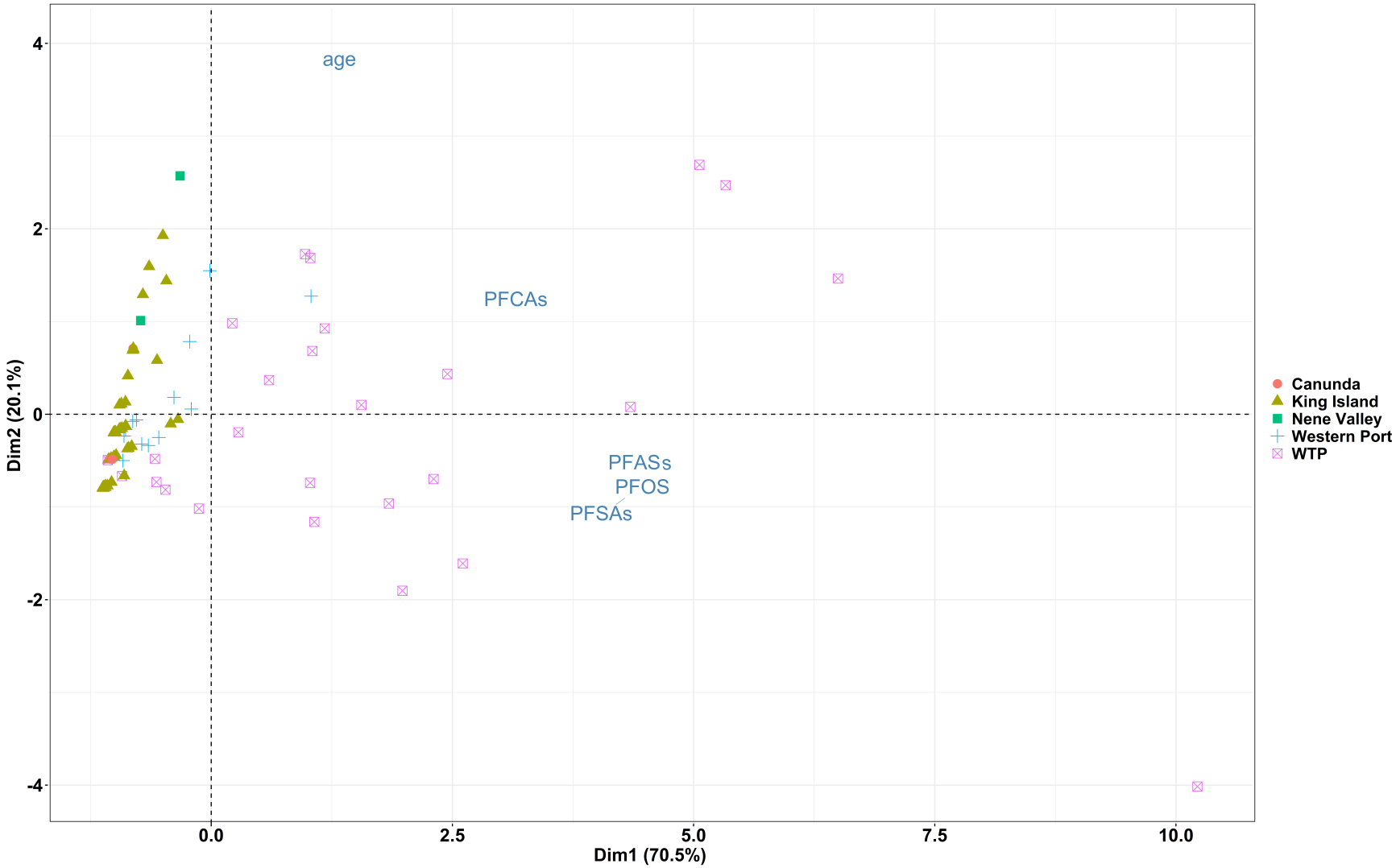

Figure 4.8.: PCA biplot of age and absolute concentrations PFOS, PFCAs (ΣPFCA), PFSAs (ΣPFSA) and PFASs (ΣPFAS) grouped by region. Western Port corresponds to Yallock Creek.

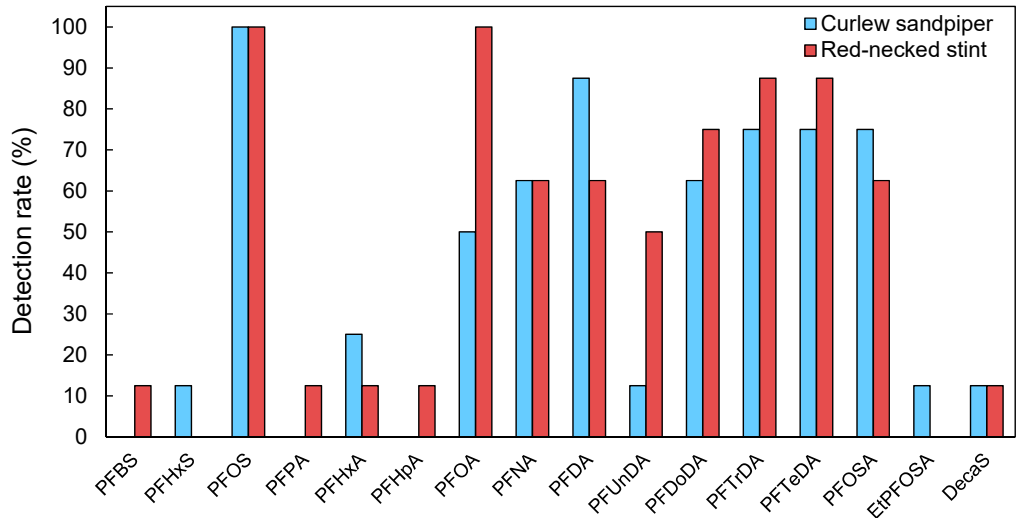

Figure 4.9.: Detection rates (%) of PFASs and one non-fluorinated compound (DecaS) in curlew sandpipers (n=8) and red-necked stint (n=8) at the Western Treatment Plant in the year 2013-14.

Although the median ΣPFAS concentrations in curlew sandpipers (40.1 ng g^{-1}) and red-necked stints (117 ng g^{-1}) differed overall, they were heavily influenced by the number of samples included from sites with less human influence (Yallock Creek; curlew sandpipers, n=11; red-necked stints, n=4). At their common WTP sample site, median ΣPFAS concentrations were similar between curlew sandpipers (187 ng g^{-1}) and red-necked stints (129 ng g^{-1}). As sampling of curlew sandpipers and red-necked stints only co-occured in 2013 and 2014, and because differences in PFAS concentrations in later sampling years could not be ruled out, a species-comparison of occurrence profiles was based only on 2013 and 2014 samples of these species.

Detection rates of PFASs in curlew sandpipers (n=8) and red-necked stints (n=8) at the WTP in 2013-14 are presented in Figure 4.9, and the corresponding concentrations of the most detected PFASs are presented in Figure 4.10. Median PFOS concentrations were 204 ng g^{-1} in curlew sandpipers and 127 ng g^{-1} red-necked stints. These were a magnitude higher than other contaminants concentrations at the site. Although median PFOS concentrations were higher in curlew sandpipers, the distribution of PFOS was not significantly different between the two species. In fact, the distribution of contaminants between species were not significantly different for any of the investigated compounds at the WTP. As can be seen from Figure 4.10 most contaminants showed similar profiles between species. Detection rates were also similar between species (Figure 4.9), with the major differences being detection rates of PFOA and PFUnDA, which were

considerably higher in red-necked stints (PFOA, 100%; PFUnDA, 50%) compared to curlew sandpipers (PFOA, 50%; PFUnDA, 13%). This is interesting, and could potentially indicate a difference in the uptake and/or exposure of these chemicals, but due to the small sample size in this comparison, caution should be applied in the interpretation of these differences.

In summary, major differences in PFAS rbc concentrations were observed between ruddy turstones sampled on King Island and the species frequenting marine areas near the city of Melbourne. These shorebirds are primarily exposed to environmental contaminants through their foraging for small invertebrates in marine areas. Species differences in measured contaminant concentrations can be caused by unequal exposure through diet, foraging and migration, as well as metabolic differences [91, 193]. Assuming similar metabolic capacity between the investigated species, these results indicate that ruddy turnstones are less exposed to PFASs on shorelines of King Island, compared to curlew sandpipers and red-necked stints frequenting areas of more human influence. This is in accordance with what was previously known regarding the environmental fate of PFASs. The similar occurrence profiles of curlew sandpipers and red-necked stints at their common sample sites can be explained by these birds having similar diets and are at times observed foraging together in mixed flocks. Their dietary exposure is therefore expected to be similar within the same habitat.

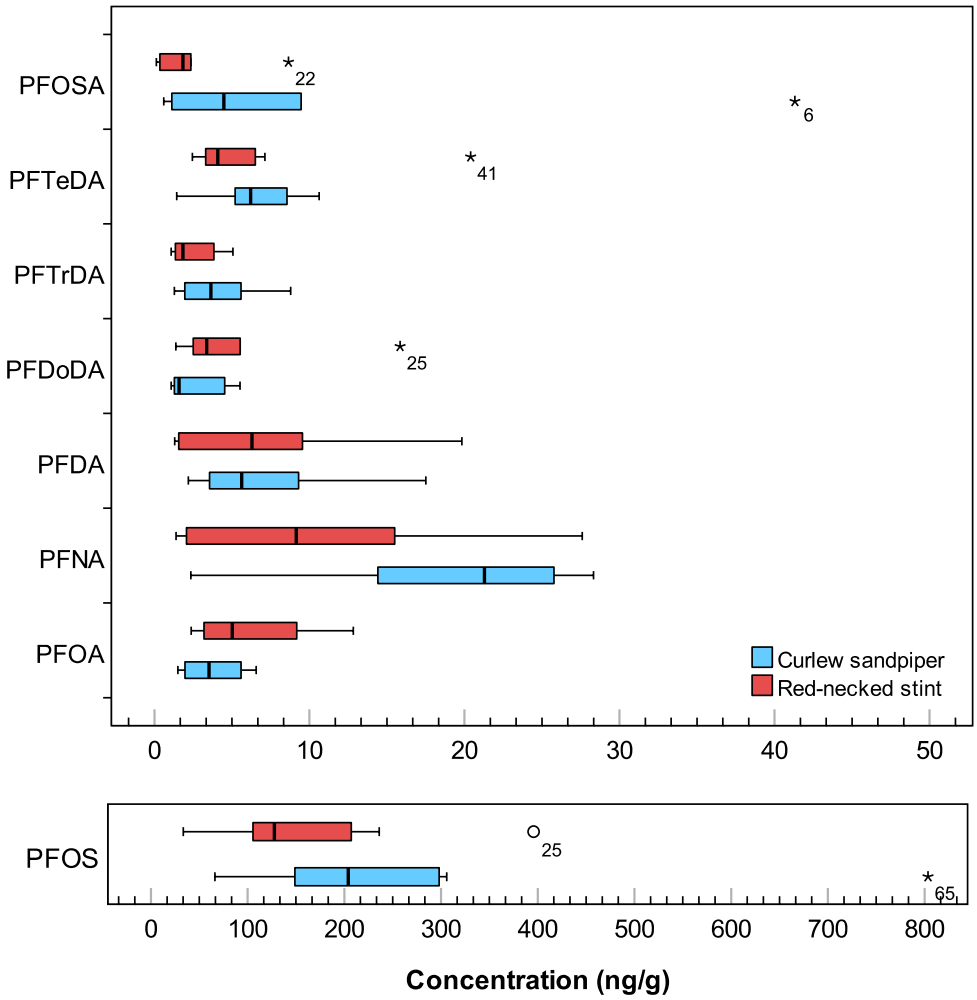

Figure 4.10.: Box and whisker plots with rbc concentrations of the most detected PFASs in curlew sandpipers (n=8) and red-necked stints (n=8) sampled at the Western Treatment Plant in 2013-14. The magnitude of the axes are different. Outliers are labeled (o) and (*) if outside 1.5 and 3 times the interquartile range, respectively.

4.6. Implications of results

In this study, indications of shorebird exposure to PFASs were investigated by determining contamination levels in avian rbc. Toxicological parameters associated with the exposure were not studied, and thus the potential adverse effects on these shorebirds were not assessed. Potential implications of the observed concentrations can be loosely estimated by comparing levels to previous toxicological studies on PFASs in birds. The avian toxicity reference value (TRV, $1700\,\mathrm{ng\,mL^{-1}}$) and predicted no-effect concentration (PNEC, $1000\,\mathrm{ng\,mL^{-1}}$) of PFOS in serum, derived by Newsted et al. [51], is often used for this purpose. The reference value is derived based on characteristics of an avian predator to be protective of all avian species. Sensitivity may still vary depending on species and other biological factors.

PFOS concentrations in red blood cells of ruddy turnstones sampled on King Island and curlew sandpipers and red-necked stints sampled at Yallock Creek were several orders of magnitude lower than the TRV and PNEC derived by Newsted et al.[51]. The significantly higher PFOS levels found in curlew sandpipers and red-necked stint at the WTP site were also a magnitude or more lower than the reference values. There are no reference values reported for rbc separately, and the serum PFOS concentrations of these birds can only be estimated. As PFOS accumulates in serum, it is assumed that the red blood cell concentrations serve as lower estimates of the serum concentrations in these birds. Taking this into account, the birds with the highest PFOS rbc concentrations, such as the curlew sandpiper with PFOS rbc concentration of $804\,\mathrm{ng\,g^{-1}}$ at the WTP site, may have serum concentrations close to the PNEC value. The TRV and PNEC was based on endpoints relating to survival and reproduction and the overall findings of PFOS in these shorebirds suggest that the majority of birds were not at risk from the PFOS exposure at their Australian sites. However, this does not mean that the birds are not subjected to other sub-lethal effects such as endocrine disruption and immunotoxicity.

Observed PFOS rbc concentrations at the WTP site were in some birds higher than the serum concentrations associated with adverse immunological effects in Peden–Adams et al.'s [52] *in ovo* experiment on chickens ($154\,\mathrm{ng\,g^{-1}}$). However, research on immunological effects on PFASs in shorebirds is not available.

Although the occurrence and abundance of PFASs in shorebirds sampled in Western Port Bay and King Island were generally lower than what has been associated with adverse effects, the birds may still be exposed to other toxicants. Other environmental pollutants such as metals, pesticides and pharmaceuticals have been identified as potential contaminants of concern in the Western Port Bay environment [166]. Analysis of these contaminants in sediments of the bay indicated contamination levels of arsenic, nickel and mercury exceeding quality guidelines posing a moderate risk to the ecosystem [194]. The future analysis of

metals and metalloids in the investigated study population is therefore of interest to gain more knowledge on the exposure to contaminants at non-breeding sites in Australia.

4.7. Potential shortcomings and future improvements

PFAS concentrations in red blood cells of the three investigated shorebird species indicated that the exposure at the non-breeding sites in Australia was relatively low in most habitats, except for the WTP site, especially in 2013-14. As these contaminants are usually not studied in rbc separately, nor in these species, it remains challenging to compare levels with previous biomonitoring and toxicological studies. Thus, more studies on PFASs in shorebirds, and studies comparing PFAS concentrations in red blood cells to plasma and whole blood are needed in order to make better comparisons. Further studies should also aim to investigate the exposure of other contaminants in the study population to gain deeper insight into toxicant exposure at the non-breeding grounds. Analysis of other persistent organic pollutants in the remaining plasma fraction are in the works. In addition, samples analyzed for PFASs in this thesis were also prepared for element analysis, and the upcoming results will give insight to not only exposure to toxic metals and metalloids but can be used to explore associations between classes of pollutants.

Exploring the role of pollution in the population decline of migratory shorebirds of the EAAF is of importance for the conservation of these species. Future and ongoing studies on these shorebirds aim to assess exposure concentrations following different migratory routes and assess potential hotspots of pollution at stop-over sites. In this study, effects of migratory route prior to arrival at the non-breeding sites on PFAS concentrations were not assessed, and may be a confounding factor. As concentrations measured in blood reflect more recent dietary exposure [41, 190], contamination levels were assumed to mainly stem from exposure at non-breeding sites. Still, this is not straightforward in migrants.

A drawback of the present study was identified to be low sample sizes per year, making comparisons between sites and species challenging and statistical analysis weaker. In the sample selection process for this project, the number of sample locations were reduced from the larger collection of available sites, in order to maintain a sufficient number of samples per location. In this process, the potential influence of temporal trends was not taken into account, thus leaving only a few samples at each location feasible for comparison per year. This could have been improved by focusing on a smaller number of groups (species+site+year) or by increasing the number of processed samples. Increasing sample sizes in each group would also

make it possible to apply other multivariate techniques such as generalized linear models, in which one could investigate how different factors such as age separately influence the concentrations of PFASs [58].

As samples of curlew sandpipers and red-necked stints were not analyzed from locations other than the WTP in 2013-14, further work should look into analyzing samples collected at other sites these years to investigate if PFOS exposure was generally high in birds in the earlier sampling years or if the WTP is a hotspot for exposure to PFASs at their non-breeding sites. Of the remaining samples that were not selected for this thesis, samples of red-necked stints from Yallock Creek and other locations in Western Port Bay these years are available.

Since only data above the detection limit was used for statistics, the degree of representativeness depended greatly on detection frequency. As the overall detection frequencies were low, this limited the discussion to only a few compounds. Methods for including left-censored data for statistical analysis would improve the results and discussion. Numerous methods exists for this purpose, and usually substitution of non-detects with constants such as 0, LOD, LOD/2 and LOD/$\sqrt{2}$ is used when there is a small degree of censored data [195]. Other methods include estimating the central tendency and spread of censored data, which provides a less biased approach. In this study, with the majority of the data being censored, the latter approach is more fitting, and methods such as robust maximum likelyhood estimation (rMLE) or Kaplan-Meier techniques should be looked into [195].

Lastly, future work into method development should focus on increasing absolute recoveries during extraction of PFASs from small volume blood samples. Although relative recoveries were acceptable, and the low absolute recoveries showed good precision and consistency, sample loss is challenging when analytes are present in trace amounts and may influence the degree of non-detects.

5. Conclusion

Concentrations of 15 selected PFASs in red blood cells (rbc) of three migratory shorebirds at their non-breeding grounds in Australia were successfully determined. The analytical method demonstrated satisfactory linearity, sensitivity and precision, as well as acceptable extraction efficiency. PFASs were detected in 78% of the analyzed avian rbc samples, illustrating the presence of these contaminants also in this compartment of blood, which has previously not been studied.

Observed differences in PFAS concentrations and detection rates between species and sites suggest that the exposure of these shorebirds to PFASs at non-breeding locations is strongly influenced by the degree of urbanization at the site they frequent. While the ΣPFAS exposure in ruddy turnstones sampled on shorelines of King Island appeared to be low, the exposure to curlew sandpipers and red-necked stints foraging in the marine areas of Melbourne, Yallock Creek and the Western Treatment Plant (WTP), seemed to be higher, which coincides with previous studies finding higher levels of PFASs in wildlife in areas impacted by industrial and urban activities. Differences between sample sites were mainly driven by varying concentrations of PFOS, which were strongly correlated with ΣPFAS concentrations. The PFOS predominance, in addition to dominance of long-chained PFCAs as opposed to short-chained homologues, was also accordant with previous avian studies. Although species differences were mainly attributed to the degree of pollution at the sampling site, biological factors can still influence contaminant concentrations. This was the case for age, which was slightly positively correlated with ΣPFCA. This relationship has been less explored and can be a reflection of the bioaccumulative properties of the long-chained PFCAs.

The rbc concentrations of PFOS, long-chained PFCAs and PFOSA in curlew sandpipers and red-necked stints at the WTP were concerning as they are in the upper scale of what has previously been reported in plasma and blood of avian species, including top-predators, and were in the range associated with potential sublethal health effects. The observed decreases in PFOS and ΣPFAS in later sample years (2016-2018) at the WTP were interesting, potentially indicating that contaminant levels are decreasing at the site. Nevertheless, the reason for this decrease, and whether if it is related to lower emissions at the WTP or generally lower concentrations of PFASs in arriving migrants in later sample years, remains unexplored.

The overall exposure concentrations of PFOS in ruddy turnstones sampled on

King Island and curlew sandpipers and red-necked stints frequenting Yallock Creek suggest that these birds are not at risk from PFOS exposure with regards to the avian toxicity reference value and predicted no-effect concentration derived by Newsted et al. [51] based on survival and reproduction. However, the role of other sub-lethal effects, such as endocrine disruption and immunomodulation, in these shorebirds, as well as exposure during migration, should be explored in future studies. In addition, these birds are susceptible to a wide range of other environmental pollutants, and further studies should therefore also investigate other contaminants of concern in order to gain deeper insights to the exposure to pollutants at non-breeding sites.

Bibliography

1. Paul, A. G., Jones, K. C. & Sweetman, A. J. A first global production, emission, and environmental inventory for perfluorooctane sulfonate. *Environmental Science and Technology* **43,** 386–392 (2009).
2. Krafft, M. P. & Riess, J. G. Selected physicochemical aspects of poly- and perfluoroalkylated substances relevant to performance, environment and sustainability-Part one. *Chemosphere* **129,** 4–19 (2015).
3. Prevedouros, K., Cousins, I. T., Buck, R. C. & Korzeniowski, S. H. Sources, fate and transport of perfluorocarboxylates. *Environmental Science and Technology* **40,** 32–44 (2006).
4. Giesy, J. P. & Kannan, K. Perfluorochemical Surfractants in the Environment. *Environmental Science & Technology* **36,** 146A–152A (2002).
5. Moody, C. A. & Field, J. A. Perfluorinated surfactants and the environmental implications of their use in fire-fighting foams. *Environmental Science and Technology* **34,** 3864–3870 (2000).
6. Giesy, J. P. & Kannan, K. Global Distribution of Perfluorooctane Sulfonate in Wildlife. *Environmental Science & Technology* **35,** 1339–1342 (2001).
7. OECD. *OECD/UNEP Global PFC Group, Synthesis paper on per- and polyfluorinated chemicals (PFCs), Environment, Health and Safety, Environment Directorate* tech. rep. (OECD, 2013).
8. Hansen, K. J., Clemen, L. A., Ellefson, M. E. & Johnson, H. O. Compound-Specific, Quantitative Characterization of Organic Fluorochemicals in Biological Matrices. *Environmental Science & Technology* **35,** 766–770 (2001).
9. Kannan, K., Koistinen, J., Beckmen, K., Evans, T., Gorzelany, J. F., Hansen, K. J., Jones, P. D., Helle, E., Nyman, M. & Giesy, J. P. Accumulation of Perfluorooctane Sulfonate in Marine Mammals. *Environmental Science & Technology* **35,** 1593–1598 (2001).
10. UNEP. *SC-4/17: Listing of perfluorooctane sulfonic acid, its salts and perfluorooctane sulfonyl fluoride* (2009).

11. UNEP. *Candidate POPs: Perfluorohexane sulfonic acid (PFHxS), its salts and PFHxS-related compounds*
URL: http://chm.pops.int/Portals/0/download.aspx?d=UNEP-POPS-PUB-factsheet-PFHxS-201803.English.pdf (accessed on May 24, 2020).
12. UNEP. *SC-9/13: Actions related to perfluorooctanoic acid (PFOA), its salts and PFOA-related compounds* (2019).
13. ECHA. *Inclusion of Substances of Very High Concern in the Candidate List* ED/169/2012 (2012).
14. ECHA. *Inclusion of Substances of Very High concern in the Candidate List for eventual inclusion in Annex XIV* ED/30/2017 (2017).
15. ECHA. *Inclusion of Substances of Very High Concern in the Candidate List for eventual inclusion in Annex XIV* ED/01/2017 (2017).
16. ECHA. *Inclusion of Substances of Very High Concern in the Candidate List for eventual inclusion in Annex XIV* ECHA/01/2020 (2020).
17. Studds, C. E. *et al.* Rapid population decline in migratory shorebirds relying on Yellow Sea tidal mudflats as stopover sites. *Nature Communications* **8,** 14895 (2017).
18. Commonwealth of Australia. *Wildlife Conservation Plan for Migratory Shorebirds* (2015).
19. Melville, D. S., Chen, Y. & Ma, Z. Shorebirds along the Yellow Sea coast of China face an uncertain future - A review of threats. *Emu* **116,** 100–110 (2016).
20. Hargreaves, A. L., Whiteside, D. P. & Gilchrist, G. Concentrations of 17 elements, including mercury, and their relationship to fitness measures in arctic shorebirds and their eggs. *Science of The Total Environment* **408,** 3153–3161 (2010).
21. Honda, M., Robinson, M. & Kannan, K. A rapid method for the analysis of perfluorinated alkyl substances in serum by hybrid solid-phase extraction. *Environmental Chemistry* **15,** 92–99 (2018).
22. Houde, M., Martin, J. W., Letcher, R. J., Solomon, K. R. & Muir, D. C. G. Biological Monitoring of Polyfluoroalkyl Substances: A Review. *Environmental Science & Technology* **40,** 3463–3473 (2006).
23. KEMI. *Occurrence and use of highly fluorinated substances and alternatives* tech. rep. (2015), 27–51.

24. Buck, R. C., Franklin, J., Berger, U., Conder, J. M., Cousins, I. T., de Voogt, P., Jensen, A. A., Kannan, K., Mabury, S. A. & van Leeuwen, S. P. J. Perfluoroalkyl and polyfluoroalkyl substances in the environment: terminology, classification, and origins. eng. *Integrated environmental assessment and management* **7,** 513–541 (2011).

25. Aleksunes, L. M. & Eaton, D. L. *Casarett & Doull´s Toxicology: The Basic Science of Poisons* 9th ed. Chap. 2 (McGraw-Hill Education, 2019).

26. Wang, Z., Cousins, I. T., Scheringer, M. & Hungerbühler, K. Fluorinated alternatives to long-chain perfluoroalkyl carboxylic acids (PFCAs), perfluoroalkane sulfonic acids (PFSAs) and their potential precursors. *Environment International* **60,** 242–248 (2013).

27. Martin, J. W., Mabury, S. A., Solomon, K. R. & Muir, D. C. Bioconcentration and Tissue Distribution of Perfluorinated Acids in Rainbow Trout (*Oncorhynchus Mykiss*). *Environmental Toxicology and Chemistry* **22,** 196 (2003).

28. Scheringer, M., Trier, X., Cousins, I. T., de Voogt, P., Fletcher, T., Wang, Z. & Webster, T. F. Helsingør Statement on poly- and perfluorinated alkyl substances (PFASs). *Chemosphere* **114,** 337–339 (2014).

29. Key, B. D., Howell, R. D. & Criddle, C. S. Fluorinated organics in the biosphere. *Environmental Science and Technology* **31,** 2445–2454 (1997).

30. Krafft, M. P. & Riess, J. G. Per- and polyfluorinated substances (PFASs): Environmental challenges. *Current Opinion in Colloid and Interface Science* **20,** 192–212 (2015).

31. Arvaniti, O. S. & Stasinakis, A. S. Review on the occurrence, fate and removal of perfluorinated compounds during wastewater treatment. *Science of the Total Environment* **524-525,** 81–92 (2015).

32. Fang, X., Wang, Q., Zhao, Z., Tang, J., Tian, C., Yao, Y., Yu, J. & Sun, H. Distribution and dry deposition of alternative and legacy perfluoroalkyl and polyfluoroalkyl substances in the air above the Bohai and Yellow Seas, China. *Atmospheric Environment* **192,** 128–135 (2018).

33. Butt, C. M., Berger, U., Bossi, R. & Tomy, G. T. Levels and trends of poly- and perfluorinated compounds in the arctic environment. *Science of The Total Environment* **408,** 2936–2965 (2010).

34. Routti, H., Gabrielsen, G. W., Herzke, D., Kovacs, K. M. & Lydersen, C. Spatial and temporal trends in perfluoroalkyl substances (PFASs) in ringed seals (*Pusa hispida*) from Svalbard. *Environmental Pollution* **214,** 230–238 (2016).

35. Ahrens, L., Rakovic, J., Axelson, S. & Kallenborn, R. *Source tracking and impact of per- and polyfluoroalkyl substances at Svalbard* tech. rep. (2016).

36. Ellis, D. A., Martin, J. W., De Silva, A. O., Mabury, S. A., Hurley, M. D., Sulbaek Andersen, M. P. & Wallington, T. J. Degradation of Fluorotelomer Alcohols: A Likely Atmospheric Source of Perfluorinated Carboxylic Acids. *Environmental Science & Technology* **38,** 3316–3321 (2004).

37. Kannan, K., Yun, S. H. & Evans, T. J. Chlorinated, brominated, and perfluorinated contaminants in livers of polar bears from Alaska. *Environmental Science and Technology* **39,** 9057–9063 (2005).

38. Palmer, K., Bangma, J. T., Reiner, J. L., Bonde, R. K., Korte, J. E., Boggs, A. S. & Bowden, J. A. Per- and polyfluoroalkyl substances (PFAS) in plasma of the West Indian manatee (*Trichechus manatus*). *Marine Pollution Bulletin* **140,** 610–615 (2019).

39. Bossi, R., Riget, F. F. & Dietz, R. Temporal and Spatial Trends of Perfluorinated Compounds in Ringed Seal (*Phoca hispida*) from Greenland. *Environmental Science & Technology* **39,** 7416–7422 (2005).

40. Kannan, K., Choi, J.-W., Iseki, N., Senthilkumar, K., Kim, D. H., Masunaga, S. & Giesy, J. P. Concentrations of perfluorinated acids in livers of birds from Japan and Korea. *Chemosphere* **49,** 225–231 (2002).

41. Escoruela, J., Garreta, E., Ramos, R., González-Solís, J. & Lacorte, S. Occurrence of Per- and Polyfluoroalkyl substances in Calonectris shearwaters breeding along the Mediterranean and Atlantic colonies. *Marine Pollution Bulletin* **131,** 335–340 (2018).

42. Gómez-Ramírez, P., Bustnes, J., Eulaers, I., Herzke, D., Johnsen, T., Lepoint, G., Pérez-García, J., García-Fernández, A. & Jaspers, V. Per- and polyfluoroalkyl substances in plasma and feathers of nestling birds of prey from northern Norway. *Environmental Research* **158,** 277–285 (2017).

43. Weiss, J. M., Andersson, P. L., Lamoree, M. H., Leonards, P. E., Van Leeuwen, S. P. & Hamers, T. Competitive binding of poly- and perfluorinated compounds to the thyroid hormone transport protein transthyretin. *Toxicological Sciences* **109,** 206–216 (2009).

44. Zabaleta, I., Bizkarguenaga, E., Prieto, A., Ortiz-Zarragoitia, M., Fernández, L. A. & Zuloaga, O. Simultaneous determination of perfluorinated compounds and their potential precursors in mussel tissue and fish muscle tissue and liver samples by liquid chromatography-electrospray-tandem mass spectrometry. *Journal of Chromatography A* **1387,** 13–23 (2015).

45. Tomy, G. T., Budakowski, W., Halldorson, T., Helm, P. A., Stern, G. A., Friesen, K., Pepper, K., Tittlemier, S. A. & Fisk, A. T. Fluorinated organic compounds in an Eastern arctic marine food web. *Environmental Science and Technology* **38,** 6475–6481 (2004).

46. Seacat, A. M., Thomford, P. J., Hansen, K. J., Olsen, G. W., Case, M. T. & Butenhoff, J. L. Subchronic toxicity studies on perfluorooctanesulfonate potassium salt in cynomolgus monkeys. *Toxicological Sciences* **68,** 249–264 (2002).

47. Lau, C., Butenhoff, J. L. & Rogers, J. M. The developmental toxicity of perfluoroalkyl acids and their derivatives. *Toxicology and Applied Pharmacology* **198,** 231–241 (2004).

48. Dewitt, J. C., Peden-Adams, M. M., Keller, J. M. & Germolec, D. R. Immunotoxicity of Perfluorinated Compounds: Recent Developments. *Toxicologic Pathology* **40,** 300–311 (2012).

49. Chang, S.-C., Noker, P. E., Gorman, G. S., Gibson, S. J., Hart, J. A., Ehresman, D. J. & Butenhoff, J. L. Comparative pharmacokinetics of perfluorooctanesulfonate (PFOS) in rats, mice, and monkeys. *Reproductive Toxicology* **33,** 428–440 (2012).

50. Pizzurro, D. M., Seeley, M., Kerper, L. E. & Beck, B. D. Interspecies differences in perfluoroalkyl substances (PFAS) toxicokinetics and application to health-based criteria. *Regulatory Toxicology and Pharmacology* **106,** 239–250 (2019).

51. Newsted, J. L., Jones, P. D., Coady, K. & Giesy, J. P. Avian toxicity reference values for perfluorooctane sulfonate. *Environmental Science and Technology* **39,** 9357–9362 (2005).

52. Peden-Adams, M. M. *et al.* Developmental toxicity in white leghorn chickens following in ovo exposure to perfluorooctane sulfonate (PFOS). *Reproductive Toxicology* **27,** 307–318 (2009).

53. Costantini, D., Blévin, P., Herzke, D., Moe, B., Gabrielsen, G. W., Bustnes, J. O. & Chastel, O. Higher plasma oxidative damage and lower plasma antioxidant defences in an Arctic seabird exposed to longer perfluoroalkyl acids. *Environmental Research* **168,** 278–285 (2019).

54. Smithwick, M. *et al.* Circumpolar study of perfluoroalkyl contaminants in polar bears (*Ursus maritimus*). *Environmental Science and Technology* **39,** 5517–5523 (2005).

55. Martin, J. W., Smithwick, M. M., Braune, B. M., Hoekstra, P. F., Muir, D. C. & Mabury, S. A. Identification of Long-Chain Perfluorinated Acids in Biota from the Canadian Arctic. *Environmental Science and Technology* **38,** 373–380 (2004).

56. Kannan, K., Franson, J. C., Bowerman, W. W., Hansen, K. J., Jones, P. D. & Giesy, J. P. Perfluorooctane Sulfonate in Fish-Eating Water Birds Including Bald Eagles and Albatrosses. *Environmental Science & Technology* **35,** 3065–3070 (2001).

57. Roscales, J. L., Vicente, A., Ryan, P. G., González-Solís, J. & Jiménez, B. Spatial and Interspecies Heterogeneity in Concentrations of Perfluoroalkyl Substances (PFASs) in Seabirds of the Southern Ocean. *Environmental Science and Technology* **53,** 9855–9865 (2019).

58. Bustnes, J. O., Borgå, K., Erikstad, K. E., Lorentsen, S.-H. & Herzke, D. Perfluorinated, brominated, and chlorinated contaminants in a population of lesser black-backed gulls (*Larus fuscus*). *Environmental Toxicology and Chemistry* **27,** 1383 (2008).

59. Blévin, P., Angelier, F., Tartu, S., Bustamante, P., Herzke, D., Moe, B., Bech, C., Gabrielsen, G. W., Bustnes, J. O. & Chastel, O. Perfluorinated substances and telomeres in an Arctic seabird: Cross-sectional and longitudinal approaches. *Environmental Pollution* **230,** 360–367 (2017).

60. Guruge, K. S., Yeung, L. W., Li, P., Taniyasu, S., Yamashita, N. & Nakamura, M. Fluorinated alkyl compounds including long chain carboxylic acids in wild bird livers from Japan. *Chemosphere* **83,** 379–384 (2011).

61. Jaspers, V. L., Herzke, D., Eulaers, I., Gillespie, B. W. & Eens, M. Perfluoroalkyl substances in soft tissues and tail feathers of Belgian barn owls (*Tyto alba*) using statistical methods for left-censored data to handle non-detects. *Environment International* **52,** 9–16 (2013).

62. Russell, M. C., Newton, S. R., McClure, K. M., Levine, R. S., Phelps, L. P., Lindstrom, A. B. & Strynar, M. J. Per- and polyfluoroalkyl substances in two different populations of northern cardinals. *Chemosphere* **222,** 295–304 (2019).

63. Leat, E. H., Bourgeon, S., Eze, J. I., Muir, D. C., Williamson, M., Bustnes, J. O., Furness, R. W. & Borgå, K. Perfluoroalkyl substances in eggs and plasma of an avian top predator, great skua (*Stercorarius skua*), in the north Atlantic. *Environmental Toxicology and Chemistry* **32,** 569–576 (2013).

64. Barghi, M., Jin, X., Lee, S., Jeong, Y., Yu, J.-P., Paek, W.-K. & Moon, H.-B. Accumulation and exposure assessment of persistent chlorinated and fluorinated contaminants in Korean birds. *Science of The Total Environment* **645,** 220–228 (2018).

65. Elliott, S. M., Route, W. T., DeCicco, L. A., VanderMeulen, D. D., Corsi, S. R. & Blackwell, B. R. Contaminants in bald eagles of the upper Midwestern U.S.: A framework for prioritizing future research based on in-vitro bioassays. *Environmental Pollution* **244,** 861–870 (2019).

66. Holmström, K. E., Johansson, A. K., Bignert, A., Lindberg, P. & Berger, U. Temporal trends of perfluorinated surfactants in Swedish peregrine falcon eggs (*Falco peregrinus*), 1974-2007. *Environmental Science and Technology* **44,** 4083–4088 (2010).

67. Herzke, D., Nygård, T., Berger, U., Huber, S. & Røv, N. Perfluorinated and other persistent halogenated organic compounds in European shag (*Phalacrocorax aristotelis*) and common eider (*Somateria mollissima*) from Norway: A suburban to remote pollutant gradient. *Science of The Total Environment* **408,** 340–348 (2009).

68. Haukås, M., Berger, U., Hop, H., Gulliksen, B. & Gabrielsen, G. W. Bioaccumulation of per- and polyfluorinated alkyl substances (PFAS) in selected species from the Barents Sea food web. *Environmental Pollution* **148,** 360–371 (2007).

69. Munoz, G., Labadie, P., Geneste, E., Pardon, P., Tartu, S., Chastel, O. & Budzinski, H. Biomonitoring of fluoroalkylated substances in Antarctica seabird plasma: Development and validation of a fast and rugged method using on-line concentration liquid chromatography tandem mass spectrometry. *Journal of Chromatography A* **1513,** 107–117 (2017).

70. Custer, C. M., Custer, T. W., Delaney, R., Dummer, P. M., Schultz, S. & Karouna-Renier, N. Perfluoroalkyl Contaminant Exposure and Effects in Tree Swallows Nesting at Clarks Marsh, Oscoda, Michigan, USA. *Archives of Environmental Contamination and Toxicology* **77,** 1–13 (2019).

71. Løseth, M. E. *et al.* White–tailed eagle (*Haliaeetus albicilla*) feathers from Norway are suitable for monitoring of legacy, but not emerging contaminants. *Science of the Total Environment* **647,** 525–533 (2019).

72. Senthilkumar, K., Ohi, E., Sajwan, K., Takasuga, T. & Kannan, K. Perfluorinated compounds in river water, river sediment, market fish, and wildlife samples from Japan. *Bulletin of Environmental Contamination and Toxicology* **79,** 427–431 (2007).

73. Taniyasu, S., Kannan, K., Horii, Y., Hanari, N. & Yamashita, N. A survey of perfluorooctane sulfonate and related perfluorinated organic compounds in water, fish, birds, and humans from Japan. *Environmental Science and Technology* **37,** 2634–2639 (2003).

74. Verreault, J., Houde, M., Gabrielsen, G. W., Berger, U., Haukås, M., Letcher, R. J. & Muir, D. C. Perfluorinated alkyl substances in plasma, liver, brain, and eggs of glaucous gulls (*Larus hyperboreus*) from the Norwegian Arctic. *Environmental Science and Technology* **39,** 7439–7445 (2005).

75. Vorkamp, K., Falk, K., Møller, S., Bossi, R., Rigét, F. F. & Sørensen, P. B. Perfluoroalkyl substances (PFASs) and polychlorinated naphthalenes (PCNs) add to the chemical cocktail in peregrine falcon eggs. *Science of The Total Environment* **648,** 894–901 (2019).

76. Yoo, H., Kannan, K., Seong, K. K., Kyu, T. L., Newsted, J. L. & Giesy, J. P. Perfluoroalkyl acids in the egg yolk of birds from Lake Shihwa, Korea. *Environmental Science and Technology* **42,** 5821–5827 (2008).

77. Sedlak, M. D., Benskin, J. P., Wong, A., Grace, R. & Greig, D. J. Per- and polyfluoroalkyl substances (PFASs) in San Francisco Bay wildlife: Temporal trends, exposure pathways, and notable presence of precursor compounds. *Chemosphere* **185,** 1217–1226 (2017).

78. Bossi, R., Riget, F. F., Dietz, R., Sonne, C., Fauser, P., Dam, M. & Vorkamp, K. Preliminary screening of perfluorooctane sulfonate (PFOS) and other fluorochemicals in fish, birds and marine mammals from Greenland and the Faroe Islands. *Environmental Pollution* **136,** 323–329 (2005).

79. Kannan, K., Tao, L., Sinclair, E., Pastva, S. D., Jude, D. J. & Giesy, J. P. Perfluorinated compounds in aquatic organisms at various trophic levels in a Great Lakes food chain. *Archives of Environmental Contamination and Toxicology* **48,** 559–566 (2005).

80. Kannan, K., Corsolini, S., Falandysz, J., Oehme, G., Focardi, S. & Giesy, J. P. Perfluorooctanesulfonate and related fluorinated hydrocarbons in marine mammals, fishes, and birds from coasts of the Baltic and the Mediterranean Seas. *Environmental Science and Technology* **36,** 3210–3216 (2002).

81. Sinclair, E., Mayack, D. T., Roblee, K., Yamashita, N. & Kannan, K. Occurrence of perfluoroalkyl surfactants in water, fish, and birds from New York State. *Archives of Environmental Contamination and Toxicology* **50,** 398–410 (2006).

82. Ehresman, D. J., Froehlich, J. W., Olsen, G. W., Chang, S.-C. & Butenhoff, J. L. Comparison of human whole blood, plasma, and serum matrices for the determination of perfluorooctanesulfonate (PFOS), perfluorooctanoate (PFOA), and other fluorochemicals. *Environmental Research* **103,** 176–184 (2007).

83. Kelly, B. C., Ikonomou, M. G., Blair, J. D., Surridge, B., Hoover, D., Grace, R. & Gobas, F. A. Perfluoroalkyl contaminants in an arctic marine food web: Trophic magnification and wildlife exposure. *Environmental Science and Technology* **43,** 4037–4043 (2009).

84. Jones, P. D., Hu, W., De Coen, W., Newsted, J. L. & Giesy, J. P. Binding of perfluorinated fatty acids to serum proteins. *Environmental Toxicology and Chemistry* **22,** 2639–2649 (2003).

85. Kannan, K. *et al.* Perfluorooctanesulfonate and Related Fluorochemicals in Human Blood from Several Countries. *Environmental Science & Technology* **38,** 4489–4495 (2004).

86. Sanchez Garcia, D., Sjödin, M., Hellstrandh, M., Norinder, U., Nikiforova, V., Lindberg, J., Wincent, E., Bergman, Å., Cotgreave, I. & Munic Kos, V. Cellular accumulation and lipid binding of perfluorinated alkylated substances (PFASs) – A comparison with lysosomotropic drugs. *Chemico-Biological Interactions* **281,** 1–10 (2018).

87. Kärrman, A., van Bavel, B., Järnberg, U., Hardell, L. & Lindström, G. Perfluorinated chemicals in relation to other persistent organic pollutants in human blood. *Chemosphere* **64,** 1582–1591 (2006).

88. Hanssen, L., Dudarev, A. A., Huber, S., Odland, J. Ø., Nieboer, E. & Sandager, T. M. Partition of perfluoroalkyl substances (PFASs) in whole blood and plasma, assessed in maternal and umbilical cord samples from inhabitants of artic Russia and Uzbekistan. *Science of The Total Environment* **447,** 430–437 (2013).

89. Furness, R. W. *Birds as monitors of pollutants* in *Birds as Monitors of Environmental Change* 1st ed. Chap. 3 (Chapman & Hall, 1993).

90. Becker, P. H. *Chapter 19 Biomonitoring with birds* in *Bioindicators & Biomonitors* 677–736 (Elsevier, 2003).

91. Burger, J. & Gochfeld, M. Marine Birds as Sentinels of Environmental Pollution. *EcoHealth* **1,** 263–274 (2004).

92. Walker, C., Sibly, R., Hopkin, S. & Peakall, D. *Principles of Ecotoxicology* 4th ed. (CRC Press, 2012).

93. BirdLife Australia. *Migratory Shorebird Factsheet*
URL: http://birdlife.org.au/documents/Shorebirds-FactSheet.pdf (accessed on May 24, 2020).

94. Melbourne Water. *Preparing for mass migration at Western Treatment Plant*
URL: https://www.melbournewater.com.au/what-we-are-doing/news/preparing-mass-migration-western-treatment-plant (accessed on May 24, 2020).

95. Battley, P. F. & Rogers, D. I. *Migration* in *Shorebirds of Australia* (CSIRO Publishing, 2007).

96. Stewart, D., Rogers, A. & Rogers, D. I. *Species descriptions* in *Shorebirds of Australia* chap. 6 (CSIRO Publishing, 2007).

97. Hayman, P., Marchant, J. & Prater, T. *Shorebirds: An indentification guide to the waders of the world* (Christopher Helm Publishers, 2011).

98. Australian Government. *Conservation advice: Calidris ferruginea*
URL: http://www.environment.gov.au/biodiversity/threatened/species/pubs/856-conservation-advice.pdf (accessed on May 24, 2020).

99. BirdLife Australia. *Curlew Sandpiper*
URL: http://www.birdlife.org.au/bird-profile/curlew-sandpiper (accessed on May 24, 2020).

100. BirdLife International. *Calidris ferruginea (amended version of 2016 assessment). The IUCN Red List of Threatened Species 2017: e.T22693431A110631069*
URL: https://dx.doi.org/10.2305/IUCN.UK.2017-1.RLTS.T22693431A110631069.en (accessed on May 24, 2020).

101. Melbourne Water. *Bird Species at the Western Treatment Plant*
URL: https://www.melbournewater.com.au/community-and-education/recreation/birdwatching/bird-species-western-treatment-plant (accessed on May 24, 2020).

102. BirdLife Australia. *Red-Necked Stint*
URL: http://www.birdlife.org.au/bird-profile/red-necked-stint (accessed on May 24, 2020).

103. BirdLife International. *Calidris ruficollis. The IUCN Red List of Threatened Species 2016: e.T22693383A93401907*
URL: https://dx.doi.org/10.2305/IUCN.UK.2016-3.RLTS.T22693383A93401907.en (accessed on May 24, 2020).

104. BirdLife International. *Arenaria interpres. The IUCN Red List of Threatened Species 2016: e.T22693336A86589171* (2016).

105. BirdLife Australia. *Ruddy Turnstone*
URL: http://www.birdlife.org.au/bird-profile/ruddy-turnstone (accessed on May 24, 2020).

106. Fifield, F. W. & Haines, P. J. *Environmental Analytical Chemistry* 2nd ed. (Blackwell science Ltd, 2000).

107. Van Eeckhaut, A., Lanckmans, K., Sarre, S., Smolders, I. & Michotte, Y. Validation of bioanalytical LC–MS/MS assays: Evaluation of matrix effects. *Journal of Chromatography B* **877,** 2198–2207 (2009).

108. Ismaiel, O. A., Zhang, T., Jenkins, R. G. & Karnes, H. T. Investigation of endogenous blood plasma phospholipids, cholesterol and glycerides that contribute to matrix effects in bioanalysis by liquid chromatography/mass spectrometry. *Journal of Chromatography B* **878,** 3303–3316 (2010).

109. Miller, J. M. *Cromatography: concepts and contrasts* 2nd ed. (John Wiley & Sons, Inc., 2009).

110. Hennion, M.-C. Solid-phase extraction: method development, sorbents, and coupling with liquid chromatography. *Journal of Chromatography A* **856,** 3–54 (1999).

111. Kole, P. L., Venkatesh, G., Kotecha, J. & Sheshala, R. Recent advances in sample preparation techniques for effective bioanalytical methods. *Biomedical Chromatography* **25,** 199–217 (2011).

112. Simpson, N. J. K. *Solid-phase Extraction: Principles, Techniques, and Applications* (Marcel Decker, Inc., New York, 2000).

113. Hostettmann, K., Marston, A. & Hostettmann, M. *Preparative Chromatography Techniques: Applications in Natural Product Isolation* 2nd ed., 11 (Springer, 1997).

114. Hashemi, B., Zohrabi, P. & Shamsipur, M. Recent developments and applications of different sorbents for SPE and SPME from biological samples. *Talanta* **187,** 337–347 (2018).

115. Masqué, N., Marcé, R. & Borrull, F. New polymeric and other types of sorbents for solid-phase extraction of polar organic micropollutants from environmental water. *TrAC Trends in Analytical Chemistry* **17,** 384–394 (1998).

116. Zhang, K. & Liu, X. Mixed-mode chromatography in pharmaceutical and biopharmaceutical applications. *Journal of Pharmaceutical and Biomedical Analysis* **128,** 73–88 (2016).

117. Chambers, E., Wagrowski-Diehl, D. M., Lu, Z. & Mazzeo, J. R. Systematic and comprehensive strategy for reducing matrix effects in LC/MS/MS analyses. *Journal of Chromatography B* **852,** 22–34 (2007).

118. Kong, R. LC/MS Application in High-Throughput ADME Screen. *Separation Science and Technology* **6,** 413–446 (2005).

119. McDowall, R. Sample preparation for biomedical analysis. *Journal of Chromatography B: Biomedical Sciences and Applications* **492,** 3–58 (1989).

120. Polson, C., Sarkar, P., Incledon, B., Raguvaran, V. & Grant, R. Optimization of protein precipitation based upon effectiveness of protein removal and ionization effect in liquid chromatography–tandem mass spectrometry. *Journal of Chromatography B* **785,** 263–275 (2003).

121. Zhao, M. & Juck, L. *Protein Precipitation for Biological Fluid Samples Using Agilent Captiva EMR—Lipid 96-Well Plates* Agilent Technologies Inc. (2018), 2.

122. Pucci, V., Di Palma, S., Alfieri, A., Bonelli, F. & Monteagudo, E. A novel strategy for reducing phospholipids-based matrix effect in LC–ESI-MS bioanalysis by means of HybridSPE. *Journal of Pharmaceutical and Biomedical Analysis* **50,** 867–871 (2009).

123. Aurand, C., Trinh, A., Ye, M. & Mi, C. Introducing HybridSPE Precipitation Technology for Pharmaceutical Bioanalytical Sample Preparation. *Supelco Reporter* **26.3,** 3–6 (2008).

124. Sigma–Aldrich. *Instructions & Troubleshooting for HybridSPE – Phospholipid (PL) 96-well Plates & Cartridges*
URL: https://www.sigmaaldrich.com/content/dam/sigma-aldrich/docs/Supelco/Product_Information_Sheet/t708008.pdf (accessed on May 24, 2020).

125. Sigma–Aldrich. *HybridSPE – Phospholipid*
URL: https://www.sigmaaldrich.com/catalog/product/supelco/55261u (accessed on May 24, 2020).

126. Ardjomand-Woelkart, K., Kollroser, M., Li, L., Derendorf, H., Butterweck, V. & Bauer, R. Development and validation of a LC-MS/MS method based on a new 96-well Hybrid-SPE™-precipitation technique for quantification of CYP450 substrates/metabolites in rat plasma. *Analytical and Bioanalytical Chemistry* **400,** 2371–2381 (2011).

127. Asimakopoulos, A. G. & Thomaidis, N. S. Bisphenol A, 4-t-octylphenol, and 4-nonylphenol determination in serum by Hybrid Solid Phase Extraction-Precipitation Technology technique tailored to liquid chromatography-tandem mass spectrometry. *Journal of Chromatography B: Analytical Technologies in the Biomedical and Life Sciences* (2015).

128. Baranowska, I. *Handbook of Trace Analysis* (Springer International Publishing, 2016).

129. Islam, M. S., Aryasomayajula, A. & Selvaganapathy, P. R. A review on macroscale and microscale cell lysis methods. *Micromachines* **8** (2017).

130. Li, W., Jian, W. & Fu, Y. *Sample Preparation in LC-MS Bioanalysis* 1st ed. (Wiley, 2019).

131. Vilkhu, K., Mawson, R., Simons, L. & Bates, D. Applications and opportunities for ultrasound assisted extraction in the food industry — A review. *Innovative Food Science & Emerging Technologies* **9,** 161–169 (2008).

132. Nguyen, D. T., Guillarme, D., Rudaz, S. & Veuthey, J. L. Fast analysis in liquid chromatography using small particle size and high pressure. *Journal of Separation Science* **29,** 1836–1848 (2006).

133. Ekman, R., Silberring, J., Westman-Brinkmalm, A. M. & Kraj, A. *Mass Spectrometry: Instrumentation, interpretation and applications* (John Wiley & Sons, Inc., 2009).

134. Ardrey, R. E. *Liquid Chromotography-Mass Spectrometry: an Introduction* **9** (John Wiley & Sons Ltd, 2003).

135. Dass, C. *Fundamentals of Contemporary Mass Spectrometry* (2006).

136. McMaster, M. C. *LC/MS: A Practical User's Guide* (John Wiley & Sons, Inc., 2005).

137. Watson, J. T. & Sparkman, O. D. *Introduction to Mass Spectrometry: Instrumentation, Applications and Strategies for Data Interpretation* 4th ed. (John Wiley & Sons Ltd, 2007).

138. De Hoffmann, E. & Stroobant, V. *Mass Spectrometry: Principles and Applications* 3rd ed. (John Wiley & Sons Ltd, 2007).

139. Niessen, W. M. A. *Liquid Chromatography-Mass Spectrometry* 3rd ed. (Taylor & Francis Group, LLC, 2006).

140. Taylor, P. J. Matrix effects: the Achilles heel of quantitative high-performance liquid chromatography–electrospray–tandem mass spectrometry. *Clinical Biochemistry* **38,** 328–334 (2005).

141. Stahnke, H., Reemtsma, T. & Alder, L. Compensation of matrix effects by postcolumn infusion of a monitor substance in multiresidue analysis with LC-MS/MS. *Analytical Chemistry* **81,** 2185–2192 (2009).

142. Souverain, S., Rudaz, S. & Veuthey, J.-L. Matrix effect in LC-ESI-MS and LC-APCI-MS with off-line and on-line extraction procedures. *Journal of Chromatography A* **1058,** 61–66 (2004).

143. Benijts, T., Dams, R., Lambert, W. & De Leenheer, A. Countering matrix effects in environmental liquid chromatography- electrospray ionization tandem mass spectrometry water analysis for endocrine disrupting chemicals. *Journal of Chromatography A* **1029,** 153–159 (2004).

144. Carmical, J. & Brown, S. The impact of phospholipids and phospholipid removal on bioanalytical method performance. *Biomedical Chromatography* **30,** 710–720 (2016).

145. Miller, J. N. & Miller, J. C. *Statistics and Chemometrics for Analytical Chemistry* 5th ed. (Pearson Education Limited, 2005).

146. Ettre, L. Relative retention expressions in chromatography. *Journal of Chromatography A* **198,** 229–234 (1980).

147. Arvaniti, O. S., Asimakopoulos, A. G., Dasenaki, M. E., Ventouri, E. I., Stasinakis, A. S. & Thomaidis, N. S. Simultaneous determination of eighteen perfluorinated compounds in dissolved and particulate phases of wastewater, and in sewage sludge by liquid chromatography-tandem mass spectrometry. *Analytical Methods* **6,** 1341–1349 (2014).

148. Dettmer–Wilde, K. & Engewald, W. *Practical Gas Chromatography: A Comprehensive Reference* 902 (2014).

149. Lynch, K. L. *Toxicology: Liquid chromatography mass spectrometry* in *Mass Spectrometry for the Clinical Laboratory* chap. 6 (Elsevier Inc., 2017).

150. Asheim, J. *Benzotriazoles, Benzothiazoles and Inorganic Elements as Markers of Road Pollution Sources in a Sub-Arctic Urban Setting (Trondheim, Norway)* NTNU (2018).

151. Poole, C. F. *The Essence of Chromatography* 1st ed. (Elsevier B.V., 2003).

152. Kang, J., Hick, L. A. & Price, W. E. Using calibration approaches to compensate for remaining matrix effects in quantitative liquid chromatography/electrospray ionization multistage mass spectrometry analysis of phytoestrogens in aqueous environmental samples. *Rapid Communications in Mass Spectrometry* **21,** 1457–1466 (2007).

153. Taverniers, I., De Loose, M. & Van Bockstaele, E. Trends in quality in the analytical laboratory. II. Analytical method validation and quality assurance. *TrAC Trends in Analytical Chemistry* **23,** 535–552 (2004).

154. Prichard, E., Crosby, N. T., Day, J. A., Hardcastle, W. A., Holcombe, D. G. & Treble, R. D. *Quality in the Analytical Chemistry Laboratory* 1st ed. (John Wiley & Sons Ltd, 1995).

155. Mitra, S. *Sample Preparation Techniques in Analytical Chemistry* 1st ed. **2** (John Wiley & Sons, Inc., 2003).

156. Skoog, D. A., West, D. M., Holler, J. F. & Crouch, S. R. *Fundamentals of Analytical Chemistry* 9th ed. (Brooks/Cole, Cengage Learning, 2014).

157. Matuszewski, B. K., Constanzer, M. L. & Chavez-Eng, C. M. Strategies for the assessment of matrix effect in quantitative bioanalytical methods based on HPLC-MS/MS. *Analytical Chemistry* **75,** 3019–3030 (2003).

158. Viswanathan, C. T., Bansal, S., Booth, B., DeStefano, A. J., Rose, M. J., Sailstad, J., Shah, V. P., Skelly, J. P., Swann, P. G. & Weiner, R. Quantitative bioanalytical methods validation and implementation: Best practices for chromatographic and ligand binding assays. *Pharmaceutical Research* **24,** 1962–1973 (2007).

159. Asimakopoulos, A. G., Wang, L., Thomaidis, N. S. & Kannan, K. A multiclass bioanalytical methodology for the determination of bisphenol A diglycidyl ethers, p-hydroxybenzoic acid esters, benzophenone-type ultraviolet filters, triclosan, and triclocarban in human urine by liquid chromatography–tandem mass spectromet. *Journal of Chromatography A* **1324,** 141–148 (2014).

160. Caban, M., Migowska, N., Stepnowski, P., Kwiatkowski, M. & Kumirska, J. Matrix effects and recovery calculations in analyses of pharmaceuticals based on the determination of β-blockers and β-agonists in environmental samples. *Journal of Chromatography A* **1258,** 117–127 (2012).

161. Lee, S. & Lee, D. K. What is the proper way to apply the multiple comparison test? *Korean Journal of Anesthesiology* **71,** 353–360 (2018).

162. Lever, J., Krzywinski, M. & Altman, N. Points of Significance: Principal component analysis. *Nature Methods* **14,** 641–642 (2017).

163. Jolliffe, I. *Principal components analysis* 2nd ed. (Springer, 2002).

164. Melbourne Water. *Western Treatment Plant*
URL: https://www.melbournewater.com.au/community-and-education/water-and-sewage-treatment-plants/western-treatment-plant (accessed on May 24, 2020).

165. Melbourne Water. *Birdwatching*
URL: https://www.melbournewater.com.au/community-and-education/recreation/birdwatching (accessed on May 24, 2020).

166. Keough, M. *Understanding the Western Port Environment: A summary of current knowledge and priorities for future research* tech. rep. (Melbourne Water, State Government Victoria, Port Phillip and Westernport CMA, 2011).

167. Australian Bureau of Statistics. *2016 Census QuickStats: King Island*
URL: https://quickstats.censusdata.abs.gov.au/census_services/getproduct/census/2016/quickstat/604031093 (accessed on May 24, 2020).

168. Silcock, P., Karrman, A. & Van Bavel, B. *Advancing perfluorinated compounds analysis using simultaneous matrix monitoring* (Waters, 2009), 1–7.

169. Shoemaker, J., Grimmett, P. & Boutin, B. *Determination of Selected Perfluorinated Alkyl Acids in Drinking Water by Solid Phase Extraction and Liquid Chromatography/Tandem Mass Spectrometry (LC/MS/MS)* in *EPA Document 600/R-08/092* (U.S. Environmental Protection Agency, 2009).

170. Asimakopoulos, A. G., Xue, J., De Carvalho, B. P., Iyer, A., Abualnaja, K. O., Yaghmoor, S. S., Kumosani, T. A. & Kannan, K. Urinary biomarkers of exposure to 57 xenobiotics and its association with oxidative stress in a population in Jeddah, Saudi Arabia. *Environmental Research* **150,** 573–581 (2016).

171. Ahmad, S., Kalra, H., Gupta, A., Raut, B., Hussain, A. & Rahman, M. A. HybridSPE: A novel technique to reduce phospholipid-based matrix effect in LC-ESI-MS Bioanalysis. eng. *Journal of pharmacy & bioallied sciences* **4,** 267–275 (2012).

172. Trimmel, S. *Simultaneous determination of 15 PFCs in harbour porpoises from the Norwegian coast* NTNU (2020).

173. Powley, C. R., George, S. W., Ryan, T. W. & Buck, R. C. Matrix Effect-Free Analytical Methods for Determination of Perfluorinated Carboxylic Acids in Environmental Matrixes. *Analytical Chemistry* **77,** 6353–6358 (2005).

174. Antignac, J. P., De Wasch, K., Monteau, F., De Brabander, H., Andre, F. & Le Bizec, B. The ion suppression phenomenon in liquid chromatography-mass spectrometry and its consequences in the field of residue analysis. *Analytica Chimica Acta* **529,** 129–136 (2005).

175. Kärrman, A., Van Bavel, B., Järnberg, U., Hardell, L. & Lindström, G. Development of a Solid-Phase Extraction-HPLC/Single Quadrupole MS Method for Quantification of Perfluorochemicals in Whole Blood. *Analytical Chemistry* **77,** 864–870 (2005).

176. Borgå, K., Fisk, A. T., Hoekstra, P. F. & Muir, D. C. Biological and chemical factors of importance in the bioaccumulation and trophic transfer of persistent organochlorine contaminants in arctic marine food webs. *Environmental Toxicology and Chemistry* **23,** 2367–2385 (2004).

177. Wang, Z., Cousins, I. T., Scheringer, M. & Hungerbuehler, K. Hazard assessment of fluorinated alternatives to long-chain perfluoroalkyl acids (PFAAs) and their precursors: Status quo, ongoing challenges and possible solutions. *Environment International* **75,** 172–179 (2015).

178. Kotthoff, M. & Bücking, M. Four Chemical Trends Will Shape the Next Decade's Directions in Perfluoroalkyl and Polyfluoroalkyl Substances Research. *Frontiers in Chemistry* **6,** 103 (2018).

179. Australian Government Department of Environment and Energy. *National phase out of PFOS: Ratification of the Stockholm Convention amendment on PFOS*
URL: https://www.environment.gov.au/system/files/consultations/52aef54d-1588-471a-b0f0-c5f67bd36e0d/files/pfos-ris-consultation-national-phase-out.pdf (accessed on May 24, 2020).

180. Newsted, J. L., Beach, S. A., Gallagher, S. P. & Giesy, J. P. Pharmacokinetics and acute lethality of perfluorooctanesulfonate (PFOS) to juvenile mallard and northern bobwhite. *Archives of Environmental Contamination and Toxicology* **50,** 411–420 (2006).

181. Sun, J. *et al.* White–Tailed Eagle (*Haliaeetus albicilla*) Body Feathers Document Spatiotemporal Trends of Perfluoroalkyl Substances in the Northern Environment. *Environmental Science and Technology* **53,** 12744–12753 (2019).

182. Sun, H., Gerecke, A. C., Giger, W. & Alder, A. C. Long-chain perfluorinated chemicals in digested sewage sludges in Switzerland. *Environmental Pollution* **159,** 654–662 (2011).

183. Jouanneau, W., Bårdsen, B.-J., Herzke, D., Johnsen, T. V., Eulaers, I. & Bustnes, J. O. Spatiotemporal Analysis of Perfluoroalkyl Substances in White–Tailed Eagle (*Haliaeetus albicilla*) Nestlings from Northern Norway—A Ten-Year Study. *Environmental Science & Technology* **54,** 5011–5020 (2020).

184. Bolong, N., Ismail, A. F., Salim, M. R. & Matsuura, T. A review of the effects of emerging contaminants in wastewater and options for their removal. *Desalination* **239,** 229–246 (2009).

185. Loos, R. *et al.* EU-wide monitoring survey on emerging polar organic contaminants in wastewater treatment plant effluents. *Water Research* **47,** 6475–6487 (2013).

186. Coggan, T. L., Moodie, D., Kolobaric, A., Szabo, D., Shimeta, J., Crosbie, N. D., Lee, E., Fernandes, M. & Clarke, B. O. An investigation into per- and polyfluoroalkyl substances (PFAS) in nineteen Australian wastewater treatment plants (WWTPs). *Heliyon* **5,** e02316 (2019).

187. Schultz, M. M., Barofsky, D. F. & Field, J. A. Quantitative determination of fluorinated alkyl substances by large-volume-injection liquid chromatography tandem mass spectrometry - Characterization of municipal wastewaters. *Environmental Science and Technology* **40,** 289–295 (2006).

188. Eriksson, U., Haglund, P. & Kärrman, A. Contribution of precursor compounds to the release of per- and polyfluoroalkyl substances (PFASs) from waste water treatment plants (WWTPs). *Journal of Environmental Sciences* **61,** 80–90 (2017).

189. Braune, B. M. & Noble, D. G. Environmental contaminants in Canadian shorebirds. *Environmental Monitoring and Assessment* **148,** 185–204 (2009).

190. Pearson, S. F., Levey, D. J., Greenberg, C. H. & Martínez Del Rio, C. Effects of elemental composition on the incorporation of dietary nitrogen and carbon isotopic signatures in an omnivorous songbird. *Oecologia* **135,** 516–523 (2003).

191. Reiner, J. L. & Place, B. J. *Perfluorinated Alkyl Acids in Wildlife* in *Toxicological Effects of Perfluoroalkyl and Polyfluoroalkyl Substances* chap. 5 (Springer International Publishing, 2015).

192. Borg, D., Lund, B. O., Lindquist, N. G. & Håkansson, H. Cumulative health risk assessment of 17 perfluoroalkylated and polyfluoroalkylated substances (PFASs) in the Swedish population. *Environment International* **59,** 112–123 (2013).

193. Jaspers, V., Covaci, A., Voorspoels, S., Dauwe, T., Eens, M. & Schepens, P. Brominated flame retardants and organochlorine pollutants in aquatic and terrestrial predatory birds of Belgium: levels, patterns, tissue distribution and condition factors. *Environmental Pollution* **139,** 340–352 (2006).

194. Sharp, S., Myers, J. & Pettigrove, V. *An assessment of sediment toxicants in Western Port and major tributaries* tech. rep. 27 (Centre for Aquatic Pollution Identification and Management (CAPIM), 2013).

195. Shoari, N. & Dubé, J. S. Toward improved analysis of concentration data: Embracing nondetects. *Environmental Toxicology and Chemistry* **37,** 643–656 (2018).

A. Sample information

Sample data on species, sample site, sample date and age of birds SampleIDs, species, band number, location and date of sampling, age of birds, and blood cell sample weights and treatment are given in Table A.1. Samples treated with ethanol pre-treatment (Chapter 3.1.3) are marked EtOH=1.

Table A.1.: Sample data of curlew sandpiper, red-necked stint and ruddy turnstone blood cell samples. EtOH denotes sample pre-treatment. Table continues over multiple pages.

Nr	SampleID	Species	BandNr	Location	Date	Longitude	Latitude	Region	age	Weight [mg]	EtOH
1	6228	Curlew sandpiper	4262566	WTP	18/12/2013	144.59	-37.98	WTP	4	40	1
2	6421	Curlew sandpiper	4254074	WTP	29/12/2013	144.59	-37.98	WTP	6	10	1
3	6801	Curlew sandpiper	4232924	WTP 270S	28/12/2014	144.64	-37.997	WTP	13	7	1
4	6804	Curlew sandpiper	4271960	WTP 270S	28/12/2014	144.64	-37.997	WTP	0	10	1
5	6806	Curlew sandpiper	4271961	WTP 270S	28/12/2014	144.64	-37.997	WTP	1	21	1
6	7285	Curlew sandpiper	4272013	WTP 270S	28/12/2014	144.64	-37.997	WTP	0	45	1
7	12337	Curlew sandpiper	4271887	Yallock Creek	24/02/2018	145.48	-38.23	Western Port	4	23	1
8	12338	Curlew sandpiper	4271686	Yallock Creek	24/02/2018	145.48	-38.23	Western Port	4	24	1
9	12374	Curlew sandpiper	4278458	Yallock Creek	07/03/2018	145.48	-38.23	Western Port	1	15	1
10	12381	Curlew sandpiper	4277854	Yallock Creek	07/03/2018	145.48	-38.23	Western Port	1	30	1
11	12395	Curlew sandpiper	4278815	Yallock Creek	07/03/2018	145.48	-38.23	Western Port	1	17	1
12	13635	Curlew sandpiper	4283060	WTP	29/12/2018	144.59	-37.98	WTP	0	27	0
13	13640	Curlew sandpiper	4278745	WTP	29/12/2018	144.59	-37.98	WTP	1	37	0
14	13660	Curlew sandpiper	4278746	WTP	29/12/2018	144.59	-37.98	WTP	1	38	0
15	13673	Curlew sandpiper	4273359	WTP	29/12/2018	144.59	-37.98	WTP	4	43	0
16	13707	Curlew sandpiper	4278269	Yallock Creek	12/01/2019	145.48	-38.23	Western Port	2	12	1
17	13713	Curlew sandpiper	4278376	Yallock Creek	12/01/2019	145.48	-38.23	Western Port	2	39	0
18	13714	Curlew sandpiper	4277854	Yallock Creek	12/01/2019	145.48	-38.23	Western Port	2	35	0
19	13716	Curlew sandpiper	4278815	Yallock Creek	12/01/2019	145.48	-38.23	Western Port	2	59	0
20	13721	Curlew sandpiper	4278458	Yallock Creek	12/01/2019	145.48	-38.23	Western Port	2	15	1
21	13723	Curlew sandpiper	4278377	Yallock Creek	12/01/2019	145.48	-38.23	Western Port	2	15	1
22	5465	Red-necked stint	3615434	WTP	28/12/2013	144.59	-37.98	WTP	9	14	1
23	5817	Red-necked stint	3621571	WTP	28/12/2013	144.59	-37.98	WTP	7	19	1
24	6289	Red-necked stint	3680908	WTP	29/12/2013	144.59	-37.98	WTP	0	27	1

Nr	SampleID	Species	BandNr	Location	Date	Longitude	Latitude	Region	age	Weight[mg]	EtOH
25	6314	Red-necked stint	3603654	WTP	29/12/2013	144.59	-37.98	WTP	10	13	1
26	7355	Ruddy turnstone	5272901	Central Manuka	25/11/2014	143.8457	-39.878	King Island	1	71	0
27	7362	Ruddy turnstone	5272357	Central Manuka	25/11/2014	143.8457	-39.878	King Island	1	58	0
28	7363	Ruddy turnstone	5272327	Central Manuka	25/11/2014	143.8457	-39.878	King Island	1	11	1
29	7533	Ruddy turnstone	5272377	Burges Bay	28/11/2014	143.843703	-39.939042	King Island	1	24	1
30	7539	Ruddy turnstone	5272383	Burges Bay	28/11/2014	143.843703	-39.939042	King Island	1	72	0
31	7546	Ruddy turnstone	5272917	Burges Bay	28/11/2014	143.843703	-39.939042	King Island	0	68	0
32	7565	Ruddy turnstone	5272923	Burges Bay	28/11/2014	143.843703	-39.939042	King Island	0	28	1
33	7572	Ruddy turnstone	5272925	Central Manuka	29/11/2014	143.8457	-39.878	King Island	0	21	1
34	7580	Ruddy turnstone	5272928	North Manuka	30/11/2014	143.853	-39.867	King Island	1	47	0
35	7585	Ruddy turnstone	5272934	North Manuka	30/11/2014	143.853	-39.867	King Island	1	26	1
36	7587	Ruddy turnstone	5272281	North Manuka	30/11/2014	143.853	-39.867	King Island	1	35	0
37	7592	Ruddy turnstone	5272933	North Manuka	30/11/2014	143.853	-39.867	King Island	1	22	1
38	7593	Ruddy turnstone	5272934	North Manuka	30/11/2014	143.853	-39.867	King Island	1	41	0
39	6860	Red-necked stint	3686433	WTP 270S	28/12/2014	144.64	-37.997	WTP	0	22	1
40	6863	Red-necked stint	3657108	WTP 270S	28/12/2014	144.64	-37.997	WTP	6	19	1
41	6872	Red-necked stint	3658183	WTP 270S	28/12/2014	144.64	-37.997	WTP	5	24	1
42	7205	Red-necked stint	3686430	WTP 270S	28/12/2014	144.64	-37.997	WTP	0	62	0
43	9738	Red-necked stint	3653909	WTP	28/12/2016	144.59	-37.98	WTP	9	16	1
44	9758	Red-necked stint	3647144	WTP	28/12/2016	144.59	-37.98	WTP	11	15	1
45	9767	Red-necked stint	3653890	WTP	28/12/2016	144.59	-37.98	WTP	9	13	1
46	9792	Red-necked stint	3675666	WTP	29/12/2016	144.59	-37.98	WTP	6	33	0
47	11246	Red-necked stint	3690484	Yallock Creek	14/04/2017	145.48	-38.23	Western Port	2	13	1
48	11254	Red-necked stint	3685159	Yallock Creek	14/04/2017	145.48	-38.23	Western Port	3	16	1
49	12176	Red-necked stint	3693968	WTP	30/12/2017	144.59	-37.98	WTP	1	16	1
50	12177	Red-necked stint	3696112	WTP	30/12/2017	144.59	-37.98	WTP	0	21	1
51	12184	Red-necked stint	3696079	WTP	30/12/2017	144.59	-37.98	WTP	0	17	1
52	13819	Red-necked stint	3676462	Yallock Creek	11/03/2019	145.48	-38.23	Western Port	7	18	1
53	13864	Red-necked stint	3675877	Yallock Creek	11/03/2019	145.48	-38.23	Western Port	7	14	1
54	8919	Ruddy turnstone	5260527	Blackfellows Cave	08/11/2015	140.5	-37.93	Canunda	5	28	0
55	8925	Ruddy turnstone	5259960	Blackfellows Cave	08/11/2015	140.5	-37.93	Canunda	5	22	1

Nr	SampleID	Species	BandNr	Location	Date	Longitude	Latitude	Region	age	Weight[mg]	EtOH
56	8927	Ruddy turnstone	5278346	Blackfellows Cave	08/11/2015	140.5	-37.93	Canunda	1	44	0
57	8932	Ruddy turnstone	5229907	Blackfellows Cave	08/11/2015	140.5	-37.93	Canunda	10	38	1
58	9118	Ruddy turnstone	5272387	Denby Bay	30/11/2015	143.9052	-40.12176	King Island	2	3	1
59	9120	Ruddy turnstone	5272383	Denby Bay	30/11/2015	143.9052	-40.12176	King Island	2	18	1
60	9149	Ruddy turnstone	5272327	Central Manuka	03/12/2015	143.8457	-39.878	King Island	2	13	1
61	9565	Ruddy turnstone	5272893	Burges Bay	18/11/2016	143.843703	-39.939042	King Island	2	23	1
62	9602	Ruddy turnstone	5278483	Central Manuka	19/11/2016	143.8457	-39.878	King Island	0	14	1
63	9615	Ruddy turnstone	5259894	Central Manuka	19/11/2016	143.8457	-39.878	King Island	6	14	1
64	11958	Ruddy turnstone	5278229	Burges Bay	09/12/2017	143.843703	-39.939042	King Island	3	17	1
65	5459	Curlew sandpiper	4269513	WTP	28/12/2013	144.59	-37.98	WTP	0	12	1
66	9016	Ruddy turnstone	5272933	North Manuka	29/11/2015	143.853	-39.867	King Island	2	33	0
67	9019	Ruddy turnstone	5272928	North Manuka	29/11/2015	143.853	-39.867	King Island	2	75	0
68	9025	Ruddy turnstone	5272281	North Manuka	29/11/2015	143.853	-39.867	King Island	2	37	0
69	9029	Ruddy turnstone	5272870	North Manuka	29/11/2015	143.853	-39.867	King Island	1	54	0
70	9081	Ruddy turnstone	5278246	Denby Bay	30/11/2015	143.9052	-40.12176	King Island	1	36	0
71	9110	Ruddy turnstone	5272376	Denby Bay	30/11/2015	143.9052	-40.12176	King Island	2	52	0
72	9151	Ruddy turnstone	5270126	Central Manuka	03/12/2015	143.8457	-39.878	King Island	4	26	0
73	9153	Ruddy turnstone	5270122	Central Manuka	03/12/2015	143.8457	-39.878	King Island	4	60	0
74	9155	Ruddy turnstone	5272337	Central Manuka	03/12/2015	143.8457	-39.878	King Island	2	84	0
75	9554	Ruddy turnstone	5260980	Burges Bay	18/11/2016	143.843703	-39.939042	King Island	3	51	0
76	9555	Ruddy turnstone	5278229	Burges Bay	18/11/2016	143.843703	-39.939042	King Island	2	56	0
77	9559	Ruddy turnstone	5278524	Burges Bay	18/11/2016	143.843703	-39.939042	King Island	0	58	0
78	9611	Ruddy turnstone	5272870	Central Manuka	19/11/2016	143.8457	-39.878	King Island	2	51	0
79	9613	Ruddy turnstone	5259530	Central Manuka	19/11/2016	143.8457	-39.878	King Island	7	61	0
80	9655	Ruddy turnstone	5259886	Nene Valley	27/11/2016	140.51	-37.98	Nene Valley	6	67	0
81	9661	Ruddy turnstone	5229907	Nene Valley	27/11/2016	140.51	-37.98	Nene Valley	11	58	0
82	11964	Ruddy turnstone	5278908	Burges Bay	09/12/2017	143.843703	-39.939042	King Island	1	38	0
83	11970	Ruddy turnstone	5272888	Burges Bay	09/12/2017	143.843703	-39.939042	King Island	3	36	0
84	11984	Ruddy turnstone	5278981	Burges Bay	09/12/2017	143.843703	-39.939042	King Island	0	26	1
85	12015	Ruddy turnstone	5272901	Central Manuka	10/12/2017	143.8457	-39.878	King Island	4	17	1
86	12026	Ruddy turnstone	5272902	Central Manuka	10/12/2017	143.8457	-39.878	King Island	4	17	1

Nr	SampleID	Species	BandNr	Location	Date	Longitude	Latitude	Region	age	Weight[mg]	EtOH
87	12745	Ruddy turnstone	5272933	North Manuka	09/12/2018	143.853	-39.867	King Island	5	16	1
88	12763	Ruddy turnstone	5286666	North Manuka	09/12/2018	143.853	-39.867	King Island	0	15	1
89	12901	Ruddy turnstone	5286069	Central Manuka	09/12/2018	143.8457	-39.878	King Island	0	15	1
90	12905	Ruddy turnstone	5286070	Central Manuka	09/12/2018	143.8457	-39.878	King Island	0	14	1
91	13876	Ruddy turnstone	5286092	North Manuka	23/03/2019	143.853	-39.867	King Island	0	16	1
92	13883	Ruddy turnstone	5286202	North Manuka	23/03/2019	143.853	-39.867	King Island	0	21	1
93	13952	Ruddy turnstone	5259682	Central Manuka	24/03/2019	143.8457	-39.878	King Island	9	15	1
94	11986	Ruddy turnstone	5278983	Burges Bay	09/12/2017	143.843703	-39.939042	King Island	0	15	1
95	12013	Ruddy turnstone	5259530	Central Manuka	10/12/2017	143.8457	-39.878	King Island	8	50	0
96	12031	Ruddy turnstone	5259686	Central Manuka	10/12/2017	143.8457	-39.878	King Island	7	22	1
97	12764	Ruddy turnstone	5272355	North Manuka	09/12/2018	143.853	-39.867	King Island	5	48	0
98	12911	Ruddy turnstone	5286072	Central Manuka	09/12/2018	143.8457	-39.878	King Island	0	43	0
99	12926	Ruddy turnstone	5278552	North Manuka	09/12/2018	143.853	-39.867	King Island	2	55	0
100	13148	Ruddy turnstone	5286065	Burges Bay	08/12/2018	143.843703	-39.939042	King Island	0	36	0
101	13151	Ruddy turnstone	5272377	Burges Bay	08/12/2018	143.843703	-39.939042	King Island	5	39	0
102	13156	Ruddy turnstone	5278524	Burges Bay	08/12/2018	143.843703	-39.939042	King Island	2	50	0
103	13161	Ruddy turnstone	5286064	Burges Bay	08/12/2018	143.843703	-39.939042	King Island	0	38	0
104	13881	Ruddy turnstone	5286203	North Manuka	23/03/2019	143.853	-39.867	King Island	0	42	0
105	13940	Ruddy turnstone	5259748	Central Manuka	24/03/2019	143.8457	-39.878	King Island	9	32	0
106	13941	Ruddy turnstone	5259894	Central Manuka	24/03/2019	143.8457	-39.878	King Island	8	36	0
107	13948	Ruddy turnstone	5270126	Central Manuka	24/03/2019	143.8457	-39.878	King Island	7	44	0
108	5452	Curlew sandpiper	4269511	WTP	28/12/2013	144.59	-37.98	WTP	0	42	0
109	8928	Ruddy turnstone	5278348	Blackfellows Cave	08/11/2015	140.5	-37.93	Canunda	1	55	0
110	9600	Ruddy turnstone	5270126	Central Manuka	19/11/2016	143.8457	-39.878	King Island	5	60	0

B. Analysis of per- and polyflouroalkyl substances

Supplier, CAS registry numbers (CASRN) and purity of standards are given Table B.1. Accurate concentrations of the $100\,\mathrm{ng\,mL^{-1}}$ target analytes are given in Table B.2. Analyte specific MS/MS parameters for target analytes and internal standards are given in Table B.4. MRM transitions, cone voltage and collision energies in the UPLC-MS/MS analysis are given in Table B.3. Calculated matrix effects, including matrix factors are presented in Table B.5.

Table B.1.: Suppliers, CAS registry numbers and purity of obtained standards.

Compound	Name	CASRN	Purity	Supplier
DecaS	1-Decanesulfonic acid sodium salt	13419-61-9	98%	Sigma-Aldrich
PFBS	Perfluorobutanesulfonic acid tetrabutylammonium salt	108427-52-7	>98%	Sigma-Aldrich
PFHxS	Perfluorohexane sulfonic acid potassium salt	3871-99-6	>98%	Sigma-Aldrich
PFOS	Perfluorooctanesulfonic acid tetrabutylammonium salt	111873-33-7	>95%	Sigma-Aldrich
PFPA	Perfluoropentanoic acid	2706-90-3	97%	Sigma-Aldrich
PFHxA	Perfluorohexanoic acid	307-24-4	>97%	Sigma-Aldrich
PFHpA	Perfluoroheptanoic acid	375-85-9	99%	Sigma-Aldrich
PFOA	Perfluorooctanoic acid	335-67-1	95%	Sigma-Aldrich
PFNA	Perfluorononanoic acid	375-95-1	97%	Sigma-Aldrich
PFDA	Perfluorodecanoic acid	335-76-2	98%	Sigma-Aldrich
PFUnDA	Perfluoroundecanoic acid	2058-94-8	95%	Sigma-Aldrich
PFDoDA	Perfluorododecanoic acid	307-55-1	95%	Sigma-Aldrich
PFTrDA	Perfluorotridecanoic acid	72629-94-8	97%	Sigma-Aldrich
PFTeDA	Perfluorotetradecanoic acid	376-06-7	96%	Sigma-Aldrich
PFOSA	Perfluorooctane sulfonamide	754-91-6		Chiron
EtPFOSA	N-Ethyl perfluorooctane sulfonamide	4151-50-2	>98%	Sigma-Aldrich
PFOA-C13	Perfluorooctanoic acid		98%	Cambrigde Isotope Laboratories, Inc.
PFOS-C13	Perfluorooctanesulfonate sodium salt		98%	Cambrigde Isotope Laboratories, Inc.

Table B.2.: Accurate concentrations of 100 ng mL^{-1} target analyte solutions.

Compound	**Concentration** [µg mL^{-1}]
PFBS	99.75
PFHxS	100.05
PFOS	-
PFPA	100.375
PFHxA	100.86
PFHpA	100.2
PFOA	99.375
PFNA	99.975
PFDA	99.91
PFUnDA	99.91
PFDoDA	99.96
PFTrDA	99.82
PFTeDA	99.64
PFOSA	99.947
EtPFOSA	100.43

Table B.3.: Molar mass (g mol^{-1}) and MRM transitions (parent and fragment ions), cone voltage (CV) and collision energy (CE) in UPLC-MS/MS analysis.

Compound	**Molar Mass**	***Parent [m/z]***	***Fragments [m/z]***	**CV [V]**	**CE [V]**
DecaS	221.34	221	80*	58	24
			221	8	24
PFBS	299.09	299	80*	22	16
			299	8	24
PFHxS	399.11	399	80*	50	34
			399	8	34
PFOS	499.12	499	80	56	44
			99*	36	44
PFPA	264.05	263	219*	20	8
			-	-	-
PFHxA	314.05	313	119	10	18
			269*	10	8
PFHpA	364.05	363	169*	16	16
			319	16	10
PFOA	414.07	413	169	20	18
			369*	20	8
PFNA	464.08	463	219	20	16
			419*	20	10
PFDA	514.09	513	269	16	18
			469*	16	10
PFUnDA	564.09	563	269	12	18
			519*	12	10
PFDoDA	614.1	613	169	26	26
			569*	26	12
PFTrDA	664.11	663	169	28	24
			619*	28	12
PFTeDA	714.12	713	169	20	30
			669*	20	14
PFOSA	499.14	498	78*	12	28
			478	12	28
EtPFOSA	527.2	526	169*	26	44
			219	26	44
PFOA-C13	422.01	421	172*	16	16
			223	16	16
PFOS-C13	507.06	507	80*	46	56
			172	32	56

* Quantifying transition.

Table B.4.: Analyte specific MS/MS parameters for target analytes and internal standards using a Kinetex C18 (30 x 2.1 mm) column. Retention times (RTs), relative retention times (RRTs) and Ion ratios (IR%) in PFAS analysis of avian red blood cells.

	RT[a]	**RRT (IS)[b]**	**IR%[c](RSD%)**	**Quantifying ion**	**Confirmative ion**
DecaS	2.08	1.00 (PFOA-C13)	20.4 (9)	221>80*	221>221
PFBS	1.68	0.81 (PFOA-C13)	239 (6)	299>80**	299>299
PFHxS	1.97	0.95 (PFOA-C13)	75.4 (13)	399>80*	399>399
PFOS	2.18	1.00 (PFOS-C13)	135 (6)	499>99**	499>80
PFPA	1.63	0.79 (PFOA-C13)	-	263>219*	-
PFHxA	1.83	0.88 (PFOA-C13)	2.54 (12)	313>269*	313>119
PFHpA	1.96	0.95 (PFOA-C13)	890 (7)	363>169**	363>319
PFOA	2.08	1.00 (PFOA-C13)	12.2 (6)	413>369*	413>169
PFNA	2.19	1.00 (PFOS-C13)	13.7 (5)	463>419*	463>219
PFDA	2.28	1.05 (PFOS-C13)	7.85 (10)	513>469*	513>269
PFUnDA	2.37	1.09 (PFOS-C13)	13.4 (5)	563>519*	563>269
PFDoDA	2.45	1.13 (PFOS-C13)	10.5 (4)	613>569*	613>169
PFTrDA	2.53	1.16 (PFOS-C13)	13.1 (6)	663>619*	663>169
PFTeDA	2.61	1.19 (PFOS-C13)	11.8 (5)	713>669*	713>169
PFOSA	2.43	1.12 (PFOS-C13)	5.89 (8)	498>78*	498>478
EtPFOSA	2.71	1.24 (PFOS-C13)	69.9 (2)	526>169*	526>219
			Internal standards		
PFOA-C13	2.08	1 (PFOA-C13)		421>172*	421>223
PFOS-C13	2.18	1 (PFOS-C13)		507>80*	507>172

a Average RT from standard solvent calibration curve.
b The internal standard (IS) used in quantification of the respective target analytes is showed in parenthesis.
c Average ion ratio (IR%) of calibration standards (5, 10, 20, and 50 $ng\,g^{-1}$) and two fortification levels of bovine blood (33 and 66 $ng\,g^{-1}$, pre-extraction and post-extraction spiked).
* Ion transition with higher signal intensity.
** Ion transition with lower noise level.

Table B.5.: Calculated matrix factors (MF) and matrix effects (ME%) of 15 PFASs and one non-fluorinated compound (DecaS) in bovine blood and bovine serum.

	Bovine blood				**Bovine serum**			
	33 ng mL^{-1}		66 ng mL^{-1}		10 ng mL^{-1}		20 ng mL^{-1}	
	MF	ME%	MF	ME%	MF	ME%	MF	ME%
DecaS	2.12	112	2.28	128	0.30	-70	0.26	-74
PFBS	2.52	152	2.48	148	1.52	52	1.51	51
PFHxS	2.64	164	2.23	123	1.52	52	1.46	46
PFOS	1.66	66	1.60	60	1.45	45	1.47	47
PFPA	1.42	42	1.35	35	1.10	10	1.01	-1*
PFHxA	1.29	29	1.27	27	1.65	65	1.45	45
PFHpA	1.44	44	1.31	31	1.64	64	1.76	76
PFOA	1.33	33	1.27	27	1.57	57	1.51	51
PFNA	1.30	30	1.14	14	1.79	79	1.66	66
PFDA	1.53	53	1.05	5	1.63	63	1.60	60
PFUnDA	1.82	82	1.31	31	1.39	39	1.40	40
PFDoDA	1.67	67	1.22	22	1.34	34	1.40	40
PFTrDA	1.82	82	1.32	32	1.58	58	1.36	36
PFTeDA	1.70	70	1.52	52	2.34	132	1.59	59
PFOSA	2.03	103	1.95	95	1.46	46	1.44	44
EtPFOSA	2.29	130	1.98	98	1.38	38	1.34	34

* RSD=415%

C. Calibration curves

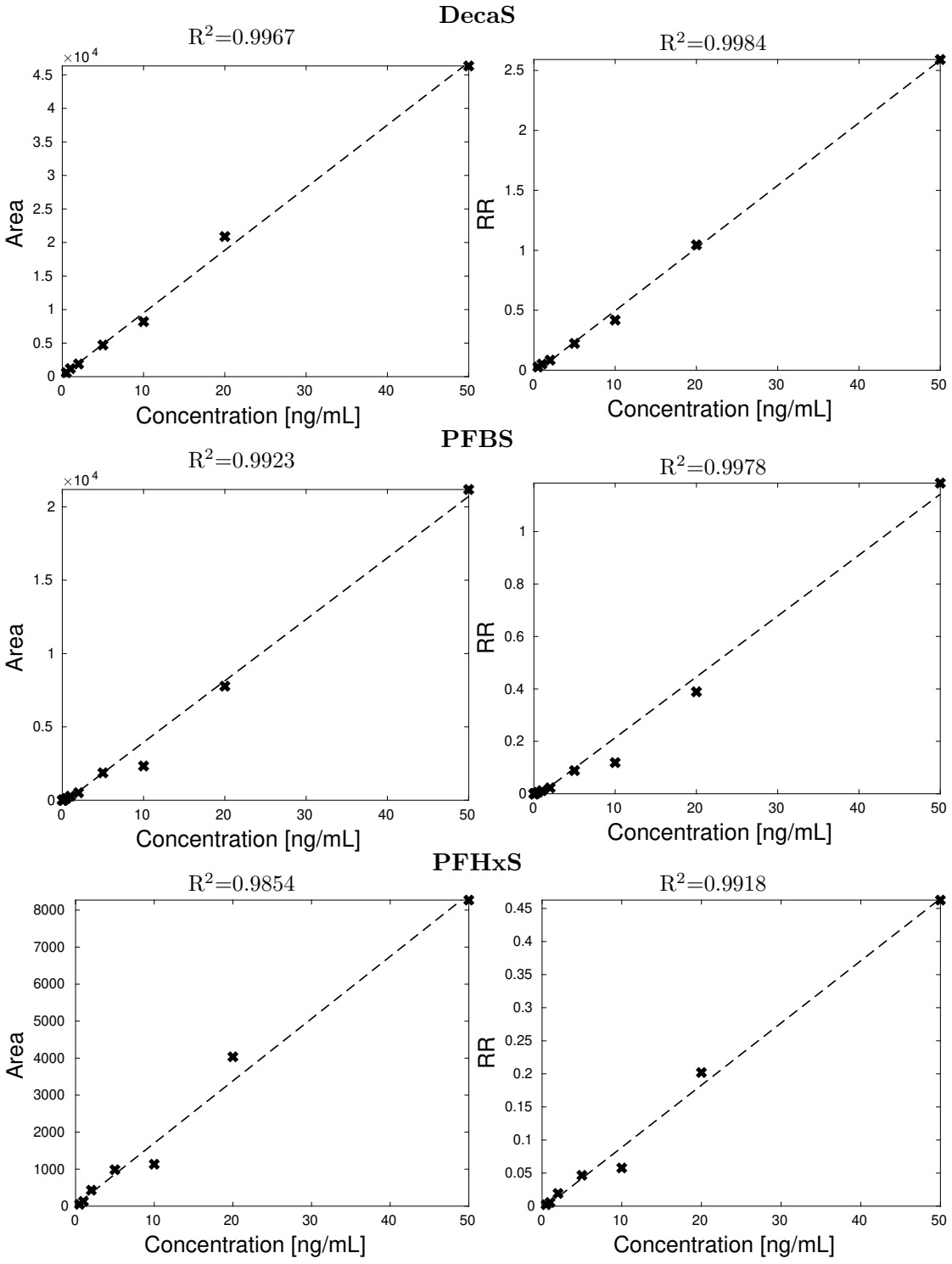

Figure C.1.: Calibration curves of target analytes based on absolute and relative areas. Part 1.

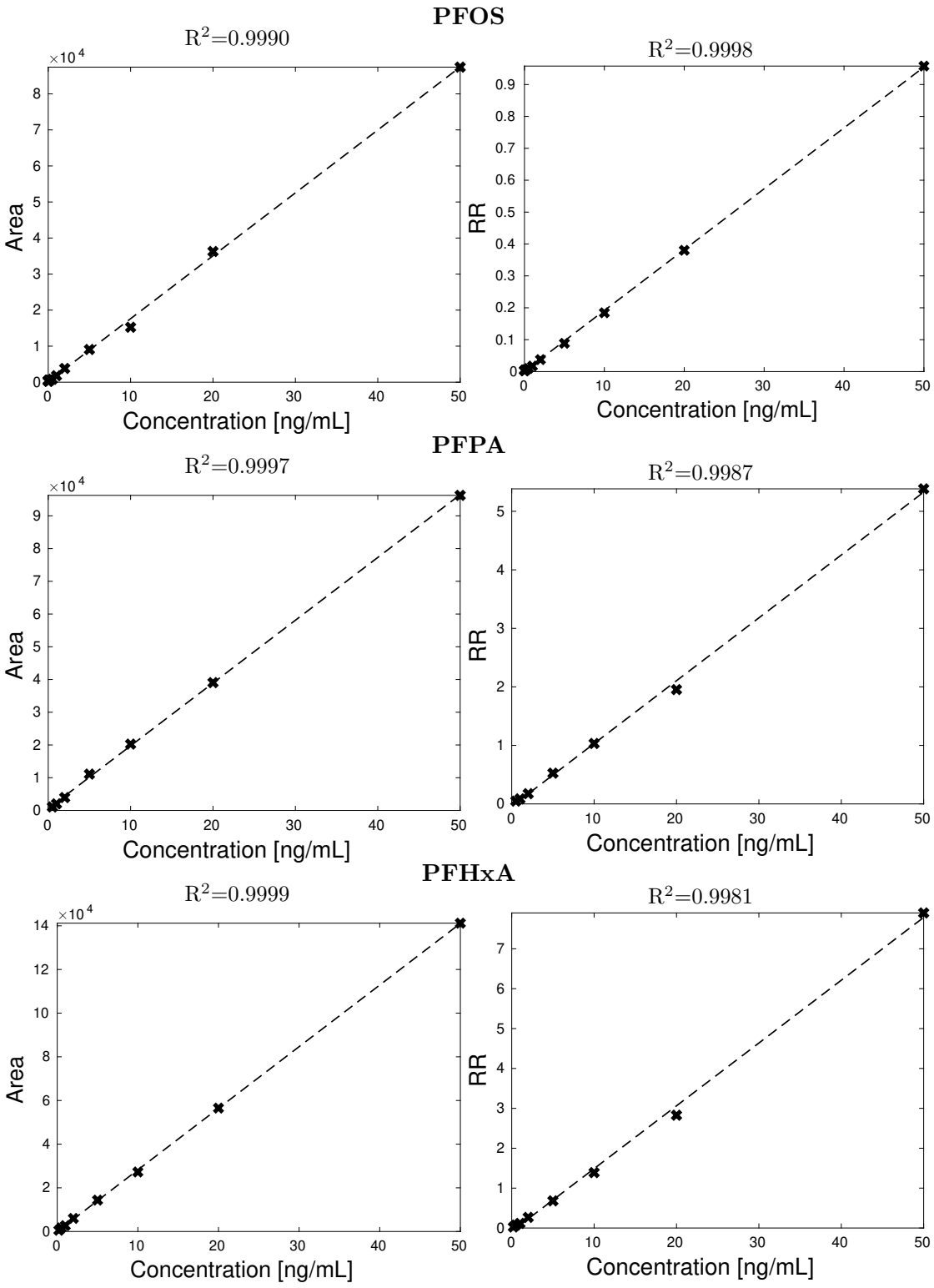

Figure C.2.: Calibration curves of target analytes based on absolute and relative areas. Part 2.

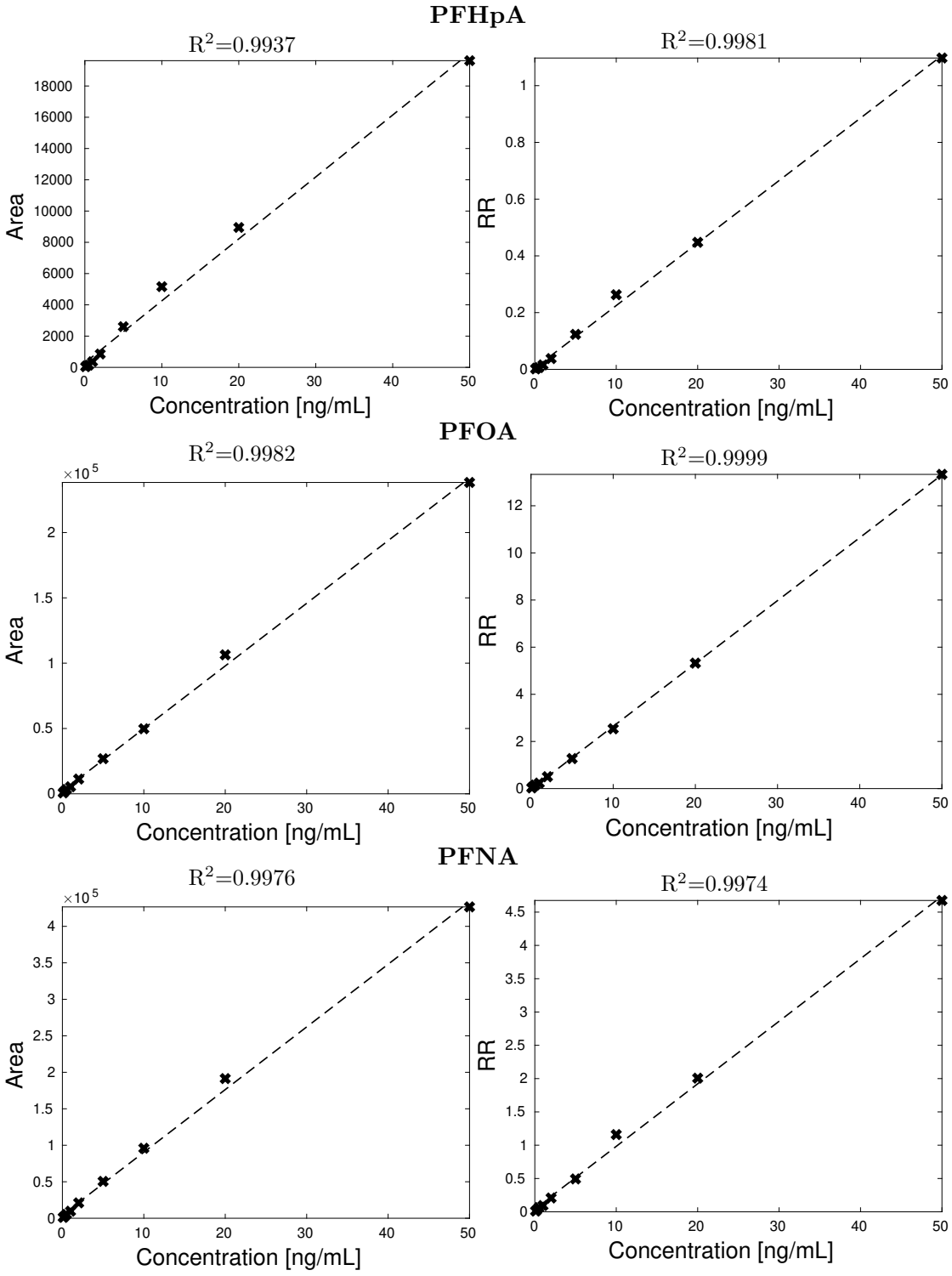

Figure C.3.: Calibration curves of target analytes based on absolute and relative areas. Part three.

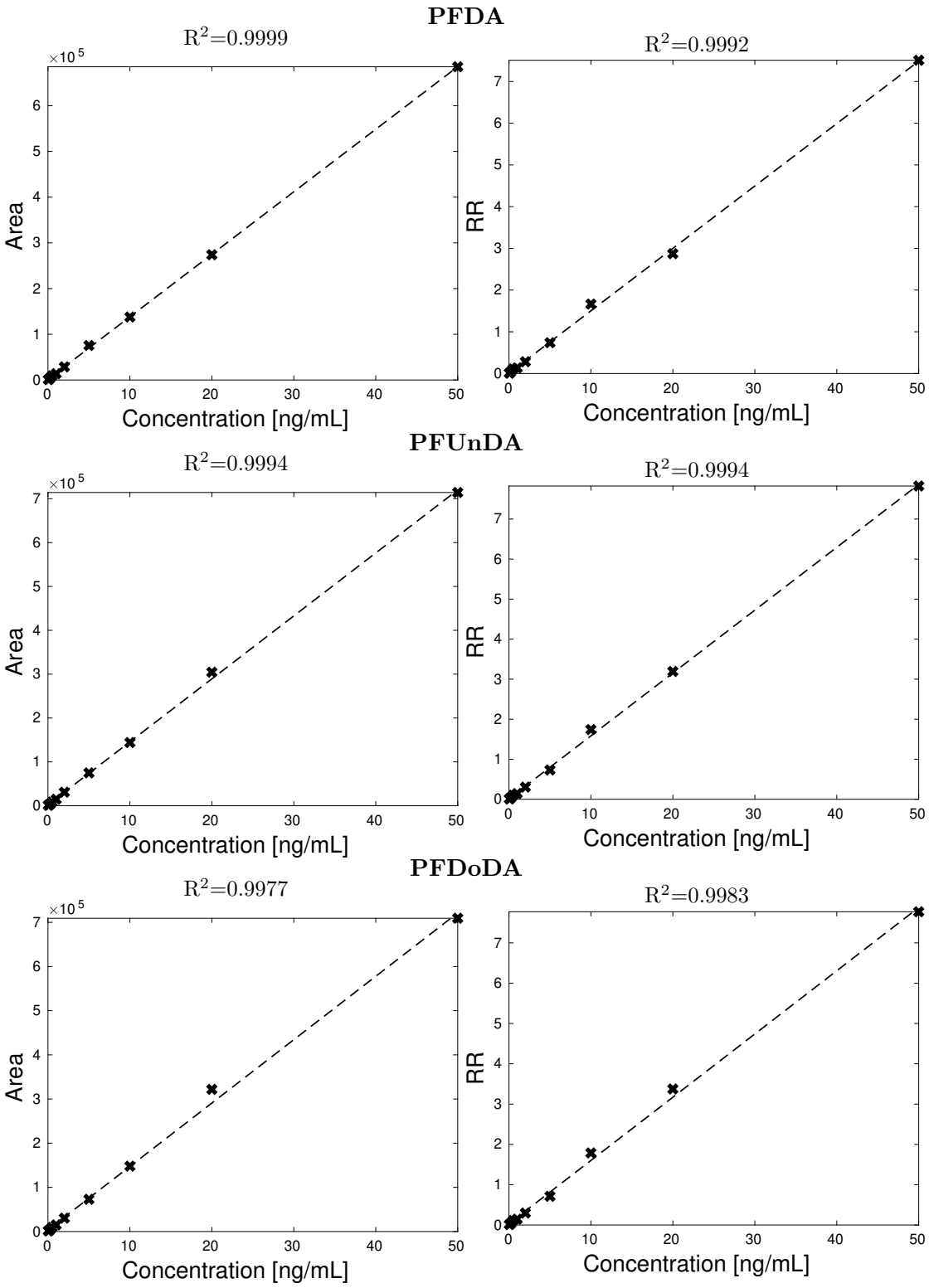

Figure C.4.: Calibration curves of target analytes based on absolute and relative areas. Part 4.

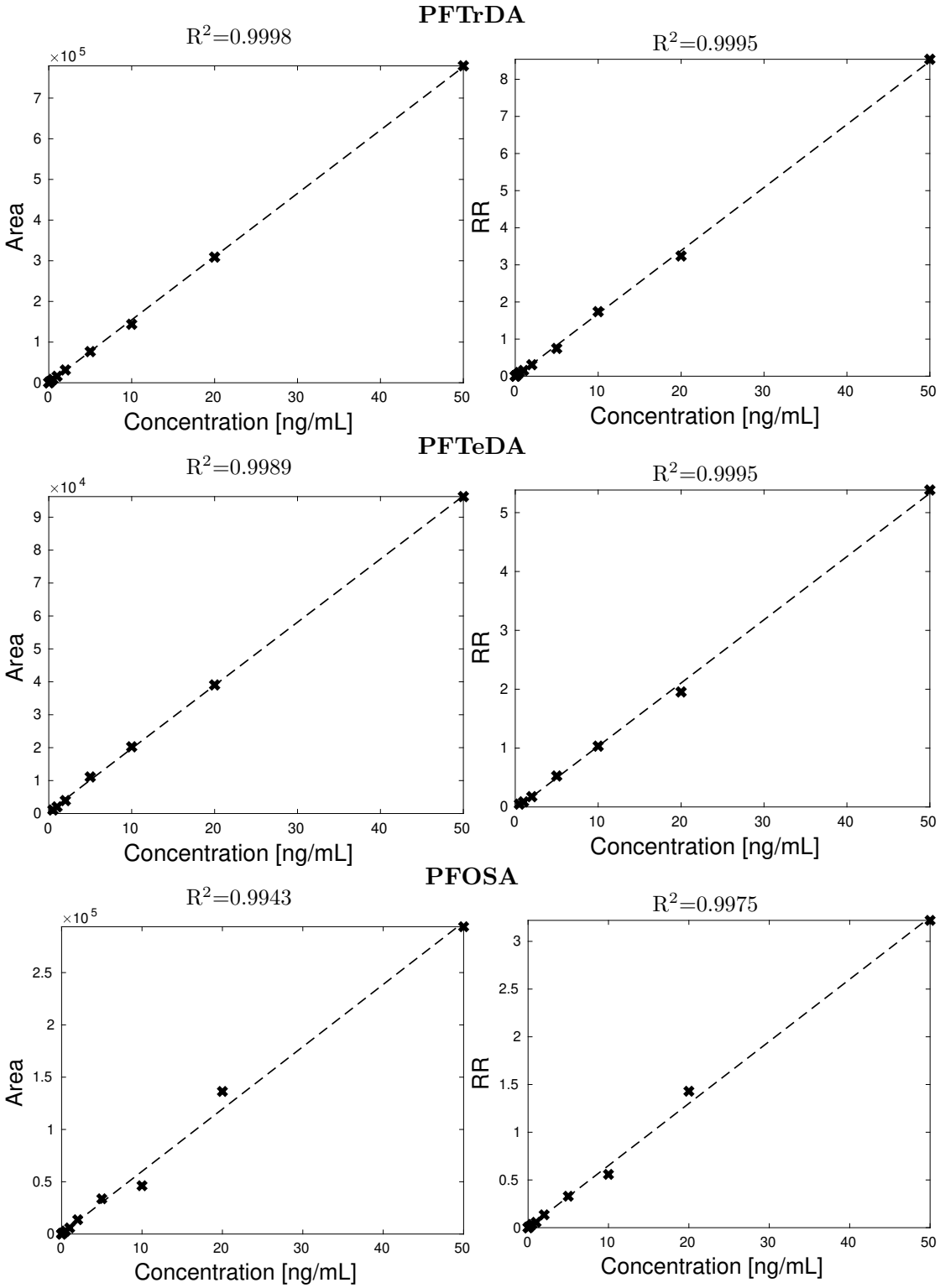

Figure C.5.: Calibration curves of target analytes based on absolute and relative areas. Part five.

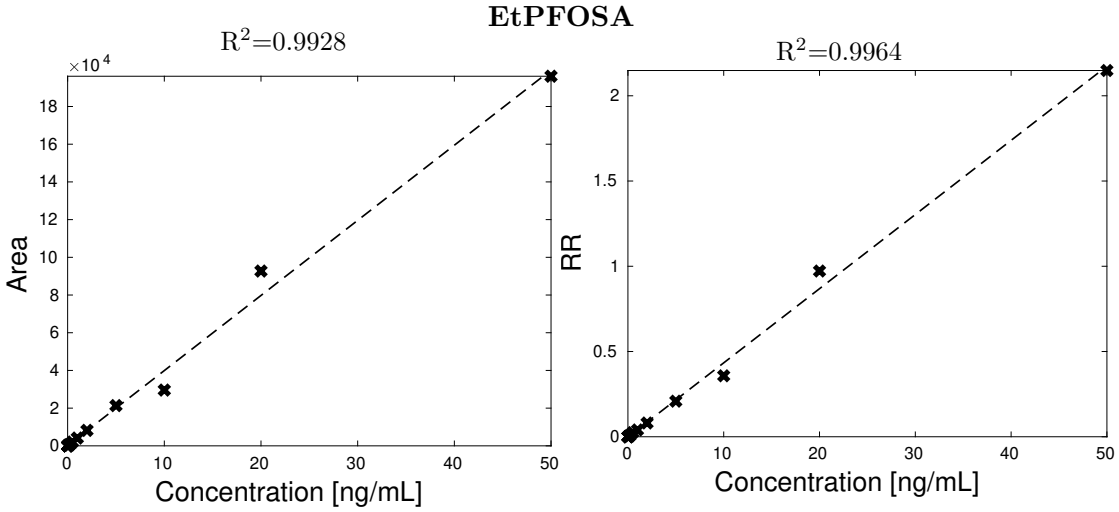

Figure C.6.: Calibration curves of target analytes based on absolute and relative areas. Part 6.

D. Chromatograms

MRM chromatograms of ^{13}C-labeled internal standards in a pre-extraction spiked matrix sample are shown in Figure D.1. MRM chromatograms of target analytes in the same sample are shown in Figures D.2-D.7.

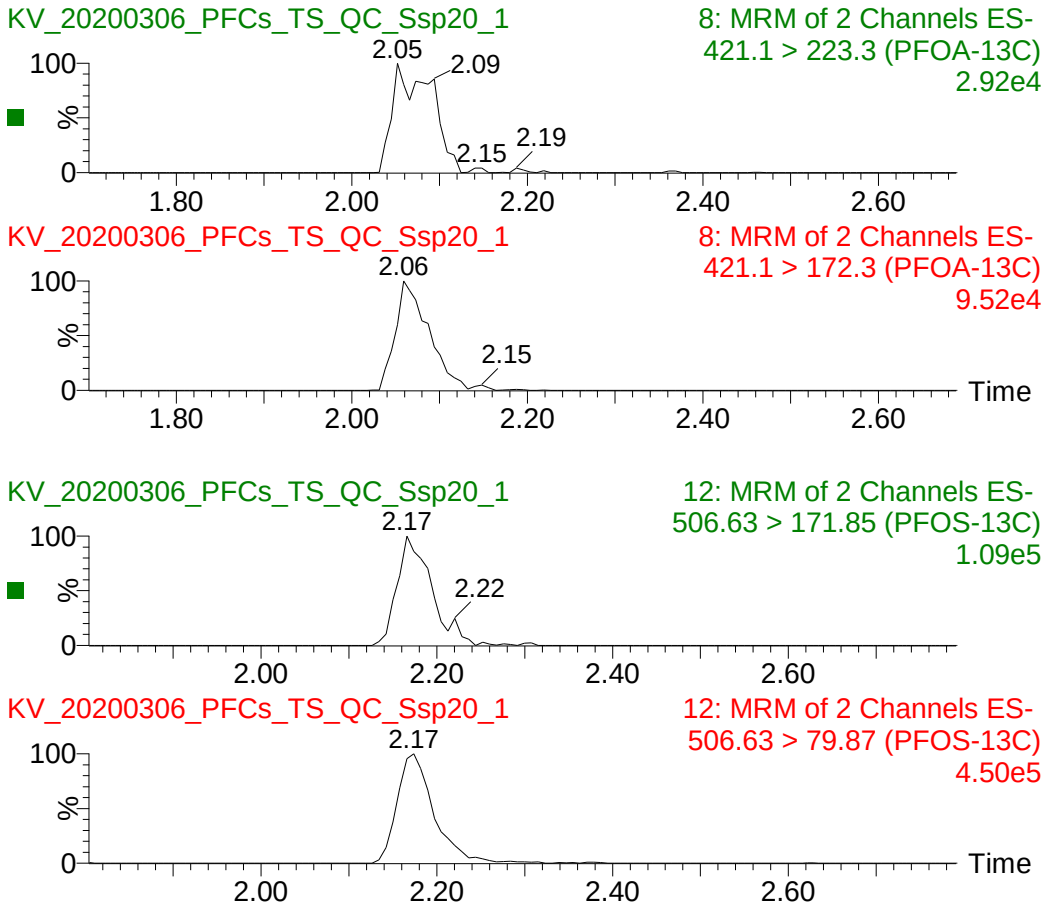

Figure D.1.: MRM chromatograms for ^{13}C-labeled internal standards, PFOA-13C and PFOS-13C, in a pre-extraction spiked matrix sample ($33\,\mathrm{ng\,mL^{-1}}$).

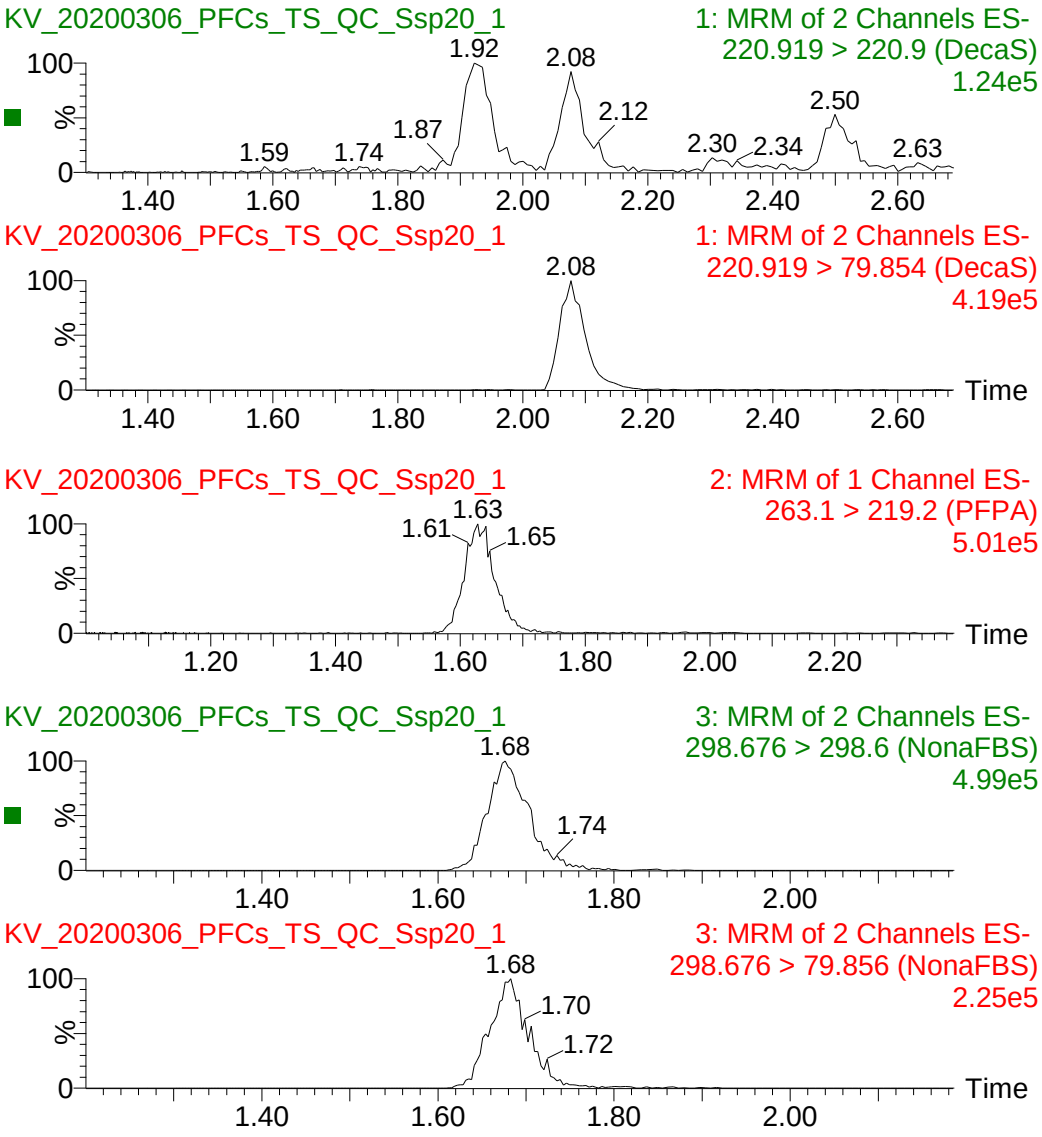

Figure D.2.: MRM chromatograms of DecaS, PFPA and PFBS (NonaFBS) in a pre-extraction spiked matrix sample (66 ng mL^{-1})

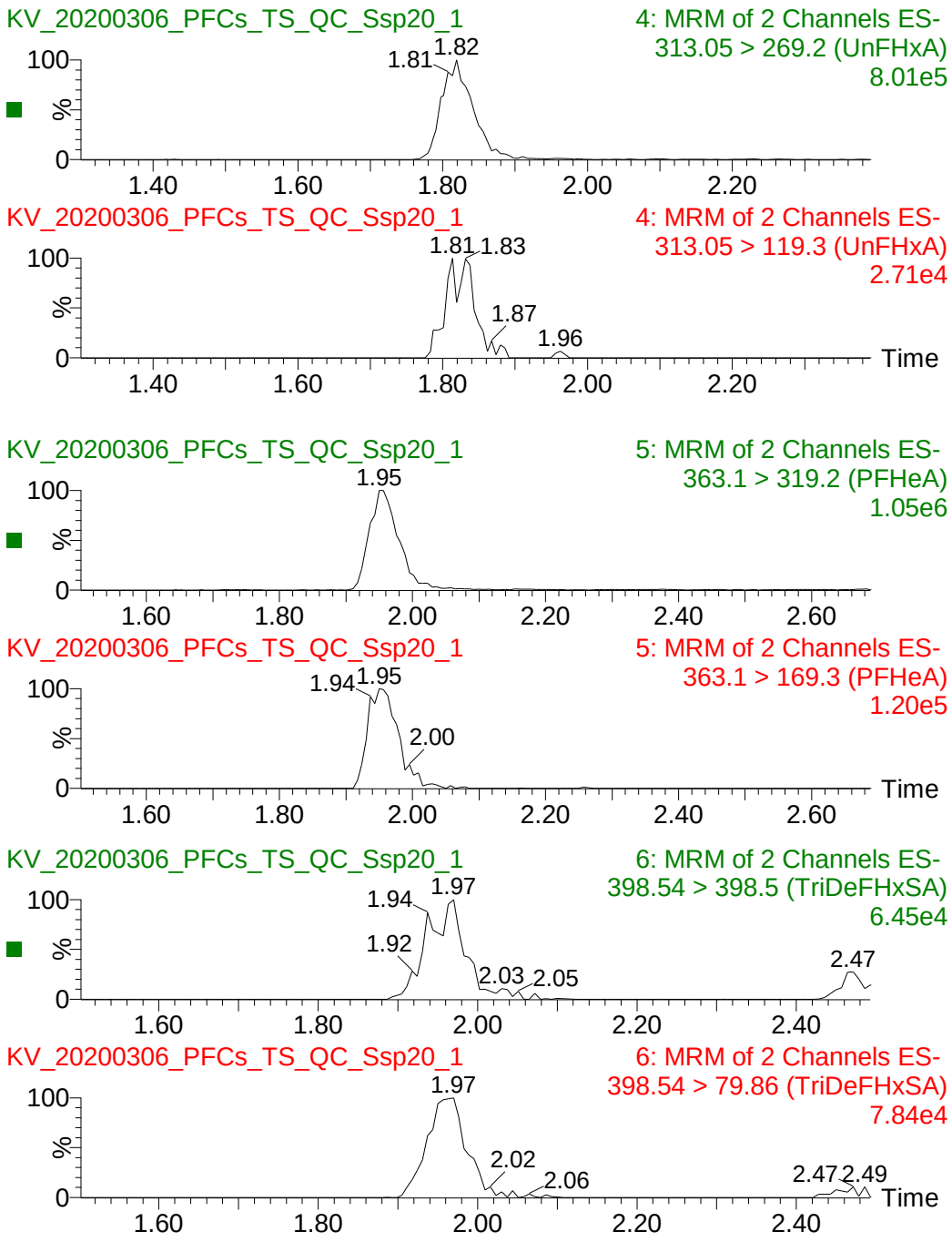

Figure D.3.: MRM chromatograms of PFHxA (UnFHxA), PFHpA (PFHeA) and PFHxS (TriDeFHxSA) in a pre-extration spiked matrix sample ($66\,\mathrm{ng\,mL^{-1}}$).

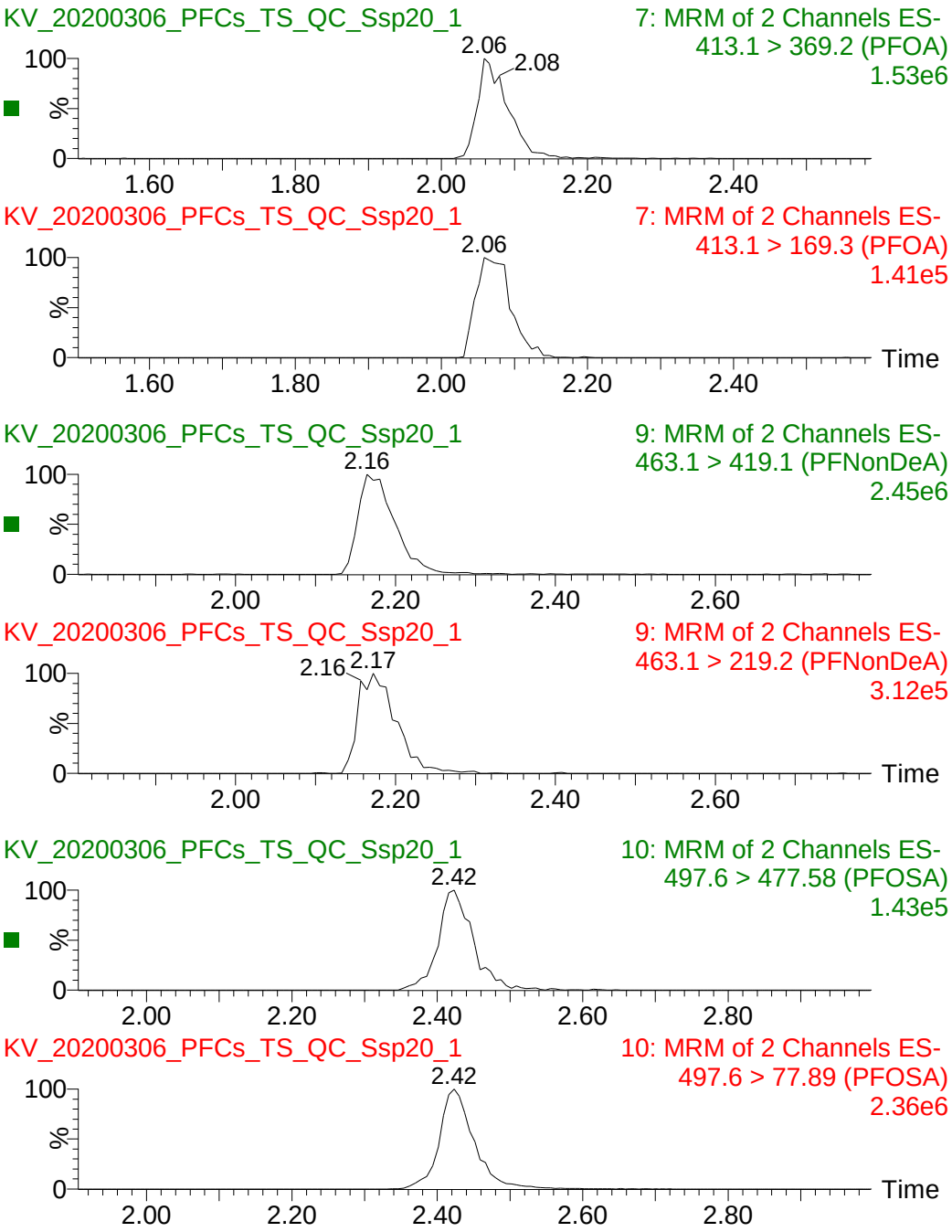

Figure D.4.: MRM chromatograms of PFOA, PFNA (PFNonDeA) and PFOSA in a pre-extration spiked matrix sample (66 ng mL^{-1}).

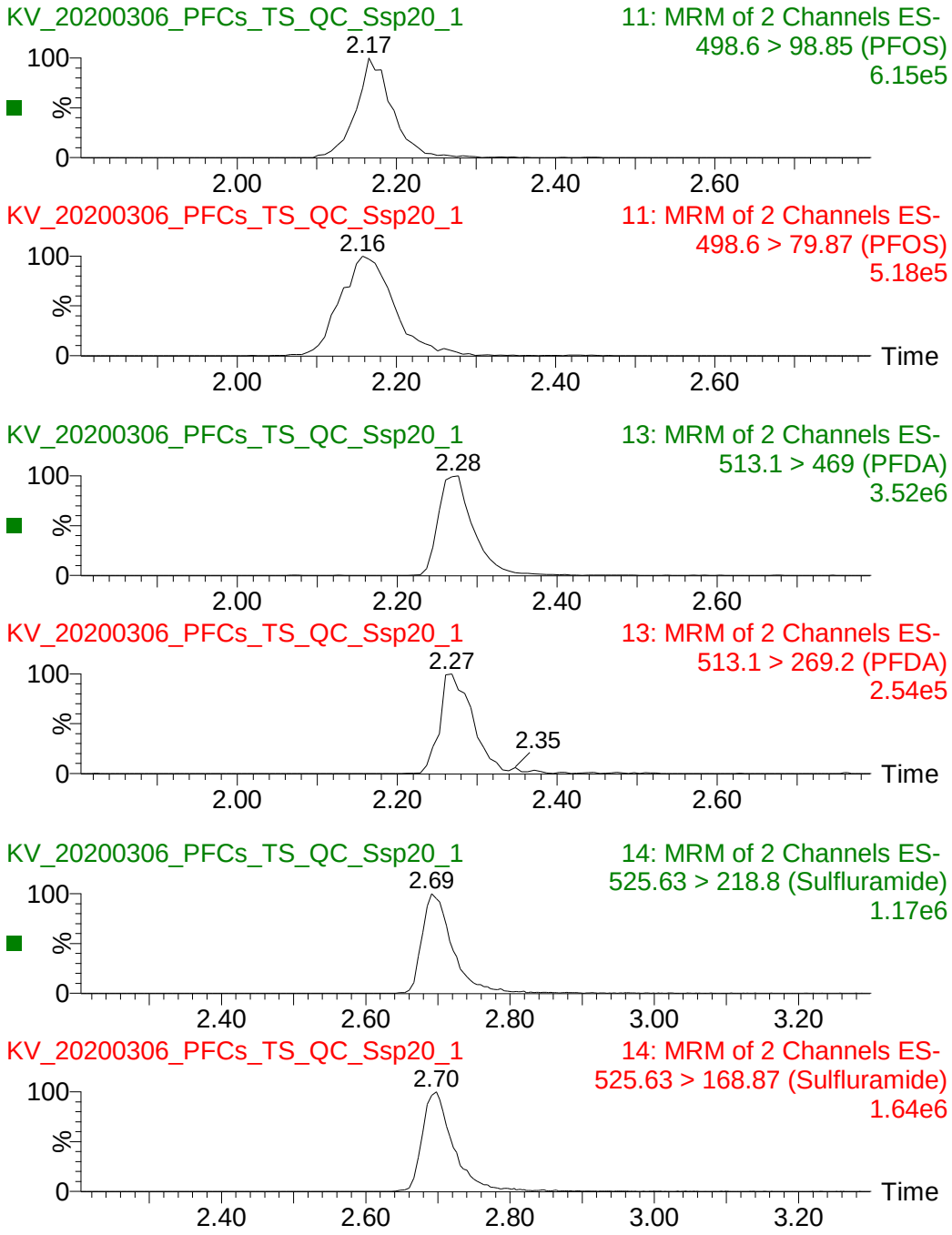

Figure D.5.: MRM chromatograms of PFOS, PFDA and EtPFOSA (Sulfuramide) in a pre-extration spiked matrix sample (66 ng mL^{-1}).

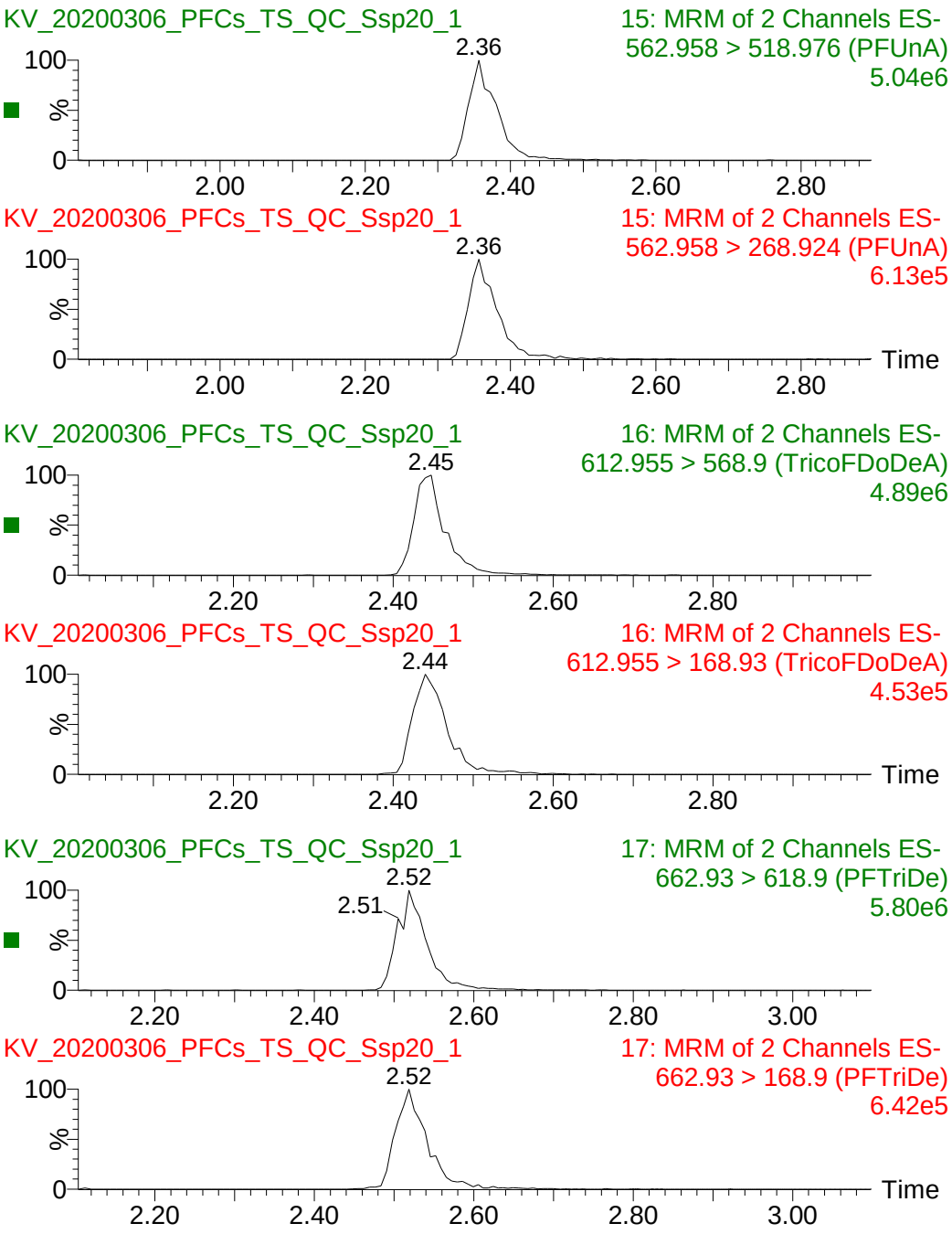

Figure D.6.: MRM chromatograms of PFUnDA (PFUnA), PFDoDA (TricoFDoDeA) and PFTrDA (PFTriDe) in a pre-extration spiked matrix sample (66 ng mL^{-1}).

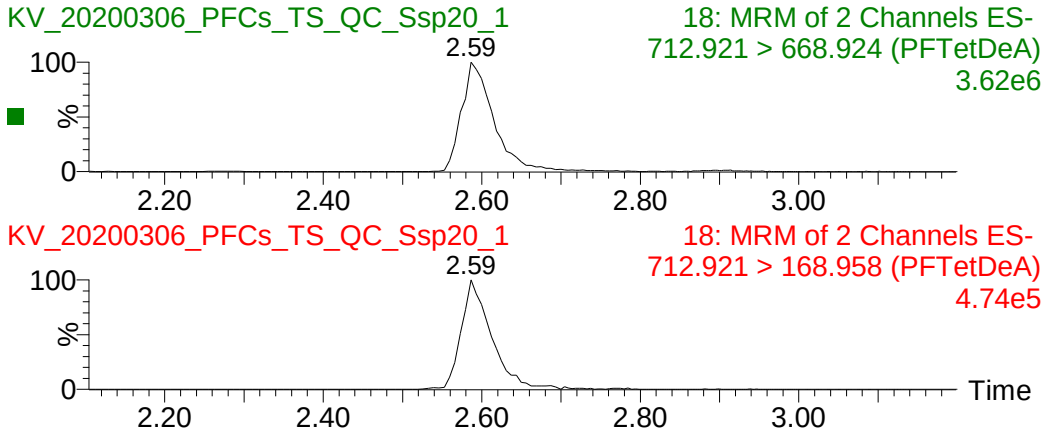

Figure D.7.: MRM chromatograms of PFTeDA (PFTetDeA) in a pre-extration spiked matrix sample (66 ng mL^{-1}).

E. Results

Concentrations of 15 per- and polyfluoroalkyl substances and one non-fluorinated target analyte in avian rbc samples are presented in Table E.1.

Table E.1.: Concentrations ($ng\,g^{-1}$, ww) og target analytes in avian red blood cell samples (n=110). Only concentrations>LOD are presented.

Nr	Species*	Location**	Year	PFBS	PFHxS	PFOS	PFPA	PFHxA	PFHpA	PFOA	PFNA	PFDA	PFUnDA	PFDoDA	PFTrDA	PFTeDA	PFOSA	EtPFOSA	DecaS
1	CUSA	WTP	2013			141						2.19		4.53	5.59	10.6	1.13		
2	CUSA	WTP	2013		20.7	306					21.3	6.18			1.96	6.74			
3	CUSA	WTP	2014			290				4.61	28.3	5.63		5.52	8.78	8.55	3.41		
4	CUSA	WTP	2014			156				6.56	25.8	4.10	13.3		2.89		5.55	0.418	26.0
5	CUSA	WTP	2014			175		3.71		2.43	2.3	3.01		1.59	4.39	5.20	9.46		
6	CUSA	WTP	2014			233		2.03				12.4				5.68	41.3		
7	CUSA	YC	2018			23.0					39.9		19.3		3.10				
8	CUSA	YC	2018			1.51				3.29	17.1		4.51						
9	CUSA	YC	2018			3.13					10.9	1.01							
10	CUSA	YC	2018			7.68				0.94	8.46		2.87						
11	CUSA	YC	2018	1.04		7.29										2.05			
12	CUSA	WTP	2018			21.6									5.12	5.35	2.47		65.8
13	CUSA	WTP	2018			40.4			3.43	9.70	5.75		1.22	3.68	4.04	3.41	3.03		19.9
14	CUSA	WTP	2018			22.4				2.36				1.92	1.36	1.83	0.50		1.85
15	CUSA	WTP	2018			74.0		1.71		5.58	3.74	3.54	1.06	1.33	1.57	1.46	0.83		7.38
16	CUSA	YC	2019							7.61									42.4
17	CUSA	YC	2019			3.42				0.76		1.35		0.95					
18	CUSA	YC	2019	0.03		0.62						3.96		1.45	1.84	1.50			
19	CUSA	YC	2019			8.27													
20	CUSA	YC	2019			18.6					13.7		5.44		2.40				10.5
21	CUSA	YC	2019			26.9				4.52									
22	RNST	WTP	2013			236	8.07	7.67	9.18	7.18	27.6	9.55	20.5	5.53	5.03	7.13	8.65		5.27
23	RNST	WTP	2013			120				3.89	1.39	1.31			1.54	4.09			
24	RNST	WTP	2013	0.74		98.7				3.87	15.5	6.29	5.98		1.17		1.84		

*Curlew sandpiper (CUSA), red-necked stint (RNST), ruddy turnstone (RUTU)

** Yallock Creek (YC); Central Manuka (CM); North Manuka (NM); Burges Bay (BB); Blackfellows Cave (BC); Nene Valley (NV); Denby Bay (DB)

Nr	Species*	Location**	Year	PFBS	PFHxS	PFOS	PFPA	PFHxA	PFHpA	PFOA	PFNA	PFDA	PFUnDA	PFDoDA	PFTrDA	PFTeDA	PFOSA	EtPFOSA	DecaS
25	RNST	WTP	2013			396				11.2	9.15	19.8	4.26	15.8	5.06	5.90	0.35		
26	RUTU	CM	2014												0.17			0.047	
27	RUTU	CM	2014												0.47				
28	RUTU	CM	2014	0.25			7.87				17.1								10.2
29	RUTU	BB	2014													8.26			47.4
30	RUTU	BB	2014																1.33
31	RUTU	BB	2014							0.70									
32	RUTU	BB	2014																
33	RUTU	CM	2014																
34	RUTU	NM	2014				2.13								0.30				
35	RUTU	NM	2014								10.7		15.1		2.16				
36	RUTU	NM	2014																
37	RUTU	NM	2014							7.78									
38	RUTU	NM	2014				3.03								0.29				
39	RNST	WTP	2014			33.4				2.37				1.38	1.08	3.69	0.12		
40	RNST	WTP	2014			112				6.16				2.50	1.84	2.93			
41	RNST	WTP	2014			178				12.8				2.97		20.4	2.35		
42	RNST	WTP	2014			135				2.52	2.06	1.57	1.66	3.76	2.65	2.45			
43	RNST	WTP	2016			94.0				6.89						8.05			
44	RNST	WTP	2016																
45	RNST	WTP	2016			88.0				6.68						9.13			
46	RNST	WTP	2016			48.3				3.84			2.21	2.26	3.87	1.34	0.77	0.65	
47	RNST	YC	2017				24.0												
48	RNST	YC	2017																
49	RNST	WTP	2017														0.12		
50	RNST	WTP	2017				8.00												
51	RNST	WTP	2017	5.39		235													
52	RNST	YC	2019																
53	RNST	YC	2019			13.1							13.2	3.26	3.66				
54	RUTU	BC	2015											0.76					
55	RUTU	BC	2015																
56	RUTU	BC	2015											0.47	0.29				
57	RUTU	BC	2015																

*Curlew sandpiper (CUSA), red-necked stint (RNST), ruddy turnstone (RUTU)

** Yallock Creek (YC); Central Manuka (CM); North Manuka (NM); Burges Bay (BB); Blackfellows Cave (BC); Nene Valley (NV); Denby Bay (DB)

Nr	Species*	Location**	Year	PFBS	PFHxS	PFOS	PFPA	PFHxA	PFHpA	PFOA	PFNA	PFDA	PFUnDA	PFDoDA	PFTrDA	PFTeDA	PFOSA	EtPFOSA	DecaS
58	RUTU	DB	2015																
59	RUTU	DB	2015									1.09			1.50				3.87
60	RUTU	CM	2015																
61	RUTU	BB	2016															0.19	
62	RUTU	CM	2016	1.14						8.47									
63	RUTU	CM	2016																
64	RUTU	BB	2017									0.76							
65	CUSA	WTP	2013			804					14.4	17.5		1.29					
66	RUTU	NM	2015																
67	RUTU	NM	2015	0.09								0.39							
68	RUTU	NM	2015	0.09						2.75		1.68		0.33					2.63
69	RUTU	NM	2015									0.78			0.54				
70	RUTU	DB	2015																
71	RUTU	DB	2015			0.63													
72	RUTU	CM	2015			1.24	8.98			3.04									
73	RUTU	CM	2015							0.75				0.31					
74	RUTU	CM	2015			0.69									0.10				
75	RUTU	BB	2016			0.05													
76	RUTU	BB	2016			0.50								0.47	2.58				
77	RUTU	BB	2016			1.28								0.17	0.55				5.27
78	RUTU	CM	2016			0.31									1.12	0.90			
79	RUTU	CM	2016																
80	RUTU	NV	2016			0.63	1.17												
81	RUTU	NV	2016									0.70		1.41	2.06	1.36			
82	RUTU	BB	2017			0.04				1.30	2.57	1.07		0.87	3.66				4.83
83	RUTU	BB	2017			0.48								0.74	1.42				
84	RUTU	BB	2017									1.40							
85	RUTU	CM	2017																
86	RUTU	CM	2017																
87	RUTU	NM	2018																
88	RUTU	NM	2018																
89	RUTU	CM	2018																
90	RUTU	CM	2018	1.73															

*Curlew sandpiper (CUSA), red-necked stint (RNST), ruddy turnstone (RUTU)

** Yallock Creek (YC); Central Manuka (CM); North Manuka (NM); Burges Bay (BB); Blackfellows Cave (BC); Nene Valley (NV); Denby Bay (DB)

Nr	Species*	Location**	Year	PFBS	PFHxS	PFOS	PFPA	PFHxA	PFHpA	PFOA	PFNA	PFDA	PFUnDA	PFDoDA	PFTrDA	PFTeDA	PFOSA	EtPFOSA	DecaS
91	RUTU	NM	2019							3.81									
92	RUTU	NM	2019																
93	RUTU	CM	2019																
94	RUTU	BB	2017																10.1
95	RUTU	CM	2017											0.21					
96	RUTU	CM	2017					9.37											
97	RUTU	NM	2018			1.22													
98	RUTU	CM	2018			0.49													
99	RUTU	NM	2018			0.89													
100	RUTU	BB	2018			0.91								0.42					
101	RUTU	BB	2018			1.16								0.33				0.083	
102	RUTU	BB	2018			0.55								0.52					
103	RUTU	BB	2018	0.24		0.88		1.70											
104	RUTU	NM	2019			0.26									0.28				
105	RUTU	CM	2019			0.94									1.02	1.86			
106	RUTU	CM	2019																
107	RUTU	CM	2019			0.08													
108	CUSA	WTP	2013			66.2				1.51				1.08	1.29	1.44	0.60		
109	RUTU	BC	2015	1.16		0.73								0.61	0.45				
110	RUTU	CM	2016											0.32	0.53				

*Curlew sandpiper (CUSA), red-necked stint (RNST), ruddy turnstone (RUTU)

** Yallock Creek (YC); Central Manuka (CM); North Manuka (NM); Burges Bay (BB); Blackfellows Cave (BC); Nene Valley (NV); Denby Bay (DB)

F. Principal component analysis and correlations

Principal component analysis biplot with loadings of age and absolute concentrations of PFOS, ΣPFAS, ΣPFSA and ΣPFAS and scores grouped by sample years is presented in Figure F.1. A heat map of correlations between age, PFOS, ΣPFAS, ΣPFSA and ΣPFCA is presented in Figure F.2.

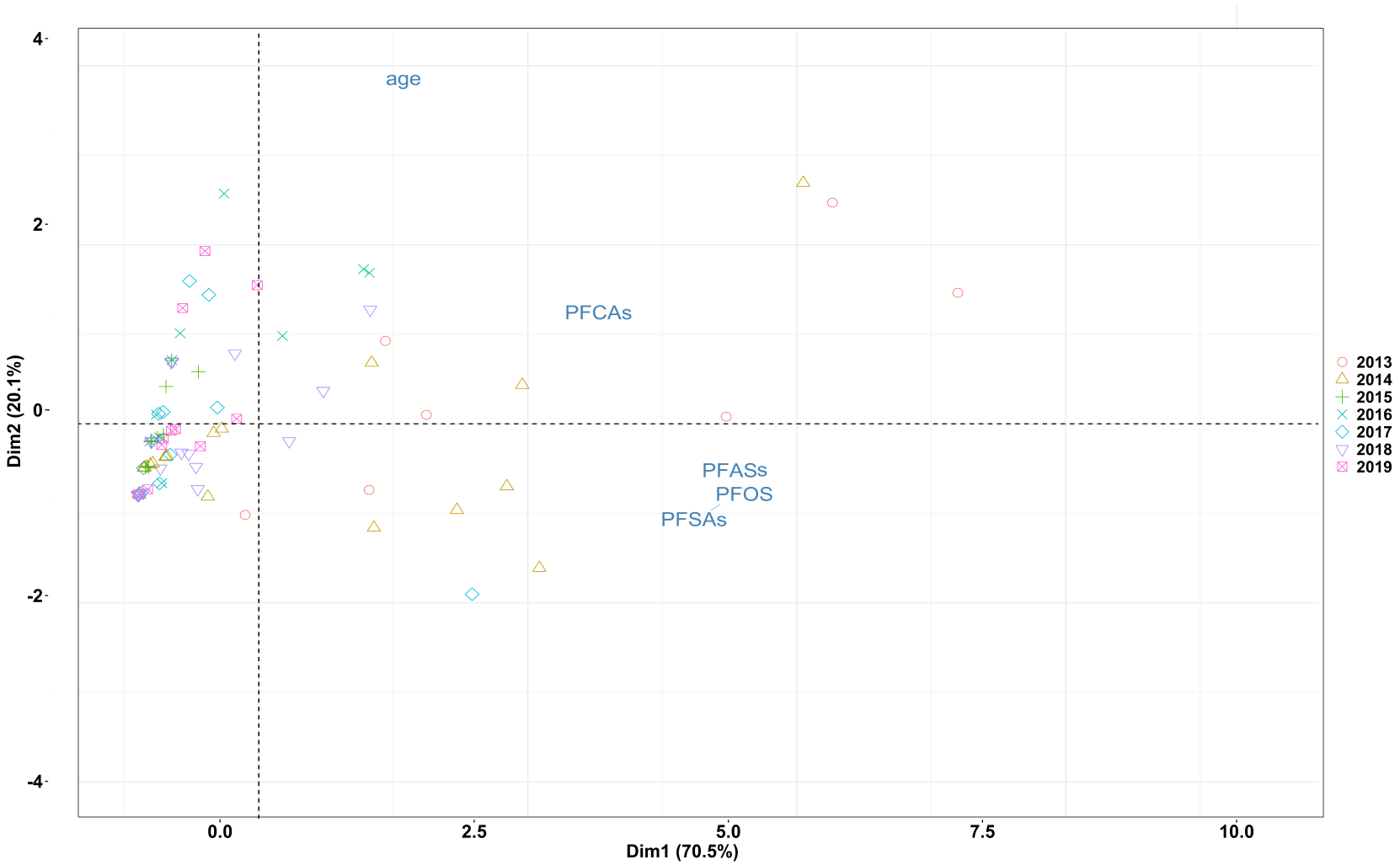

Figure F.1.: PCA biplot of age and absolute concentrations of PFOS, PFCAs (ΣPFCA), PFSAs (ΣPFSA) and PFASs (ΣPFAS) grouped by year.

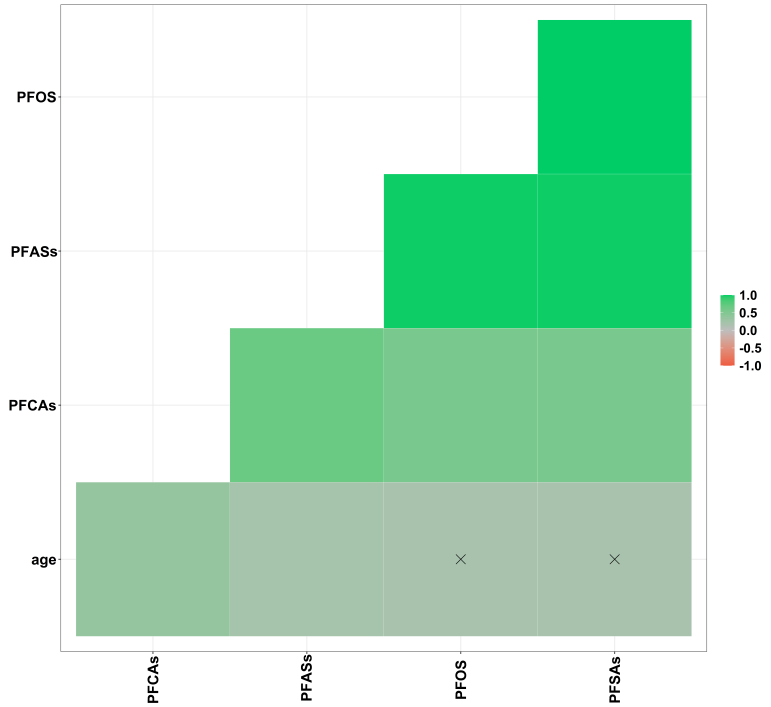

Figure F.2.: Correlation heat map of chemical groups and PFOS in avian blood cells. x denotes non-significant correlation.

G. Element analysis

Red blood cell samples (n=110) of three shorebird species were prepared for element analysis (HR-ICP-MS). Results of element analysis could not be obtained for this thesis. The sample preparation work that was performed is, however, described below.

Chemicals and materials Concentrated nitric acid (HNO_3, 50% (v/v), Ultra-Pure grade) was obtained by distillation with Milestone SubPue. MilliQ water was obtained using a water purification system (Q-option, Elga Labwater, Veolia Water Systems LTD).

Sample preparation Samples in 15mL Eppendorf tubes were digested by adding 1 mL 50% HNO_3 (v/v) before heating at 105°C for approximately 3.5 hours. Tubes in which samples had adhered to the wall above the liquid was regularly rotated to regain contact between acid and sample. Some samples were left 4.5-5 hours total to ensure complete digestion. An additional 0.5 mL 50% HNO_3 (v/v) was added to five samples to enhance digestion. Digested samples were diluted with Milli-Q water to obtain a 0.6 M HNO_3 solution.

Tonje Gottenberg Skaalvik

Per- and polyfluoroalkyl substances in shorebirds of Australia

NTNU
Kunnskap for en bedre verden